UNIVERSITEIT VAN PRETORIA
UNIVERSITY OF PRETORIA
YUNIBESITHI YA PRETORIA

1-Hexene dimerisation over a solid phosphoric acid catalyst

Renier Bernhard Schwarzer

1 February 2012

A thesis submitted to the Faculty of Engineering, the Built Environment and Information Technology of the University of Pretoria, Pretoria, South Africa, in partial fulfilment of the requirements for the degree of Philosophiae Doctor (Chemical Engineering)

Supervisor: Prof. W. Nicol
Co-supervisor: Mrs E.L. du Toit

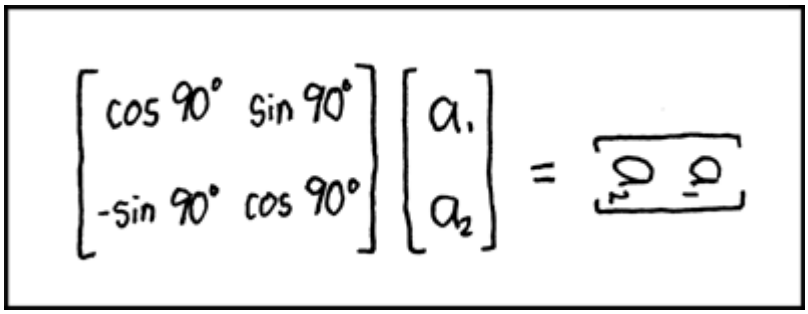

http://www.xkcd.com/184

Abstract

Solid phosphoric acid is a catalyst used for the upgrading of light olefins into fuels. To delve into the mechanism of olefin dimerisation over the catalyst, the oligomerisation of 1-hexene was investigated over a wide range of operating conditions. The reaction progression of 1-hexene dimerisation over solid phosphoric acid was interpreted by means of kinetic experiments for both a linear hexene (1-hexene) and a branched hexene (2,3-dimethyl-butene). The reaction rate for both reagents was described by using an elementary kinetic model. From the experimental data it was shown that the rate of dimerisation of branched hexenes was faster than the rate observed for linear hexene dimerisation. To correlate the two sets of kinetic data, the reaction network was expanded to incorporate skeletal isomerisation of 1-hexene with dimerisation only taking place by the co-dimerisation of linear and branched hexenes and the dimerisation of branched hexenes. The fit of the kinetic equation demonstrated that the reaction rate of 1-hexene is essentially controlled by the rate of skeletal isomerisation. Due to the large activation energy for skeletal isomerisation, low reaction temperatures favoured the co-dimerisation of linear and branched hexenes whereas at higher temperatures, the reaction rate was dominated by the dimerisation of branched hexenes. The product distribution indicated that, because of the fast rates of both cracking and secondary dimerisation (*dimerisation of cracked products*), the product distribution instantaneously reached a pseudo equilibrium after the dimerisation of hexenes. Therefore the carbon distribution was found to depend only on the reaction temperature, not on the residence time in the reactor.

Solid phosphoric acid is a supported liquid phosphoric acid where the condensed state of the acid, e.g. ortho phosphoric acid (H_3PO_4) and pyro phosphoric acid ($H_4P_2O_7$), is dependent on the quantity of water present in the reaction mixture. With a decrease in water content, the distribution of acid shifts and the ortho phosphoric acid becomes more condensed ($H_4P_2O_7$, $H_5P_3O_9$ etc.), i.e. high water content → low acid strength, low water content → high acid strength. The experiments completed at various degrees of catalyst hydration and free acid loading showed that the rate of reaction over solid phosphoric acid was dependent on the acid strength of the catalyst. The effect of acid strength on the reaction rate was integrated into the rate constants by means of an exponential dependency on acid strength. It was also shown that both the product distribution and the degree of branching remained unaffected by acid strength. The constant product indicates that the rate of cracking is limited by the rate of

oligomerisation of hexenes, irrespective of the acid strength of the catalyst. Since the product from the dimerisation of 1-hexene could be used as fuel, the quality of the desired fuel would therefore depend solely on the reaction temperature, not on the hydration of the catalyst.

The work performed in this thesis has been published in two peer-review articles:

1. Schwarzer R.B., du Toit E. and Nicol W. (2008) Kinetic model for the dimerisation of 1-hexene over a solid phosphoric acid catalyst, *Applied Catalysis A: General*, 340, 119-124.

2. Schwarzer R.B., du Toit E. and Nicol W. (2009) Solid phosphoric acid catalysts: The effect of free acid composition on selectivity and activity for 1-hexene dimerisation, *Applied Catalysis A: General*, 369, 83-89.

Acknowledgements

My journey through postgraduate at the University of Pretoria was a memorable road to traverse, even though the journey is past the memories are treasured. I would like to thank Elizbe du Toit for her inspiration and encouragement to endure with my research, her guidance is greatly appreciated, together with Willie Nicol they kept me on the straight and narrow and steered the work to completion. Thanks also go out to Sasol Technology, whom sponsored this research, and to the colleagues whom helped direct, support and dispute the research in this thesis.

Contents

Nomenclature

A	Linear hexenes isomers, mol/L
A_A	P_2O_5 weight percentage (i.e. acid strength)
B	Skeletal hexene isomers, mol/L
C_x	Concentration of molecule x, mol/L
D	Hexene depletion toward dimerised product, mol/L
E_a	Activation energy, kJ/mol.K
k_1	Kinetic constant for the rate of skeletal isomerisation, L/min.g
$k_{2,3}$	Kinetic constant for the rate of dimerisation and co-dimerisation, L^2/mol.min.g
$k_{x,o}$	Pre-exponential constant
k_{x,A_A}	Acid strength rate constant dependency
K_x	Distribution of molecule x with reference to the hexene depletion
K_{eq}	Experimentally determined equilibrium distribution of branched hexenes versus dimerised product
m_{cat}	Weight concentration of catalyst in the reaction mixture, g/L
$P_2O_5°$	SPA base phosphoric acid strength, weight fraction P_2O_5
P_2O_5 (W %)	Acid strength of SPA
t	Time, min
T	Temperature, K
$W_{Free\ acid}$	Weight-free acid determined from titration, g
W_{H2O}	Weight H_2O in the reaction mixture, g
V	Volume of reaction mixture, L

Abbreviations

AARE	Absolute average relative error
IB	Iso-butene
CD	Co-dimerisation of linear and branched hexenes
CFPP	Cold Filter Plugging Point
DLH	Dimerisation of linear hexenes
DBH	Dimerisation of branched hexenes
DMB	2,3-dimethyl-2-butene
df	Film thickness
FID	Flame ionisation detector
FT	Fischer-Tropsch
i.d.	Inside diameter
GC	Gas chromatography
MON	Motor Octane Number
2M1B	2-Methyl-1-butene
2M2B	2-Methyl-2-butene
MS	Mass-spectrometry
RON	Research octane number
SPA	Solid phosphoric acid
FA	Free acid

Figure symbols

◊	Concentration of branched hexenes
*	Concentration of linear hexenes
△	Concentration of oligomerised product

List of Figures

List of Tables

1 Introduction

The petrochemical industry has relied on the oligomerisation of short-chain olefins for blending into fuels since 1935 (Ipatieff *et al.*, 1935). Oligomerisation of short-chain olefins allows a refinery a means to incorporate lighter boiling olefins into the fuel pool and still comply with volatility specification. These short-chain olefins originate from fluid catalytic cracking (Cruz *et al.*, 2007; Chen *et al.*, 2008), steam-cracking and dehydrogenation units (Di Girolamo *et al.*, 1997). In high-temperature Fischer-Tropsch processes, short-chain alpha olefins (C_3-C_4) are also continually produced and then oligomerised (Dancuart *et al.,* 2004). Olefins present in the light naphtha fraction (specifically C_5-C_6 carbon number) are not oligomerised and instead used as feedstock for other chemical production processes (De Klerk, 2005b; Dancuart *et al.*, 2004). However, with the continued increase in global demand for fuel and international concern about dwindling oil resources (Bentley, 2002), it is increasingly becoming economically feasible to incorporate a wider range of product into the fuel pool.

The quantity of light boiling olefins that can be blended into fuel is restricted by volatility limitations, as stated earlier. These limitations will become even more significant when environmental concerns may result in the future mandatory addition of ethanol to fuels (Schmidt *et al.*, 2008). Oligomerisation/dimerisation of the C_5-C_6 olefins will result in greater flexibility for the petrochemical industry in terms of the olefin fraction that can be blended into the fuel. Oligomerisation of longer chain olefins can also be used for the production of lubrication oils (Dazeley, 1948; Sarin *et al.*, 1996) or detergents and plasticisers (Da Rosa *et al.,* 1997). Making it increasingly more important to study the oligomerisation/dimerisation reactions for these longer-chain olefins. 1-Hexene forms a substantial part of the naphtha fraction from Fischer-Tropsch processing (De Klerk, 2006a) and was selected as a model component to study these oligomerisation reactions.

Various catalysts have been investigated for the oligomerisation of olefins, examples of which include liquid phosphoric acid (Ipatieff, 1935), solid phosphoric acid (Ipatieff and Corson, 1935), sulphuric acid (Naworski and Harriott, 1969), Aluminum Chloride (Dazeley, 1948), Cobalt-Oxide-on-Carbon (Schultz, 1967), ZSM-5 (Tabak *et al.*, 1986), Ni-Aluminosilicates (Bercik *et al.*, 1978), cation exchange resins (O'Connor *et al.*, 1985) and silica-alumina (Shepard *et al.,* 1962). These are just some of the catalyst that is active for oligomerisation, a more comprehensive list can be found in the reviews of Schemrling and

Ipatieff (1950) and Skupińska (1991). Commercially oligomerisation has occurred using ZSM-5 (Tabak *et al.,* 1986), solid phosphoric acid (SPA, De Klerk, 2007a) and Ni (Commereuc *et al.,* 1982). Due to the ban of MTBE from fuel MTBE, cation exchange resins have also been investigated for the dimerisation of iso-butene (Hondela and Krause, 2003). SPA, which is used in this investigation, is manufactured by mixing diatomaceous earth (Kieselguhr) with liquid phosphoric acid (Coetzee *et al.*, 2006). The resultant catalyst consists of a layer of different phosphoric acid species, i.e. ortho, pyro, tri and poly phosphoric acid (the free acid layer), supported on a mixture of silica and silicon phosphates and is therefore known as a liquid supported catalyst. Although the silicon phosphates affect the crushing strength of the catalyst, it is accepted that the phosphates have no influence on the catalytic activity of SPA (Krawietz *et al.,* 1998).

Most of the previous work on oligomerisation reaction rates focused on the oligomerisation of shorter-chain olefins such as propene and butene (Cruz *et al.*, 2007; Honkela and Krause, 2004; Alcántara *et al.*, 2000; Cao *et al.*, 1988). There are relatively few investigations into the oligomerisation of longer-chain olefins. Where these reactions were studied, the focus was on the behaviour of various isomers at fixed residence times, without giving any consideration to the progression of the reaction. For example, during the alkylation reaction of hexene, Nel and De Klerk (2007) found that linear hexenes were selectively alkylated and branched hexenes selectively dimerised. This selective oligomerisation of branched olefins over SPA, was corroborated by De Klerk (2006b) for octene dimerisation. This indicates that skeletal isomers present in the feed is critical to the oligomerisation of heavy olefins over SPA.

Studies specifically on the oligomerisation of C_6 olefins investigated the catalyst activity at a constant residence time instead of investigating the reaction progression (Van Grieken *et al.*, 2006; Pater *et al.*, 1999). For the oligomerisation of butenes, Golombok and de Bruijn (2000) show that there is a difference in the fuel quality, depending on which double bond isomer is present initially. This observation could however be limited to oligomerisation of olefins over Amorphous Silica Alumina since the catalyst contains both Lewis and Brønsted acids since Golombok and de Bruijn (2000). For the oligomerisation of longer-chain olefins, such as 1-hexene, an even greater quantity of isomers – including skeletal isomers (Quan *et al.*, 1988) – can form part of the isomer community that contributes to the oligomerisation reaction. The reaction progression of the various isomerisation and subsequent oligomerisation reactions will then be important, since the reaction progression can influence the product selectivity. Not only is the product reaction route important but also the

temperature dependence of these rates. Due to differences in the activation energy, for each reaction rate, changing the reaction temperature could influence the product distribution. Therefore it is increasingly important not only to study the oligomerisation capabilities of the catalyst at fixed residence times, but also to gain an insight into the temperature-dependent reaction progression of the various isomers. Accordingly, in Chapter 3 the batch reaction kinetics of the dimerisation of 1-hexene is discussed regarding the temperatures around which the current oligomerisation reactors for shorter chain olefins are operated. The quality of the produced fuel will not only depend on the amount of dimerised product, however, but also on the degree of cracking and secondary oligomerisation that takes place after dimerisation. Hence, the effect of temperature and residence on the degree of cracking is also discussed in Chapter 3.

When studying the oligomerisation of propene on SPA, Cavani *et al.* (1993) report that a low water feed content is preferable where the reaction rate is concerned. The water in the reaction mixture is absorbed into the free acid layer of the catalyst and directly influences the acidity and activity of the catalyst. In addition, a variation in water content is also reported to have an influence on reaction selectivity. For instance, Prinsloo (2006) showed that there was increased diesel selectivity with decreased hydration levels for the oligomerisation of propene over SPA. De Klerk *et al.* (2006) also found that the hydration of the SPA as well as the reaction temperature affected the quality of the produced fuel when butene was oligomerised.

Phosphoric acid reacts with water to form an equilibrium distribution of the various acid oligomers, $H_{2n}P_nO_{3n+1}$: from the less condensed ortho phosphoric acid, to the more condensed pyro and tri phosphoric acids and finally to the highly condensed poly phosphoric acids (Jameson, 1959). Altering the water content on the catalyst will therefore affect the resulting acid strength as well as the composition of the phosphoric acid. Although Zhirong *et al.* (2000) report no definite trend in the total quantity of free phosphoric acid and the catalytic activity of SPA towards propene oligomerisation, they did find that the presence of pyro phosphoric acid in the free acid layer is imperative for the catalytic activity.

In Chapter 4 attention is given to the influence of acid strength and free acid content on the reaction kinetics and the product distribution. Batch kinetic data was gathered for various acid strengths by either *1)* altering the hydration of the catalyst at different temperatures or *2)* investigating the effect of altering the free acid content of the catalyst at a constant temperature of 200 °C. The vapour liquid equilibrium data of phosphoric acid together with the measurements of the free acid content after various catalyst treatment procedures, was

used to alter the P_2O_5-based acid strength and subsequently the distribution of acid oligomers in the free acid layer.

The product from the oligomerisation of 1-hexene over SPA could either be used as lubricating oil, for detergent production, or as fuel additive. The use of the product, as either, is limited by the chain length and the degree of branching of the product. Since acid strength can be assumed to affect the degree branching and chain length of the formed product, this will impact the use of the 1-hexene oligomerate over SPA. In Chapter 5 the effect of acid strength on the degree of branching and chain length of the product is discussed.

2 Literature survey

Oligomerisation of short chain olefins is by no means a new technology as it has been practised industrially since 1935 (Egloff, 1936; Ipatieff *et al.,* 1935). Reaction kinetics for oligomerisation over SPA has mostly been overlooked owing to the extent of the experimental data needed to gain an accurate kinetic model. For this reason the literature has focused on gaining insights into the effect of operating conditions and feed concentration on the quality of the produced fuel (Ipatieff and Schaad, 1938).

A literature survey is needed to understand the oligomerisation of short chain olefins over SPA so as to convey aspects of the quality of the fuel, the reaction network/mechanism, reactivity and selectivity differences of isomers, the catalyst (with regard to composition, hydration and acid strength) and the attempts that have been made to model the reaction kinetics in the literature.

2.1 Oligomerisation: Product slate

Oligomerisation of olefins can be used for the production of various products from lubrication oils, detergents and plasticiser feed stock to the production of fuels (gasoline, jet fuel and diesel). Since a large part of the literature focuses on the production of fuels from short chain olefins a basic understanding of the product slate and the properties of the product is needed.

For the production of fuels, short chain olefins are oligomerised and then fractionated into petrol, jet fuel and diesel with the cut-off points dictated by the applicability of the product to each fuel. If paraffinic hydrocarbons are considered, chain length 1 to 4 can be regarded as liquefied petroleum gas (LPG), 5-9 can be incorporated into petrol/gasoline, 11-22 can be used as diesel or jet fuel depending on the degree of branching (Dancaurt *et al.,* 2004).

To define the quality of petrol engine testing is used determine the tendency of the gasoline to auto ignite under compression, which results in knocking. For octane testing a baseline is used whereby the octane rating of 1-heptane equals zero with iso-octane (trimethyl pentane) equalling 100. For streams consisting of paraffins and olefins, the octane rating is influenced by the following:

- The chain length of the hydrocarbon: with an increase in the chain length, the octane is generally expected to decrease (if both molecules have the same branching).

- The degree of branching: with an increased degree of branching, at a fixed carbon length, the octane value is expected to increase. This is important to the oligomerisation of short chain olefins, since isomerisation and oligomerisation of short chain olefins can both occur over acid catalyst. The relative ratio of each will affect the quality of the petrol.
- The saturation of the hydrocarbon (a saturated hydrocarbon has no double/triple bonds, e.g. alkanes): unsaturated hydrocarbons tend to have a greater octane value than saturated hydrocarbons. The fraction of unsaturated hydrocarbons that can be blended into the fuel is however regulated, the Euro 4 specification for olefin content is 18% (De Klerk *et al.*, 2004)

The specifications of jet fuel and diesel overlap with regard to flash point and final boiling point, the big difference between diesel and jet fuel lies in the CFPP, freezing point and cetane. For jet fuel a low freezing point is needed (maximum freezing point of -47 °C, US Ministry of Defence Standard 91-91 Issue 6), where as for diesel a CFPP (which is a function of freezing point) between 0 and -20 °C is defined depending on the season (DIN EN 590-2009 standard). The freezing point, and CFPP, of a hydrocarbon is dependent the degree of branching, increasing the degree of branching reduces both the freezing point and CFPP. The cetane value, however, is larger for a linear hydrocarbon. Therefore if the product boils above the petrol fraction, the fuel would be more applicable as a jet fuel if the product is highly branched or as diesel if the product is highly linear.

Lubricating oils are paraffinic hydrocarbons with a chain length greater than 20 and shorter than 40 which are prevalently branched (Montanari *et al.*, 1998). Whereas for the synthesis of detergents and plasticisers, shorter chain linear ($<C_{20}$) olefins are required (Da Rosa *et al.,* 1996).

2.2 Background: Oligomerisation of short chain olefins over SPA

Industrially, mainly two catalysts are used for the oligomerisation of short chain olefins to gasoline, namely solid phosphoric acid (Ipatieff *et al.*, 1935) and ZSM-5 (Tabak *et al.*, 1986) which are used by UOP and Mobil respectively. Oligomerisation of short chain olefins have also been shown to occur thermally (Ipatieff and Pines, 1936), although the addition of a catalyst reduces the severity needed for oligomerisation.

Historically SPA was used for the upgrading of light olefins, both propylene and butenes, to fuel (Ipatieff *et al.*, 1935;Weinert and Egloff 1948; Deeter, 1950; Egloff and Welnert, 1951).

The feed to a Catalytic Polymerisation unit can originate from Fischer-Tropsch, catalytic cracking or thermal cracking, typical analysis of which is shown in Table 2-1 (Jones, 1956; De Klerk *et al.*, 2006). As is evident from the feed composition, a wide variety of olefins are fed into the reactor. This creates an assortment of dimerisation and co-dimerisation reactions which may occur; if the reaction rate between these isomers differs, a large reaction network would be required especially if the RON values differ among the varied products.

Table 2-1: Composition of feed to a catalytic polymerisation unit from Fischer-Tropsch, thermal cracking and catalytic cracking.

Component	C4 FT cut	Thermal cracking	Catalytic cracker
Hydrogen		2.1%	
Methane		31.1%	
Ethylene		19.1%	
Ethane		31.2%	0.1%
Propene		8.3%	14.4%
Propane	<0.1%	2.2%	15.9%
2-methyl-propane	4.5%		
n-butane	22.1%	4.1%	14.5%
iso-butane			22.0%
trans-2-butene	2.0%		
1-butene	54.8%	1.1%	32.8%
Butadiene		0.0%	0.1%
2-methyl-propene	5.7%		
Cis-2-butene	3.4%		
2-methyl-butane	0.4%		
n-pentane	0.2%	0.7%	0.1%
3-methyl-1-butene	1.7%		
2-methyl-2-butene	3.7%		
2-methyl-1-butene	0.2%		
other C5+ material	1.3%		

The quality of the produced gasoline is also dependent on the feed composition, if propylene is fed to the reactor the hydrogenated RON of the fuel would be less than 80, whereas if butenes are fed to the reactor a hydrogenated RON between 90-96 is viable (Egloff and Welnert, 1951). This is due to isomerisation which occurs readily over SPA. During the oligomerisation of 1-butene over SPA at mild operating conditions (< 250°C), the C_8 product spectrum indicated that isomerisation had indeed occurred before the butene oligomerised (De Klerk, 2004). Since the isomerisation of the product will improve the

quality of the gasoline, the induction of isomerisation is critical to the production of a high RON fuel (De Klerk 2004; Nel and De Klerk, 2007; Cowley *et al.*, 2006).

Unlike propylene butene has a skeletal isomer, iso-butene, which is known to influence the reaction rate and the degree of branching of the produced fuel (i.e. RON). This has bearing on the oligomerisation of 1-hexene since hexene has various branched isomers which could react differently to their linear counter parts. Ipatieff and Schaad (1938) showed that with a more pronounced presence of isobutene, not only did the oligomerisation occur more easily at less severe operating conditions but the quality of the produced fuel also improved (Table 2-2). Controlling the degree of branching in the feed is therefore important for increasing the reaction rate and optimising the quality of the gasoline produced.

Table 2-2: Effect of isobutene on oligomerisation rate and the quality of the hydrogenated produced fuel.

T (°C)	Butenes charged ($g_{butenes}/(hr.cc_{cat})$)	Isobutene percentage	Total conversion	Octane no.
80	4.75	84.8%	91.5%	98
95	6.95	96.0%	88.0%	100
120	5.40	91.4%	87.0%	98
120	1.37	46.0%	74.0%	97
120	0.58	36.5%	54.0%	96
120	0.32	25.5%	49.0%	95
149	0.87	27.1%	58.0%	95
177	0.88	0.0%	72.0%	83
177	0.77	1.4%	64.0%	85

The position of the double bond also affects the reaction rate. Paynter and Schuette (1971) noted selectivity differences for a constant feed olefin content of C_3 and C_4 olefins, depending on the fraction of 1-butene and 2-butene in the feed. As more 2-butene was introduced in the feed, the selectivity turned toward the dimerisation of C_3 and less C_4 dimerisation and co-dimerisation took place. Cao *et al.* (1988) determined that 2-butene was far less reactive than 1-butene for the oligomerisation of a light olefin feed over SPA at 115 °C. It should be noted that at temperatures below 550 °C the equilibrium distribution of butenes favours 2-butene above 1-butene. Hence to obtain a correct measurement of the

reaction rate difference between the two isomers, the equilibrium distribution should be taken into account as well as measuring the rate difference for the two isomers experimentally. Cao *et al.* (1988) took the equilibrium distribution into account but did not have kinetic data available for the two individual isomers. This could result that the difference in reaction rate predicted could be lumped in an inadequate reaction mechanism and not due to difference in the reaction rate for the two isomers. De Klerk (2004) however showed that for the oligomerisation of a pure mixture of 1-butene, cis-2-butene and trans-2-butene showed that 1-butene had a far higher conversion at the same temperature and residence time in a pack bed reactor. The presence of 1-butene seemed to ease the formation of iso-butene which reacts to far more significantly than its linear counterparts. The increased probability of 1-butene to isomerise was also present in the formation of highly branched product from 1-butene.

Golombok *et al.* (2000) found that the quality of the produced fuel would also differ; depending on which of these two olefins oligomerised, a superior gasoline was obtained for the oligomerisation of 1-butene in comparison to the 2-butene oligomerisation. The work was however done on Amorphous Silica Alumina which is both a Lewis and Brønsted acid for which the reaction pathway may differ from SPA which is predominantly a Brønsted acid. For butene oligomerisation over SPA De Klerk (2004) observed that the formation of trimethyl pentene was linked to the concentration of 1-butene and iso-butene in the reaction mixture, there for in an equilibrated mixture of n-butenes the oligomerisation to trimethyl pentene occurs through the 1-butene in the mixture. This further creates the impression that the distribution of isomers in the reaction mixture controls the fuel quality.

Since kinetic data is not available for complex mixtures of olefins, experimental studies rely on the comparison of the fuel quality at various space velocities to draw residence time-dependent trends to the quality of the fuel. For a mixed butene feed at 150 °C and 38 bars, De Klerk *et al.* (2004), showed that at high space velocities conversion dropped whereas the RON of the fuel increased (Figure 2-1). Since the selectivity to branched C_8s influences the resulting octane, it becomes a problem to limit the selectivity to the dimerised product, especially at lower space velocities which are needed to obtain high conversion.

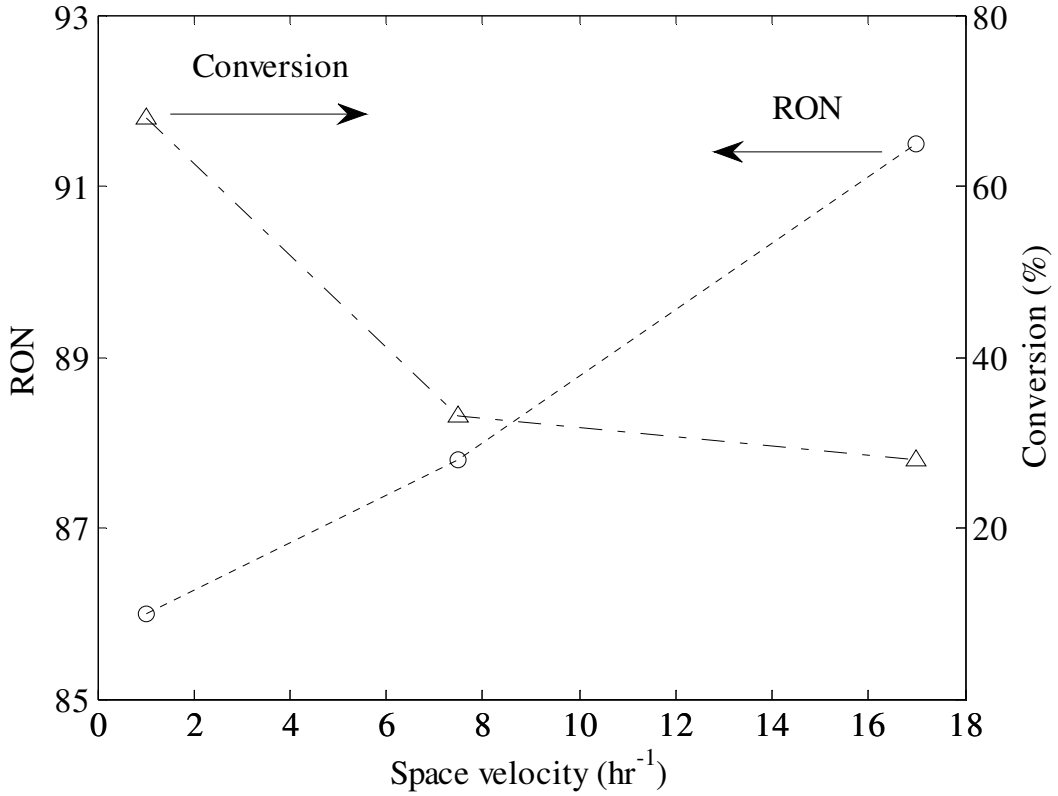

Figure 2-1: Effect of space velocity on the conversion and RON for the oligomerisation of C4 olefins over SPA, |● – RON, ▲ - Conversion (De Klerk, *et al.*, 2004).

A kinetic model would be invaluable if the increase in RON could be incorporated over the progression of the reaction. For the kinetic model to predict the rate of oligomerisation, and possibly estimate the RON, the model would have to incorporate the difference in the reactivities of olefins, together with the rate of isomerisation. This could easily result in a substantial number of parameters that would be required to model the reaction network.

2.3 Oligomerisation of light naphtha olefins over SPA

Industrial oligomerisation mainly focuses on the refining of shorter chain olefins ($<C_5$) into the fuel pool. Naphtha range products can easily be blended into the gasoline pool without further refining but the extent that can be blended is limited by the linearity of the naphtha. The oligomerisation (or isomerisation) of the naphtha fraction will allow the incorporation of a larger fraction into gasoline, jet fuel or diesel (Quan *et al.*, 1988; De Klerk, 2005b).

Early work on the dimerisation of a pentene mixture over SPA by Ipatieff and Schaad (1948) showed that pentene skeletal isomers can be dimerised over SPA at low temperatures

(83 and 100 °C). The rate was found to be faster for the dimerisation of 2-methyl-1-butene than that of 3-methyl-1-butene at similar reaction conditions. Unfortunately no comparison was available for the dimerisation of 1-pentene which would give valuable information to the route of dimerisation of longer chain olefins (e.g. via skeletal isomerisation or direct dimerisation of linear pentene isomers). As such fairly little could be extracted for the path of heavy olefin oligomerisation over SPA.

Where heavier olefins have been oligomerised over SPA, the high degree of branching seen in the product indicates the catalyst is more appropriate for the production of gasoline or jet fuels. Mashapa *et al.* (2007) focused on the effect of oxygenates on the oligomerisation of heavy olefins, however experiments done for a 1:1 mass ratio in the feed of butenes and hexenes showed that 76% and 91% of the 1-hexene converted at 150 and 180 °C respectively. Although this was higher than the extent of butene conversion, which was 27% and 44%, only 18% and 30% of the hexenes converted to oligomers (1-hexene predominantly converted to hexene isomers). Interestingly the carbon distribution of the product was also limited to the formation of dimerised product. This limited extent of oligomerisation over SPA was also noted for the alkylation of benzene with 1-hexene by Nel and De Klerk (2007). This low extent of oligomerisation with high branching negates the use of SPA for the production of lubricating oils as well as detergents and plasticisers. Therefore it seems that SPA is purpose built for the production fuel range products.

A study done by De Klerk (2006b) investigating how the degree of branching of a C_8 olefin influences the rate of dimerisation indicates that trimethyl pentene is more reactive than 1-octene at similar operating conditions. This suggests that for the oligomerisation of longer chain olefins, isomerisation needs to occur first before oligomerisation can occur. This limits the use of SPA as a catalyst for the oligomerisation of long chain alpha olefins. Due to a reduction in activity with chian length, the temperature needs to be upped until isomerisation becomes viable. Unfortunately if the temperature is raised too much coke formation will inevitably occur more freely limiting the usefulness of the catalyst. Therefore when oligomerising of light naphtha olefins to diesel, the reaction is usually catalysed by a Zeolite (Pater *et al.*, 1998; Pater *et al.*, 1999; Garwood, 1983), silica alumina (Van Grieken *et al.*, 2006; Escola *et al.*, 2006) or Ni (Fortini *et al.*, 1997; Heveling *et al.*, 2003).

When SPA is used as catalyst for the oligomerisation of longer chain olefins, the reaction rate seems to be limited by the rate of isomerisation, however no kinetic data is available for predicting the route or relative rate of dimerisation through skeletal or linear olefin isomers. If the reaction conditions could be varied to overcome this limitation, SPA would be more

viable. It also seems that due to the high degree of branching incurred by the isomerisation over SPA, SPA is more applicable for the production of a jet fuel than a diesel fuel or lubricating oils.

2.4 Solid phosphoric acid

The patent by UOP for the production of SPA has existed since 1962 (Morrell, 1962a; Morrell, 1962b; Morrell, 1964). The support on which the phosphoric acid is placed has mainly been diatomaceous earth (kiezelguhr) although the phosphoric acid has also been impregnated on quartz (Langlois & Walkey, 1951; Langlois & Walkey, 1952; Vinnik and Obraztsov, 1983) and silica gel (Kotsarenko *et al.*, 1989). Mainly kiezelguhr, such as Celite (Handlos and Nixon, 1956), is preferred as support for impregnating phosphoric acid.

When discussing SPA, certain key concepts create confusion if there is no prior knowledge of the catalyst. The catalyst is described in terms of the acid impregnated on the catalyst:

- *firstly* the total acid content describes the total quantity of acid present on the catalyst (as a weight percentage of the catalyst),
- *secondly* the "*free acid*" is used to describe the quantity of phosphoric acid present as a liquid layer in the catalyst (this excludes the quantity of chemically bound phosphoric acid on the support) and this is expressed as the weight percentage H_3PO_4 with regard to the catalyst weight,
- *thirdly* the acid strength, this describes the phosphoric acid strength of the free acid (this concept will be further elaborated in this section).

SPA is produced by mixing kiezelguhr and phosphoric acid at 200 °C (impregnation temperature) before being extruded. After extrusion, the catalyst is calcined for a predetermined length of time. During the impregnation of the kiezelguhr, the phosphoric acid bond to the silicon support and silicon phosphates originate:

Silicon ortho phosphate:

$$5SiO_2 + 6H_3PO_4 \leftrightarrow Si_5O(PO_4)_6 + 9H_2O \qquad 2\text{-}1$$

Silicon pyro phosphate

$$5SiO_2 + 10H_3PO_4 \leftrightarrow 5SiP_2O_7 + 15H_2O \qquad 2\text{-}2$$

The total phosphoric acid content in the catalyst is present as either fixed phosphorus (silicon phosphates; Equation 2-1 and 2-2) or as free acid. The total acid content of SPA is in

the order of 70%. Most of the phosphorous present in the catalyst is fixed on the support as silicon phosphates, whereas only about 20% of the acid is present as free acid (Coetzee *et al.*, 2006). The free acid on the catalyst is critical to the activity of SPA since the support (fixed phosphorous) does not contribute to the activity of the catalyst. Therefore only the supported free acid determines the activity of the catalyst (Krawietz *et al.*, 1998). The reactivity of silicon phosphates to oligomerisation is however not so simple to measure, since a small amount of water present in the feed will result in the hydration of the silicon phosphates to phosphoric acid, resulting that no forthright conclusion can be made concerning the activity or non-activity of the silicon phosphates (Schmerling and Ipatieff, 1950).

A study by Prinsloo (2007) on the production of SPA from low-quality kieselguhr showed that quartz had a negative affect on the crushing strength of the catalyst. It is believed that the crushing strength is of critical importance to the industrial applicability of the catalyst. The pressure drop measured during the operation of the catalyst has shown a steady increase with time on stream; this is coupled to the disintegration of the catalyst which is directly related to the crushing strength of the catalyst (Coetzee *et al.*, 2006). The two most important aspects of the catalyst, industrially, are its crushing strength and activity. Both of these properties are influenced by the acid strength of the phosphoric acid used for impregnation, the calcination temperature and the type of kiezelguhr impregnated. An increase in both the acid strength and the calcination temperature is beneficial to the crushing strength. This is connected to the formation of the silicon pyro phosphates, which is directly linked to the physical properties of the catalyst. However, when increasing these parameters, the free acid content of the catalyst decreases, meaning the activity decreases (Coetzee *et al.*, 2006).

As stated above, the free acid layer of phosphoric acid determines the activity of the catalyst. Therefore in order to investigate the catalyst, the properties of the free acid layer should be understood. Since the free acid layer is entirely composed of phosphoric acid, the properties of phosphoric acid have to be investigated.

Phosphoric acid (H_3PO_4) is a triprotic acid, meaning that the dissociation of phosphoric acid occurs three times (Equation 2-3 to 2-5). For each successive disassociation, the equilibrium shifts less to the formation of H_3O^+ ($Ka_1 = 7.5\times10^{-3}$, $Ka_2 = 6.2\times10^{-8}$ and $Ka_3 = 2.14\times10^{-13}$). As the first dissociation constant is significantly larger than the last two, the acid strength is determined by the first dissociation constant (Kotz & Treichel, 1999).

$$H_3PO_4 + H_2O \leftrightarrow H_2PO_4^- + H_3O^+ \qquad 2\text{-}3$$

$$H_2PO_4^- + H_2O \leftrightarrow HPO_4^{-2} + H_3O^+ \qquad 2\text{-}4$$

$$HPO_4^{-2} + H_2O \leftrightarrow PO_4^{-3} + H_3O^+ \qquad 2\text{-}5$$

Generally the activity of a catalyst is stated in terms of the equivalents of H^+. For this reason, the degree of dissociation is a measure of the activity. This is not so simple for phosphoric acid, because phosphoric acid condenses to form stronger acids, e.g. ortho phosphoric acid (H_3PO_4) → pyro phosphoric acid ($H_4P_2O_7$, Equation 2-6) → tri phosphoric acid ($H_5P_3O_{10}$, Equation 2-7), etc. For pyro phosphoric acid, ($H_4P_2O_7$) the first and second dissociation constants are 1.4×10^{-1} and 3.2×10^{-2} respectively, which are much larger than that of ortho phosphoric acid. This indicates that the more condensed the acid, the stronger the resulting acid (Weast, 1988).

$$2H_3PO_4 \leftrightarrow H_4P_2O_7 + H_2O \qquad 2\text{-}6$$

$$H_3PO_4 + H_4P_2O_7 \leftrightarrow H_5P_3O_{10} + H_2O \qquad 2\text{-}7$$

Since phosphoric acid can condense, it is not easy to describe the condensed state of the phosphoric acid present in the free acid layer without analysing the free acid. The chemical composition of the phosphoric acid depends directly, on the quantity of water present in the free acid. Various methods are used to express the acid strength of the catalyst. One method of describing the acid strength is the fraction phosphorous oxide (P_2O_5). This started because of the production of various strengths of phosphoric acid by mixing P_2O_5 with water (Equation 2-3). Another method of expressing the acid strength is by means of the weight percentage H_3PO_4. Starting with pure ortho phosphoric acid, different acid strengths can be obtained by evaporating water from the mixture. Converting between the two methods is done by the stoichiometry of mixing P_2O_5 with water to form H_3PO_4 (Equation 2-8). The conversion factors used to convert between the two methods are shown in Table 2-3.

$$P_2O_5 + 3H_2O \leftrightarrow 2H_3PO_4 \qquad 2\text{-}8$$

Table 2-3: Unit conversion between % P_2O_5 and % H_3PO_4

Compound	Chemical Formula	Molar weight [kg/kmol]	P_2O_5 [wt. %]	H_3PO_4 [wt. %]
Phosphorous pentoxide	P_2O_5	142	100	138
Ortho phosphoric acid	H_3PO_4	98	72.4	100

This still does not describe the condensed form (i.e. ortho/pyro) in which phosphoric acid will be present, it only describes the fraction of P_2O_5 and water in the acid. Jameson (1959) established how the condensed state of phosphoric acid changes by mixing P_2O_5 with water, the dependence of the acid distribution with the fraction of P_2O_5 in the mixture is shown in Figure 2-2. Below 68% P_2O_5 the acid mixture shifts completely to ortho phosphoric acid, changing to more condensed acids as the water fraction in the phosphoric acid decreases.

For the evaporation of a mixture of phosphoric acid and water, a vapour-liquid equilibrium will ensue, altering the water (or phosphoric acid content) of the liquid which will then influence the acid strength of the phosphoric acid. Brown & Whitt (1952) determined the phase equilibria for various mixtures of P_2O_5 and water (Figure 2-3). At temperatures below 300 °C phosphoric acid's vapour pressure becomes negligible and the vapour phase will contain mostly water. Increasing the temperature above 300 °C will therefore result in the evaporation of phosphorous from the catalyst.

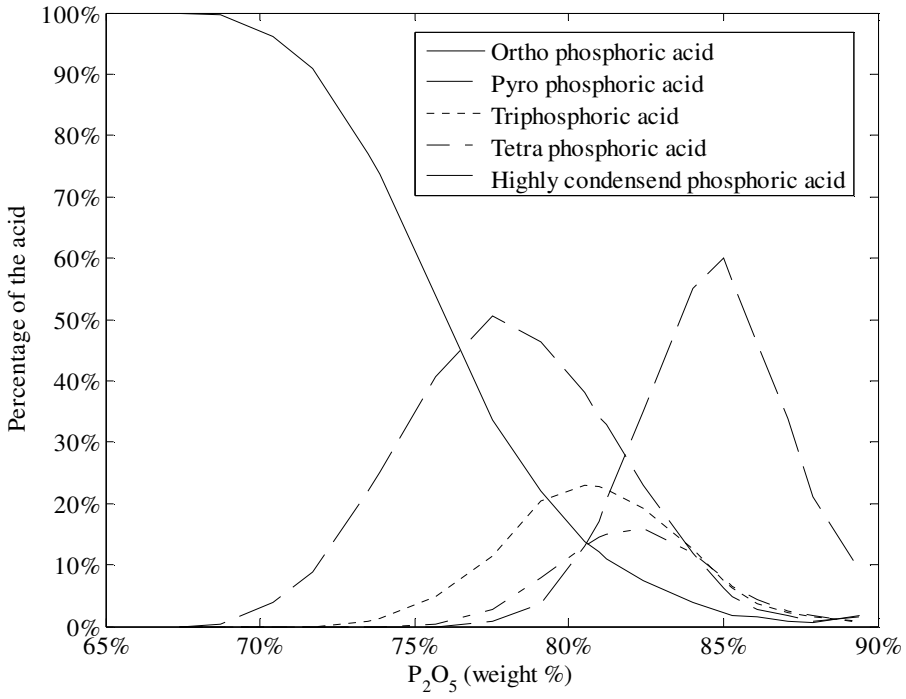

Figure 2-2: Distribution of phosphoric acid as a function of P_2O_5 content (Jameson, 1959).

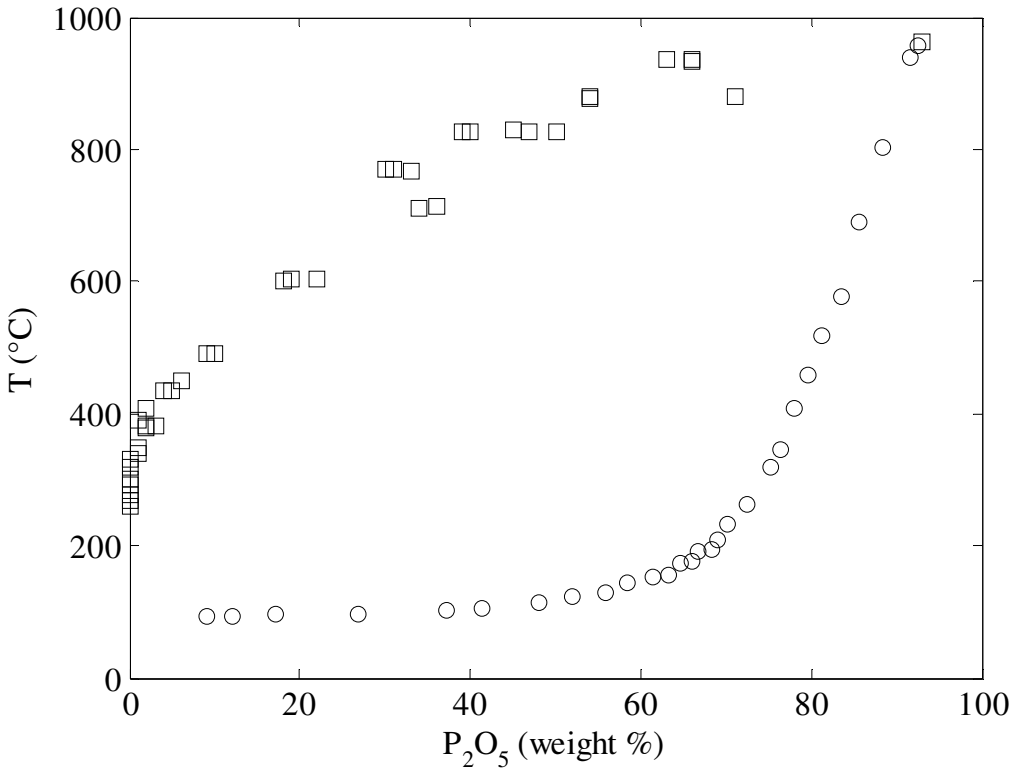

Figure 2-3: Vapour liquid equilibrium for liquid phosphoric acid (Brown & Whitt, 1952).

If the liquid phosphoric acid is however heated over an open flame at 200 °C time is not given for phase equilibrium to establish (shown in Figure 2-4).

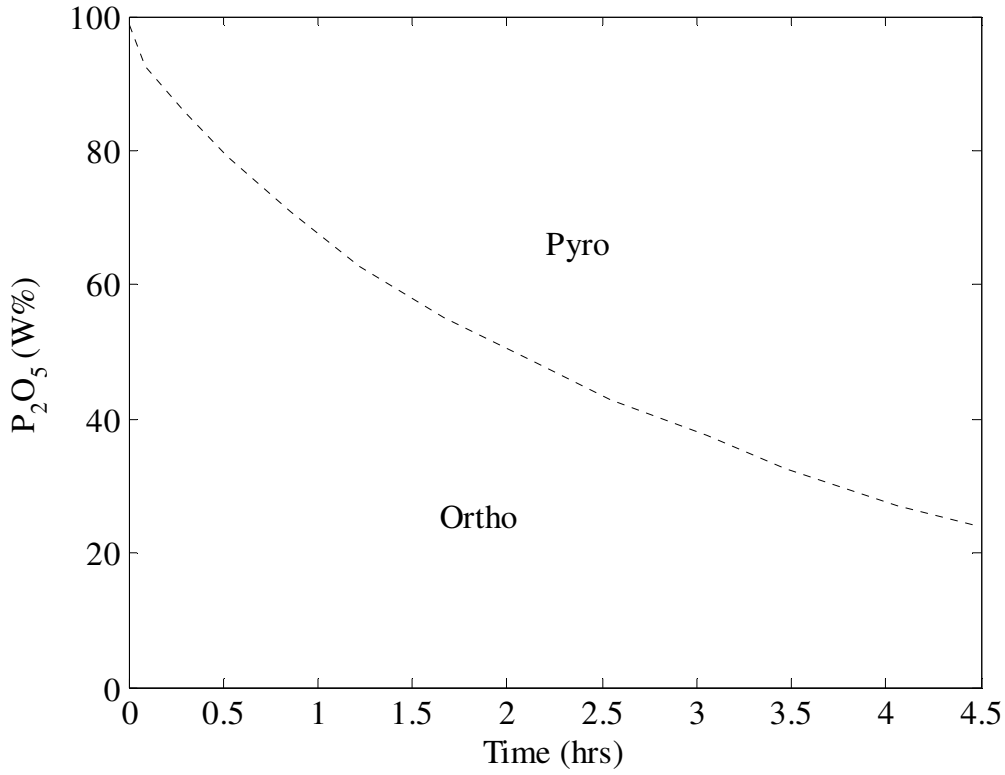

Figure 2-4: Acid distribution with time when heating liquid phosphoric acid over and open flame at 200 °C (Ohtsuka & Aomura, 1962).

If SPA, instead of liquid phosphoric acid, is rather heated in a muffle furnace it seems that the acid distribution evens out dependent on the type of support used, the distribution obtained for the heating of SPA composed of either Makkari kiezelguhr, Okayama kiezelguhr or Celite kiezelguhr is shown in Figure 2-5. If an equilibrium distribution was obtained at 200 °C the phosphoric acid strength would 70.5 W% P_2O_5, from the ortho - to pyro phosphoric distribution shown in Figure 2-5 it seems that the acid strength would equal 74.5%, 73% and 72% respectively. This stable acid distribution is quite close to what was measured by Brown and Whitt (1952) as the equilibrium distribution of the phosphoric acid which suggests that the free acid supported on the kiezelguhr support reaches a pseudo equilibrium distribution within the pores of the catalyst.

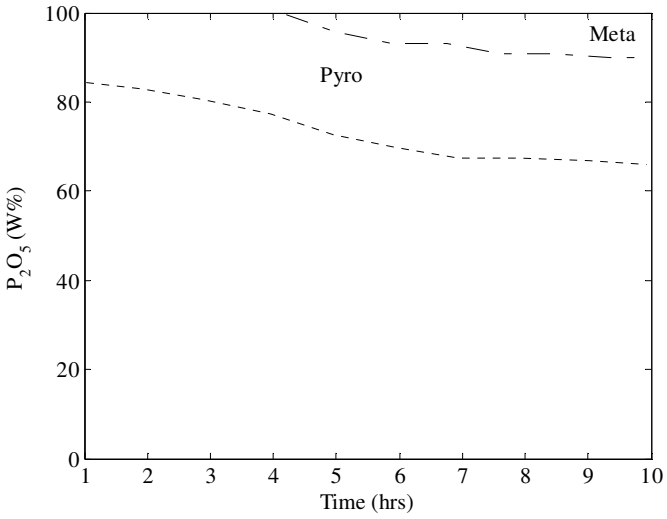

a)

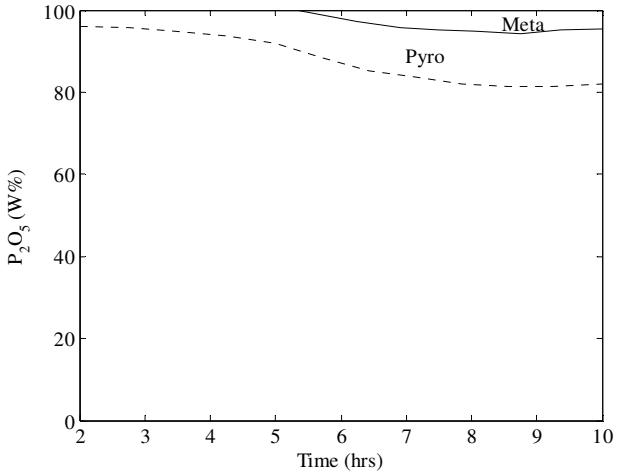

b)

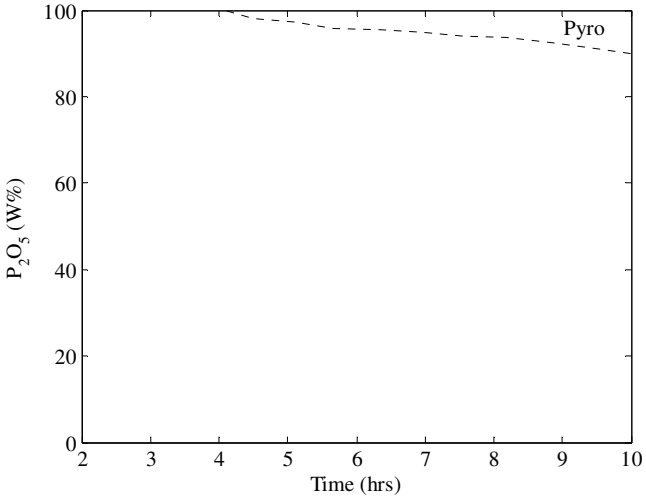

c)

Figure 2-5: Acid distribution over various kiezelguhr supports when heated in a muffle furnace at 200 °C

In short, the acid strength of the catalyst and the subsequent distribution of phosphoric acids are predominantly determined by the fraction of water present in the free acid layer. How the acid strength of the catalyst affects the activity of the catalyst is an altogether different matter.

2.5 Catalyst hydration

It is accepted that water inhibits the activity of solid acid catalysts (Okuhara, 2002). Generally this inhibition is due to the selective adsorption of water onto the acid site, effectively eliminating the active site from taking part in the reaction. Water is known to influence a phosphoric acid in various ways, *1)* blocking of active sites by selective adsorption onto the active sites, *2)* decreasing the activity of the catalyst by diluting the acid or *3)* improving the activity of the catalyst by liberation of free acid from the catalyst support (Makatun *et al.,* 1985).

For solid phosphoric acid, water is part of the free acid and will influence the distribution of phosphoric acid. As to how water will affect the reaction rate, remains indefinite. Work done by Skupińska (1991) indicates that the conversion of propene will increase with the adsorption of water onto the catalyst, whereas Cavani *et al.* (1993) state that an increased quantity of water in the feed significantly inhibits the oligomerisation rate of propene over SPA. The inhibition was found to be prominent only where the free acid content was larger than 20% (weight %), for free acid concentrations lower than 20%, the liberation of fixed phosphoric acid on the catalyst support (silicon phosphates) to the free acid layer occurs. This increases the total free acid concentration resulting in an increase in catalytic activity. According to Cavani *et al.* (1993) the inhibiting effect of increased hydration levels is believed to be twofold. Firstly, SPA is extremely hydrophilic, flooding the pores when excess water is present in the reaction mixture and restricting access to the catalytically active sites and secondly, by altering the phosphoric acid distribution (Figure 2-2). An increase in catalytic activity was also noted by Langois and Walkey (1952) when using a dry feed to the reactor for phosphoric acid impregnated on quarts.

Some water however needs to be present for catalytic activity. Deeter (1950) indicated that initial activity of a *properly* hydrated catalyst to be higher than that of a under hydrated catalyst. Therefore to control the activity of the catalyst both temperature and water need to be controlled.

Water does not only influence the activity of the catalyst but can also effect the life time, Weinert and Egloff (1948) stipulated that water is needed in the reactor feed to prevent the catalyst from becoming dehydrated. Over hydration of the catalyst results in the softening of

the catalyst, leading to the plugging of the reactor bed, whereas under hydration will result in coke formation. Over hydration will also result in leaching phosphoric acid from the catalyst which will result in corrosion of the reactors (Egloff and Welnert, 1951), further emphasizing the importance of hydration control over the reactor.

For cases where oxygenates are present in the reactor feed, as is the case for feed produced from high-temperature Fischer-Tropsch, it has been shown that the oligomerisation is significantly inhibited. This is especially true for the oligomerisation of the C_5-C_6 cut which contains a large fraction of oxygenates (3 weight %). When oligomerising 1-hexene the addition of various oxygenates to the reaction mixture inhibits the oligomerisation as well as the rate of isomerisation over SPA (De Klerk *et al.*, 2007). The inhibition of the oligomerisation rate is largely attributed to the formation of water which form from the dehydration of oxygenates. This decreases the acid strength of the free acid, resulting in the decreased activity of the catalyst (Mashapa and De Klerk, 2007).

Prinsloo (2006) showed an increased propensity toward the production of distillate range products from the oligomerisation of propene with an increase in the acid strength of the free acid. A maximum in the distillate selectivity occurs at an acid strength of 108% H_3PO_4 (78% P_2O_5, Figure 2-2) where the pyro phosphoric acid is at a maximum. Thereafter a drop in the diesel selectivity was observed. The propylene conversion was also seen to increase as the acid strength increased. The maximum observed in the selectivity, at an acid strength of 108% H_3PO_4, was not seen for conversion. The conversion increased up to 108% H_3PO_4 and then flattened out. The flattening out of activity at higher acid strengths was also noted by Ohtsuka and Aomura (1962), which attributed this to the formation of meta phosphoric acids (highly condensed phosphoric acids). This suggests that pyrophosphoric acid mostly controls the activity of phosphoric acid.

However, it is not so easy to determine the phosphoric acid distribution of the free acid supported on the kiezelguhr, as given by Jameson (1959) for liquid phosphoric acid (Figure 2-2), since the acid is supported on the catalyst and extracting the liquid acid without altering the acid distribution is difficult (Cavani *et al.*, 1993).

The quantity of free acid is usually determined by the addition of an excess of water to the catalyst, which results in the leaching of the free acid from the catalyst support. If the contact time is too long, fixed acid (silicon phosphates) will also desorb, giving an inaccurate representation of the free acid fraction (Cavani *et al.*, 1993; Coetzee *et al.*, 2006). The titration of the water liquor will indicate the quantity of hydronium ions due to the complete hydrolysis of stronger acids to ortho phosphoric acid (Equations 2-6 and 2-7). Therefore the

titration will only indicate the quantity of ortho phosphoric acid present in the free acid, not the form of the phosphoric acid (ortho/pyro).

Zhirong *et al.* (2000) used ion chromatography to determine the distribution of ortho and pyro phosphoric acid in the free acid. In the end, these researchers could not report any definite trend between the total quantity of free acid and the catalytic activity towards propene oligomerisation, but it was shown that with an increase in the pyro phosphoric acid content (i.e. less water), the conversion of propylene increased (Figure 2-6) further advocating increased activity with increased acid strength.

De Klerk *et al.* (2006) investigated the effect of operating conditions on the oligomerisation of butene over liquid phosphoric acid. The investigation focused on gaining an idea of the influence of acid strength and temperature on the degree of branching of the C_8 olefins as well as the gasoline-to-distillate ratio (gasoline was taken as all compounds boiling lighter than 175 °C). It was found that as acid strength and temperature decreased, the degree of branching of the product as well as the gasoline production increased, (see Figure 2-7 *a)*, which suggest that the optimum operating condition for gasoline production would be at a high hydration (low acidity) of the catalyst and a low temperatures.

It was suggested that both high temperature and high acid strength would result in a greater likelihood of the cracking of branched product, which would decrease the gasoline quality (De Klerk, 2006b). With the increased distillate ratio at higher acid strengths and higher temperatures, Figure 2-7 *b)*, the increased activity of the catalyst results in the formation of more trimer product (C_{12}s, boiling point 214 °C). Therefore the decreased gasoline quality at these conditions could be due to the greater reactivity of the branched C_8 olefins, selectively reacting with shorter chain olefins toward the formation of diesel range products.

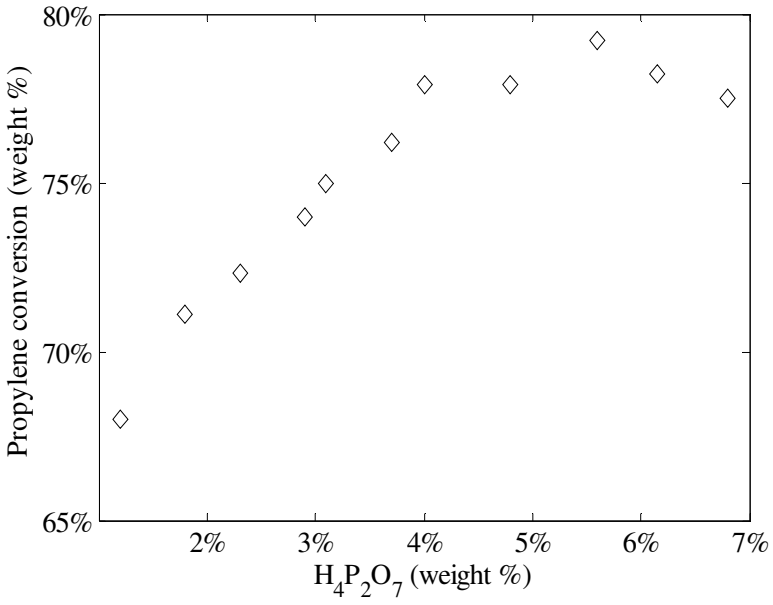

Figure 2-6: The effect of $H_4P_2O_7$ (wt %) on the conversion of propylene (Zhirong *et al.*, 2000).

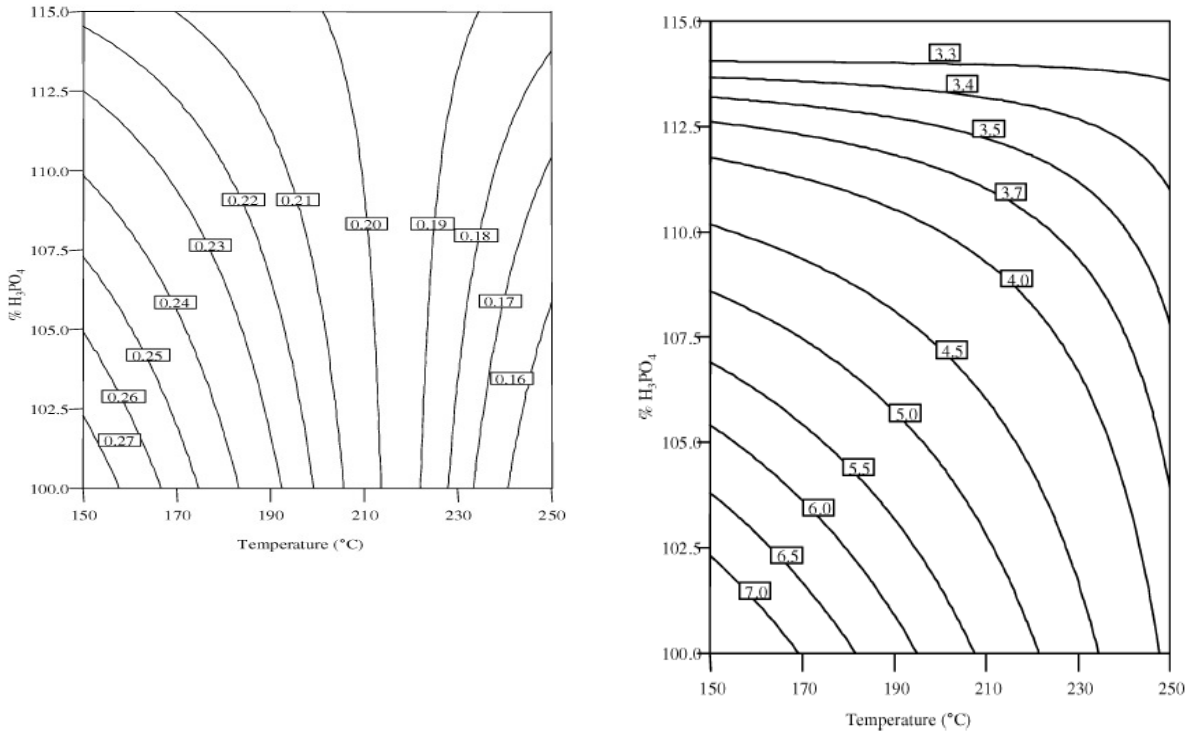

a) b)

Figure 2-7: Effect of acid strength and temperature on *a)* degree of branching of C_8 olefins and *b)* gasoline-to-distillate ratio for C_4 oligomerisation, for a constant residence time, over liquid phosphoric acid (De Klerk *et al.*, 2006).

The increase in activity with increase in acid strength is corroborated in one of the first articles studying the effect of acid strength on the rate of oligomerisation of propene using liquid phosphoric acid as catalyst. Bethea & Karchmer (1956) approximated the rate of oligomerisation of propylene for various acid strengths of the catalyst. When the acid strength was increased, the first order rate constant increased exponentially with the increase in acid strength, Figure 2-8. This increase in the reaction rate was also seen by Monroe and Gilliland (1938) for the oligomerisation of propene over dilute liquid phosphoric acid, where the reaction rate was found to be proportional to the square of the propene partial pressure, the volume of acid and the acid strength of the catalyst.

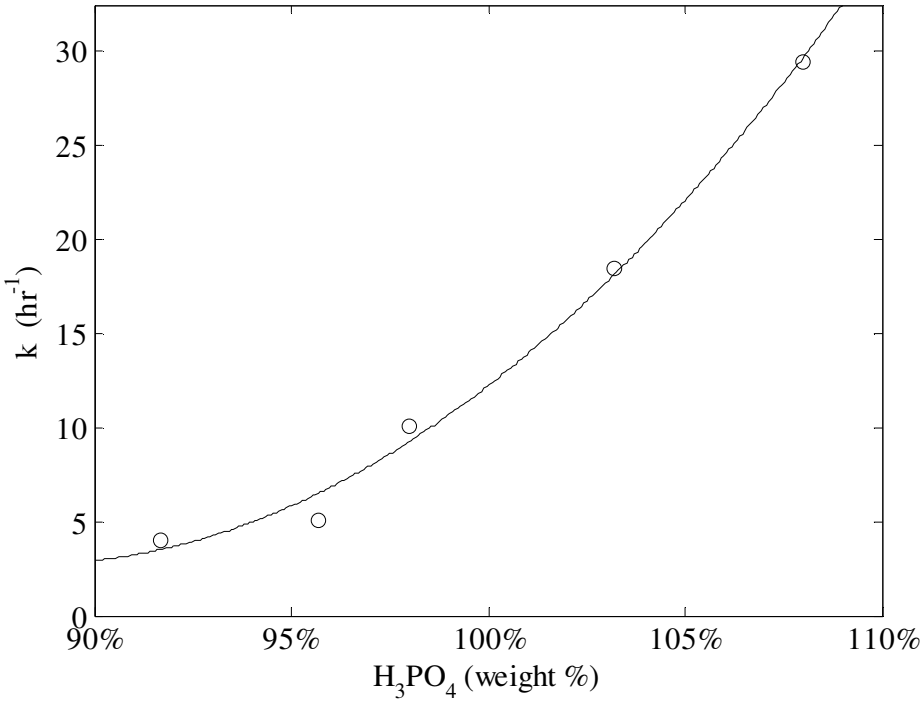

Figure 2-8: Effect of acid strength on the rate constant of Bethea & Karchmer (1956).

Therefore, the reaction rate over phosphoric acid is exponentially dependent on both the reaction temperature and the acid strength of the phosphoric acid, Figure 2-9. From the Arrhenius trend it seems that the activation energy also increases with an increase in acid strength. No attempt was made to integrate the acid strength effect with the rate constant or to relate the conversion of propylene to the resulting product. It was noted, however, that as the acid strength increased, the selectivity of the oligomerisation changed from predominantly trimerisation (C_9) to tetramerisation (C_{12}). At an acid strength of 92% H_3PO_4 the ratio of

C_9:C_{12} was 2.33:1 whereas at an acid strength of 109% H_3PO_4 the ratio changed to 1:1.56, as would be expected for a sequential reaction at increased activity of the catalyst.

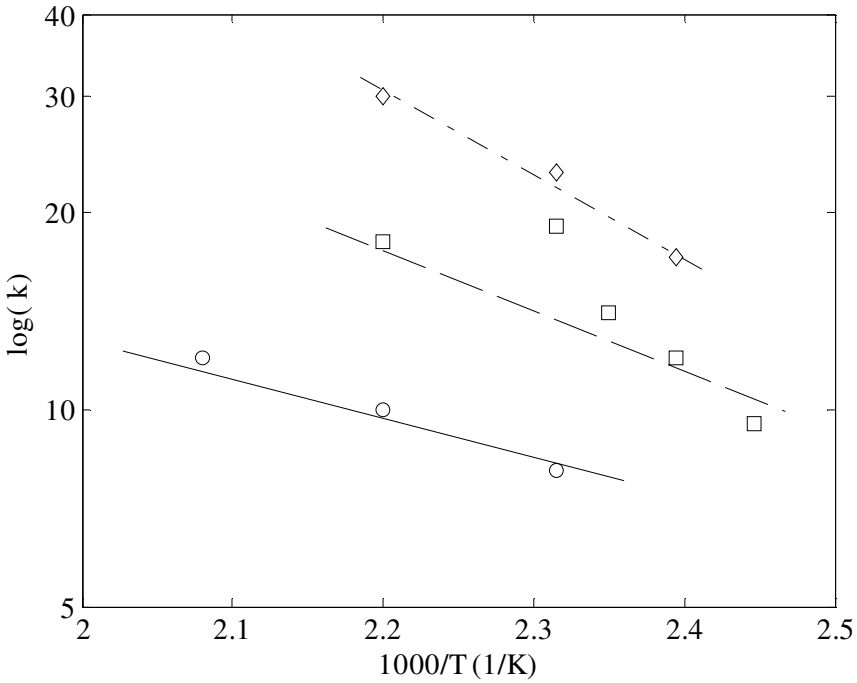

Figure 2-9: Effect of acid strength on the rate constant, ○ – 98% H_3PO_4, □ – 103% H_3PO_4, ◊ - 109% H_3PO_4 (Bethea & Karchmer , 1956).

As to how quickly the phosphoric acid stabilizes upon the introduction of water to the reaction system, Vinnik and Obraztsov (1983) showed that the introduction of water to the reactor reduces the catalytic activity but recovers to initial activity within minutes.

Fairly little work has been done in the literature on modelling the effect of acid strength on the reaction rate. The only attempt that could be found was in the doctoral thesis of McClean (1987) while modelling the rate of oligomerisation of C_3 and C_4 olefins. It was noted that when there was an increase in acid strength, the rate of oligomerisation increased. This was compensated for by adapting the rate constant as shown in Equation 2-9. However, when the model was applied to experimental data to characterise the influence of acid strength, negative activation energies ensued.

$$k_x = k_o e^{-\frac{E}{T}} .[\%H_3PO_4/100]^y \qquad 2\text{-}9$$

Conflicting arguments are present in the literature concerning the effect of water on the reaction rate and the product selectivities. Mostly the literature have focused on drawing trends based on hydration variations at a constant space velocity without taking the reaction progression into account. A kinetic evaluation of the effect of hydration would be instrumental to closing the loop to the effect of hydration on oligomerisation over SPA.

2.6 Reaction mechanism/network

When modelling the reaction kinetics for the oligomerisation of an olefin, various routes or products are plausible. The reaction mechanism/network defines these routes a reagent can follow from possible intermediates to the formation of the products, but does not delve into rate difference between these routes. For kinetic modelling the rate difference between these intermediates are critical toward predicting the formation of the desired product. This is especially true if the feed contains the different intermediates present in the reaction network.

This is true for a feed present in a petrochemical refinery. Even though mostly olefins and paraffins are present in the feed, a variety of reactions can occur in series and/or parallel, namely double bond shift, skeletal isomerisation, cracking, disproportionation and cyclisation, Figure 2-10. Since each of these reactions is important to the quality of the produced fuel, choosing the catalyst and operating conditions is critical. Over SPA all of the previously mentioned reactions occur. Cracking is limited to olefins with a carbon number greater than seven at temperatures below 275 °C (De Klerk, 2005b), this is quite important for this investigation since when oligomerising 1-hexene cracking of the feed can be excluded from the reaction scheme. Below 200 °C only acyclic mono olefins are evident (De Klerk, 2006b) with paraffin formation becoming more likely bove 300 °C (Skupińska, 1991). The scope of this study covers only isomerisation, oligomerisation and cracking of the olefin feed.

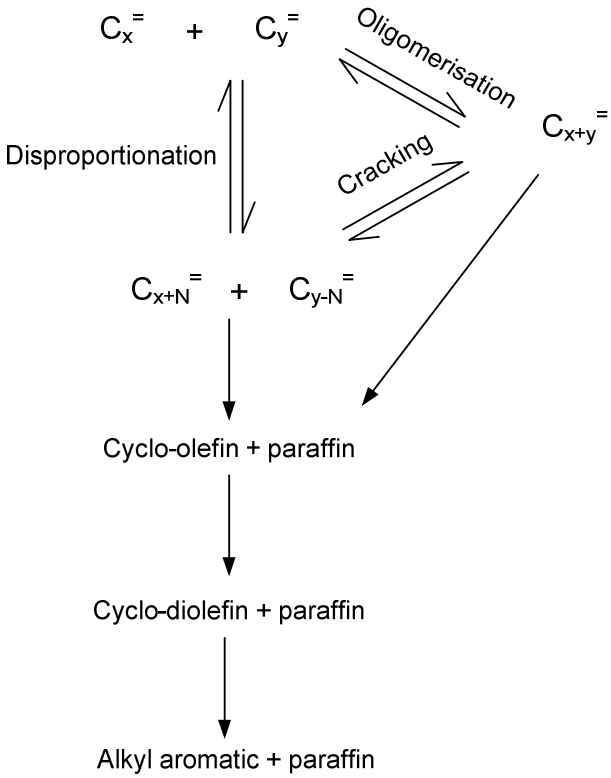

Figure 2-10: Various reactions that can occur during the oligomerisation of two olefins (Quan *et al.*, 1988).

One of the differences in the oligomerisation of olefins over phosphoric acid, is the difference in the reaction mechanism. Usually oligomerisation is assumed to occur through the classic carbocation mechanism, whereas for phosphoric acid oligomerisation occurs through a phosphoric acid ester intermediate.

2.6.1 Classic carbocation mechanism

When an acid catalyst is used for the oligomerisation of olefins, it is usually assumed that a carbocation mechanism prevails (Figure 2-11). The stability of the carbocation intermediate dictates the differences in reactivity, methyl and hydrogen migration and product selectivity. With increased substitution, the carbocation intermediate becomes more stable and therefore the reactivity increases (McMurry, 2000).

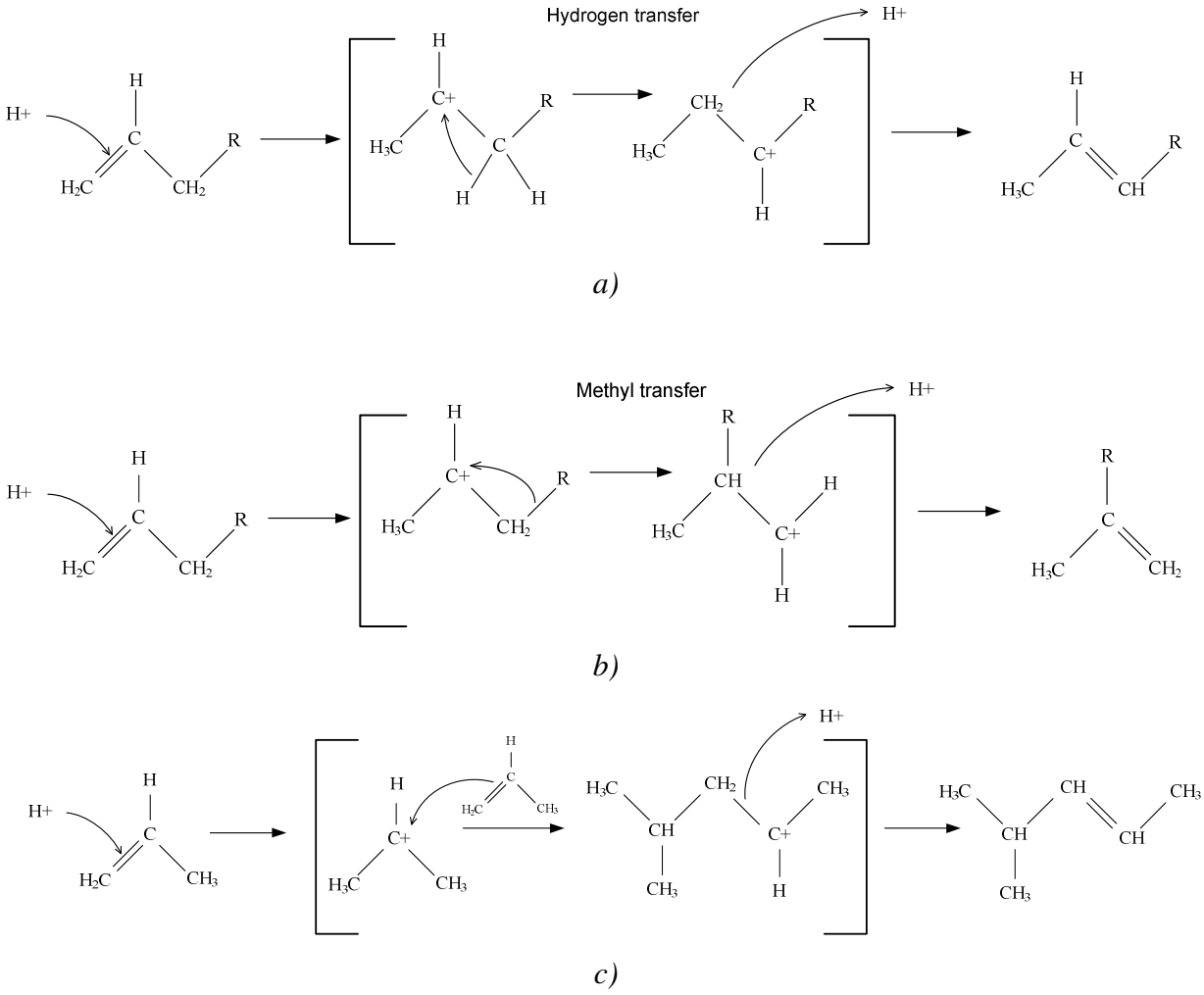

Figure 2-11: Classic oligomerisation carbocation mechanism for *a)* double bond isomerisation, *b)* skeletal isomerisation and *c)* oligomerisation.

2.6.2 Phosphoric acid ester mechanism

The formation of an ester intermediate is not limited to phosphoric acid, and has also been seen for the oligomerisation of alkenes over sulphuric acid (Schmerling and Ipatieff, 1950). Several authors in the literature propose that oligomerisation over SPA occurs through an ester intermediate (Ipatieff, 1935; Schmerling and Ipatieff, 1950; De Klerk, 2006b; Mashapa and De Klerk, 2007). The ester intermediate was first seen by Ipatieff (1935) who heated liquid phosphoric acid and an olefin in an autoclave at 10 atm. At low temperatures a single layer was present in the autoclave, this layer was found to be the phosphoric acid ester. When the mixture was heated the liquid dissolved into two layers (phosphoric acid and the olefin). Ethyl phosphoric acid ester was found to be stable up to 200 °C, whereas propyl phosphoric

acid ester was stable up to 125 °C. This suggests a temperature barrier that has to be overcome to destabilise the phosphoric acid ester before the oligomerisation reaction can occur (De Klerk *et al.,* 2004) and that the stability of the phosphoric acid ester drops with an increase in the chain length of the olefin. The stability of the ester is also dependent on the degree of branching of the olefin, owing to the increased rate of oligomerisation of branched octenes (De Klerk, 2006b).

Before oligomerisation can take place an ester is formed between the olefin and the liquid phosphoric acid, Figure 2-12 (Ipatieff, 1935).

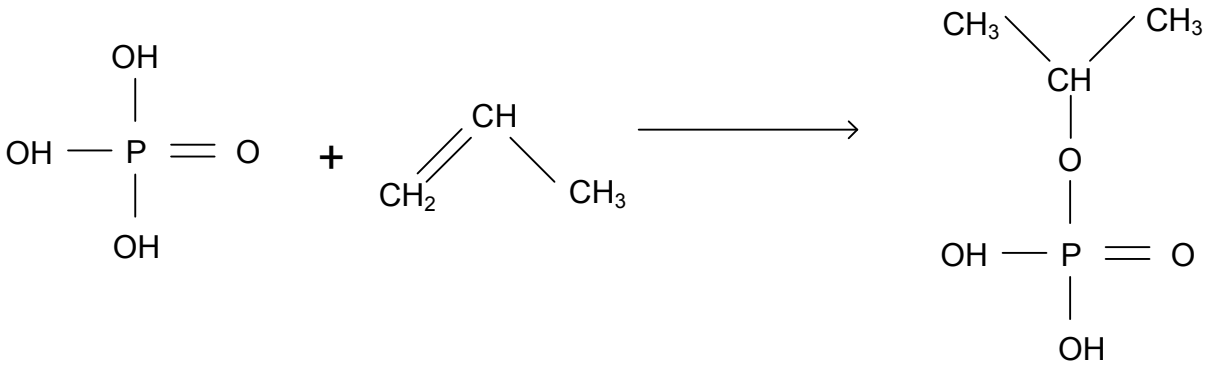

Figure 2-12: Phosphoric acid mechanism (Ipatieff, 1935)

Oligomerisation can then take place by either *1)* an ester reacting with an olefin, Figure 2-13 *a)* or *2)* by two esters reacting with each other to form a hexene isomer, Figure 2-13 *b)* (Schmerling and Ipatieff, 1950).

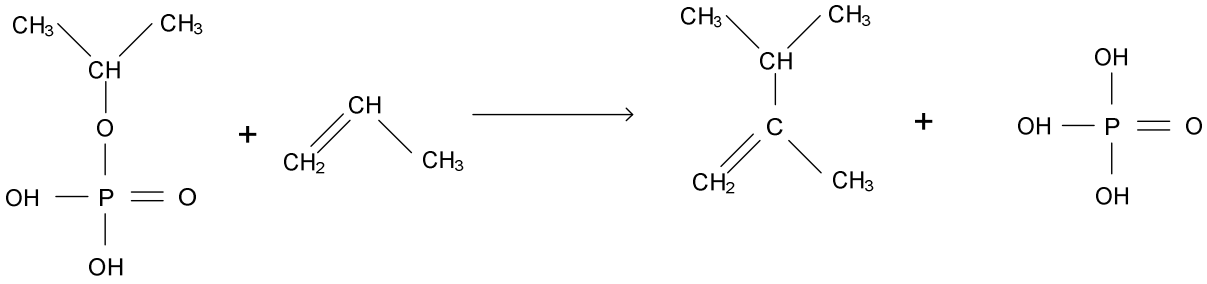

a)

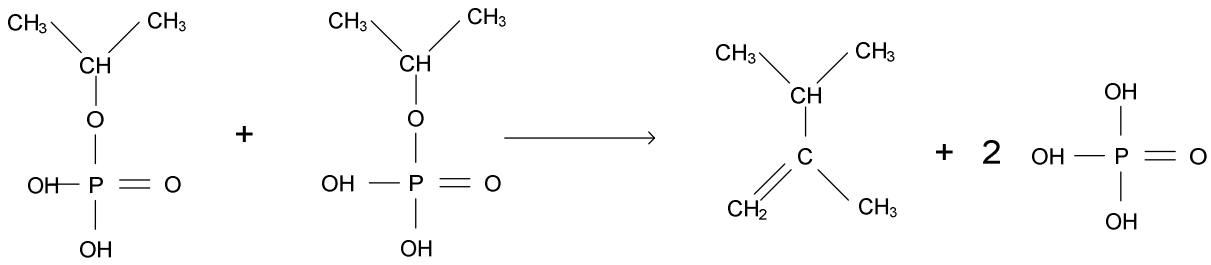

b)

Figure 2-13: The ester mechanism for a) one olefin reacting with an olefin or b) two esters dimerising.

Farkas and Farkas (1942) proposed that the formation of the phosphoric acid intermediate with the olefin by taking up hydrogen or by donating one hydrogen atom (Figure 2-14). This describes the route the molecule follows to the product as well as the stability of the intermediate, which could result in different activation energies dependent on the formed intermediate.

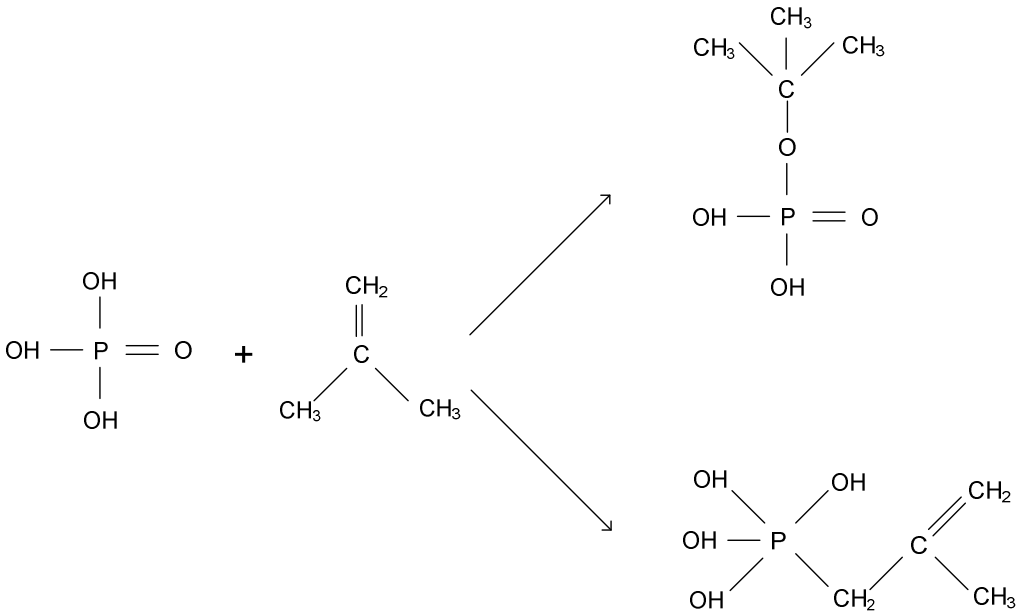

Figure 2-14: Reaction mechanism as proposed by Farkas and Farkas (1942).

Double bond shift and skeletal isomerisation both occur through the phosphoric acid intermediate, Figure 2-15 (De Klerk, 2006b). The presence of iso-butene and highly branched oligomerised product, for the oligomerisation of 1-butene at low temperatures (130 °C), indicates that SPA is adept at the isomerisation of olefins. SPA has also been shown to be capable of the skeletal isomerisation of longer chain olefins with the isomerisation of 1-hexene at elevated temperatures, 285-500 °C and atmospheric pressure (Hay *et al.*, 1945).

This ability of SPA to isomerise olefins, even at low temperatures, is advantageous to the production of gasoline, due to the increased RON value of highly branched paraffins.

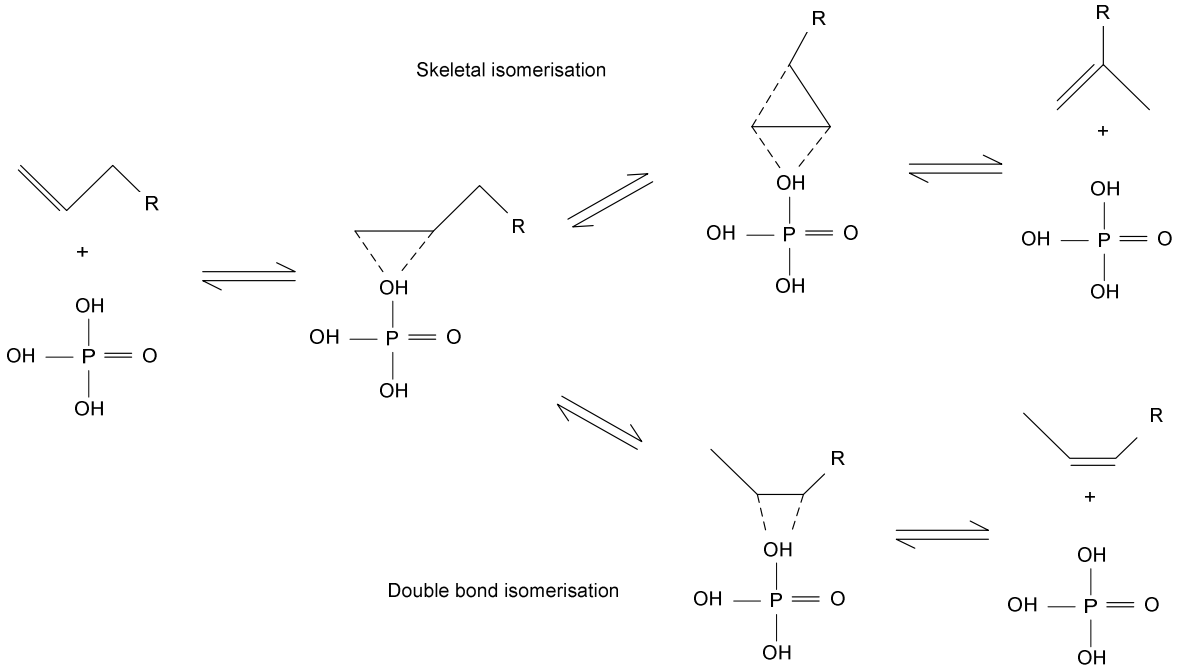

Figure 2-15: Phosphoric acid ester mechanism for skeletal and double bond isomerisation.

Since double bond -, skeletal isomerisation and oligomerisation can occur through both the carbocation and the ester mechanism the reaction route followed for both mechanisms are similar. The difference between the two would be the relative activation energies needed to model the reaction rate, since no previous kinetic parameters are available for 1-hexene oligomerisation over either catalyst no comparison is possible for the activation energies.

2.7 Kinetic modelling of oligomerisation over acid catalyst

Kinetic modelling of the reaction rate over SPA focused on the rate of oligomerisation of short chain olefins, these include the work done by Paynter & Schuette (1971), Friedman & Pinder (1971), Cao *et al.* (1988) and the doctoral thesis of McClean (1987). For other acid catalysts the literature is more prominent (Alcántara *et al.*, 2000; Honkela *et al.*, 2003; Honkela *et al.*; 2004 Cruz *et al.*, 2007;).

The oligomerisation of short chain olefins over and acid catalyst is mostly with the intent of producing petrol, therefore precautions have been taken to limit the extent of the oligomerisation, especially for the selective production of highly isomerised octenes from iso-butene. Over sulphonic cation exchange resins, the oligomerisation of iso-butene can run

away easily to form trimer and tetramer product at mild operating conditions, 100 °C and 94 kPa (Alcántara *et al.*, 2000). Although oligomerisation over a cation exchange resins follows the classical Brønsted mechanism, the increased reaction rate noticed for iso-butene with respect to the rate seen for linear butenes also holds true for SPA (McClean, 1987). Therefore the higher reactivity of skeletal isomers is valid for both traditional Brønsted acids and SPA. For cation exchange resins, one method which has been used to limit the extent of the oligomerisation is the addition of alcohols to the reactor feed. This limits the oligomerisation to a gasoline-range product and the formation of ethers which is beneficial to the octane of the resulting fuel (Di Girolamo *et al.*, 1997; Cruz *et al.*, 2007; Honkela *et al.*, 2003). The addition of ethers to the gasoline pool has been met with some concern, however, due to the contamination of ground water. For this reason, oxygenates that do not participate in the oligomerisation reaction have been used to limit the extent of oligomerisation, such as tertiary butyl alcohol (TBA) (Honkela *et al.*, 2003; Honkela *et al.*, 2004).

The use of oxygenate compounds as well as branched short chain olefins decreases the amount of possible products by negating the possibility of isomerisation. It is necessary to account for the differences in the adsorption selectivity between the oxygenates and olefins to adequately model the reaction rate. This is done by applying Langmuir-Hinshelwood adsorption to the reaction kinetics, as shown in Equation 2-10 for the dimerisation of iso-butene (IB).

$$r_{Dimerisation} = \frac{k_{Dimerisation} K_{IB}^2 \alpha_{IB}^2}{\left(K_{IB}\alpha_{IB} + K_{ITBA}\alpha_{TBA} + K_{Dimer}\alpha_{Dimer} + K_{Trimer}\alpha_{Trimer}\right)^2} \qquad 2\text{-}10$$

The reaction network, with regard to the amount of possible dimer products, grows considerably for the oligomerisation of a C_5 olefin, Figure 2-16. To simplify the reaction network, lumping of the products and reagents ensues. This simplifies the modelling of the reaction network for C_5 oligomerisation. If however a more thorough depiction of the reaction products is needed, especially when the fuel properties are highly sensitive to the composition of the product, a more complicated reaction network will result. Such is the case when modelling the rate of oligomerisation for methyl-butene, where 11 reaction constants are needed to describe the reaction network (Cruz *et al.*, 2007). Validating each of the kinetic parameters would require a great deal of experimental work with a detailed analysis of the product, which is not always a viable option. For instance, if the reaction network was rather

completed for 1-pentene, skeletal isomerisation would need to be incorporated in the reaction route, as well as the dimerisation and co-dimerisation of all the pentene isomers. This would result in a dramatic increase of the reaction network depicted below.

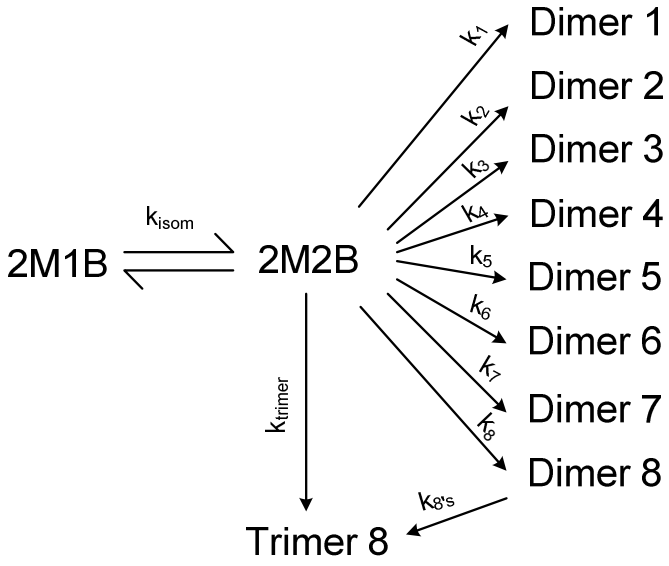

Figure 2-16: Reaction network for the oligomerisation of 2-methyl-1-butene (2M1B).

Although the increased reactivity of iso-butenes (and selectivity to highly branched petrol) have been noted for SPA oligomerisation using a FT derived feed (De Klerk *et al.*, 2004), the addition of oxygenates to limit the reaction rate of iso-butene has not been investigated due to the negative impact of oxygenates on the reaction rate over SPA (De Klerk *et al.*, 2007). Although using TBA for oligomerisation over SPA to limit the reaction rate and increase the selectivity to high RON petrol could be useful if a high fraction of iso-butene is present in the feed.

Considering that the oligomerisation of short chain olefins have been practised for some time over SPA, fairly little has been done to model the kinetics involved in the reaction. The models have also relied extensively on the lumping of species to minimise the number of parameters needed in the kinetic model. In 1971 the first attempts at modelling the oligomerisation of an olefin mixture over SPA were made, firstly by Friedman & Pinder (1971) and secondly by Paynter & Schuette (1971). Friedman & Pinder (1971) used a second order kinetic model to approximate the rate at which propene disappeared from the reaction mixture. Only an apparent rate constant was modelled as internal mass transfer was evident.

Paynter & Schuette (1971) made the first attempt at using kinetics to describe the resulting product distribution from the oligomerisation of propenes and n-butenes over SPA, as can be seen in Equations 2-11 to 2-18. Due to selectivity differences between 1-butene and 2-butene,

the reactivity of the two isomers was split, but the formation of olefins larger than C_9 was grouped under a lumped rate constant. Paynter & Schuette (1971) gathered their experimental data at mild operating conditions (115°C), this ensured that only oligomerisation needed to be modelled since at these low temperatures cracking did not occur. The reactivity difference with increased chain length was determined to be $k_2 > k_1 > k_4 > k_3 > k_5$. This suggests that the co-dimerisation of C_3 and C_4 olefins occur the fastest, followed by C_3 oligomerisation and then by C_4 oligomerisation.

$$2\,C_3 \xrightarrow{k_1} C_6 \qquad \text{2-11}$$

$$C_3 + C_{4,1} \xrightarrow{k_2} C_7 \qquad \text{2-12}$$

$$C_3 + C_{4,2} \xrightarrow{k_3} C_7 \qquad \text{2-13}$$

$$2\,C_{4,1} \xrightarrow{k_4} C_8 \qquad \text{2-14}$$

$$2\,C_{4,2} \xrightarrow{k_5} C_8 \qquad \text{2-15}$$

$$\left(C_3 + C_{4,1} + C_{4,2}\right) + \left(C_6 + C_7 + C_8\right) \xrightarrow{k_6} C_{9+} \qquad \text{2-16}$$

$$C_{4,1} \xleftrightarrow{k_7} C_{4,2} \qquad \text{2-17}$$

$$3C_3 \xrightarrow{k_8} C_{9+} \qquad \text{2-18}$$

Cao *et al.* (1988) expanded on the kinetic model proposed by Paynter & Schuette (1971) who lumped all olefins larger than C_9 under the same reaction constant. For this reason a limited perspective of the product can be formulated from the reaction network/model. Coa *et al.* (1988) proposed a kinetic model that could differentiate between the product chain lengths. For the sake of simplicity, the reagents were lumped based on the chain length with an added parameter for the isomerisation of the olefin to a non-reactive olefin (irreversibly). It was also assumed that the rate of isomeriserisation was independent of the chain length of

the olefin that was isomerised. Due to the low temperature of the investigation, cracking could still be ignored. A kinetic parameter ρ_n was used to approximate the reactivity of a lumped olefin chain length. The reactivity between two olefins was then taken as the product of the individual reactivities ($\rho_n.\rho_m$). The resulting kinetic expression used is shown in Equations 2-19 to 2-21.

$$2C_{n,1} \longrightarrow C_{2n,1}; r = p_n{}^2 C_{n,1}{}^2 \qquad 2\text{-}19$$

$$C_{n,1} \longrightarrow C_n; r = k_{iso} C_{n,1} \qquad 2\text{-}20$$

$$C_{n,1} + C_{m,1} \longrightarrow C_{n+m,1}; r = 2 p_{n,1} p_{m,1} C_{n,1} C_{m,1} \qquad 2\text{-}21$$

Only olefins up to C_7 were taken as being likely to oligomerise with the maximum chain length formed limited to C_{14}. From the kinetic modelling, the reactivity of olefins was determined to be: $\rho_6 > \rho_3 > \rho_{4,1} > \rho_7 > \rho_{4,2}$. This is similar to the reactivity sequence given by Paynter & Schuette (1971). The high reactivity of C_6 olefins is questionable, since for the oligomerisation of C_3s over SPA, a high selectivity results in C_9 and C_{12} olefins (Table 2-4). If only dimerisation and co-dimerisation propene are assumed, the optimisation of the kinetic fit would inevitably result in a high reactivity of C_6 olefins, especially in the case of the reaction mechanism proposed by Coa *et al.* (1988). Furthermore the reactivity of C_6 was not validated by spiking hexene into the reaction mixture to investigate the reactivity of the olefin. Another possibility is the one-step trimerisation of C_3 to C_9, but this was not investigated by Coa *et al.*(1988).

Table 2-4: Product spectrum for varied conversion of pure propene from McClean (1987).

Conversion of propene	5%	13.7%	32.0%
Product concentration ($mol.l^{-1} \times 10^3$)			
Butene	0.0	0.0	0.0
Pentenes	0.0	0.0	0.0
Hexenes	0.3	2.0	4.7
Heptenes	0.0	0.2	0.7
Octenes	0.0	0.4	1.3
Nonenes	3.7	12.1	30.2
Decenes	0.1	0.3	1.3
Un-decenes	0.2	0.6	1.6
Do-decenes	1.5	3.6	11.0
> Do-decene	0.1	0.3	1.1

One investigation which used SPA and did look at the oligomerisation of hexene, was that of McClean (1987). The work focused on the oligomerisation of butene and propene and, to gain an understanding of the reaction mechanism over SPA, hexene was also oligomerised. The resulting reaction network is shown in Figure 2-17. Cracking was only observed for olefins longer than C_8. No cracking products shorter than C_4 olefins was observed.

A significant difference in reactivity was observed for the oligomerisation of butene and iso-butene, but no difference in reactivity was evident for the oligomerisation of different hexene isomers. The goal of the thesis of McClean (1987) was not to model the reaction rate of 1-hexene, but rather to model the reaction rate for C_3 and C_4 oligomerisation (hexene was used as to understand the reaction progression of propene). Although a rate difference was apparent for iso-butene this was not captured in the reaction model of butene oligomerisation. This could be a critical misrepresentation of the reaction mechanism since the product spectrum from butene oligomerisation (Bekker and Prinsloo, 2009) shows a significant fraction of branching in the product. As such isomerisation of butene is critical towards the reaction route followed and ultimately towards predicting the product quality. McClean (1987) modelled the reaction kinetics for the oligomerisation of pure propene and butene, with the dimerisation and co-dimerisation of multiples of propene and butene; cracked products formed from the cracking of C_{12} olefins were lumped. The resulting optimisation of

the kinetic parameters resulted in negative activation energies, leaving questions about the empirical nature of the model.

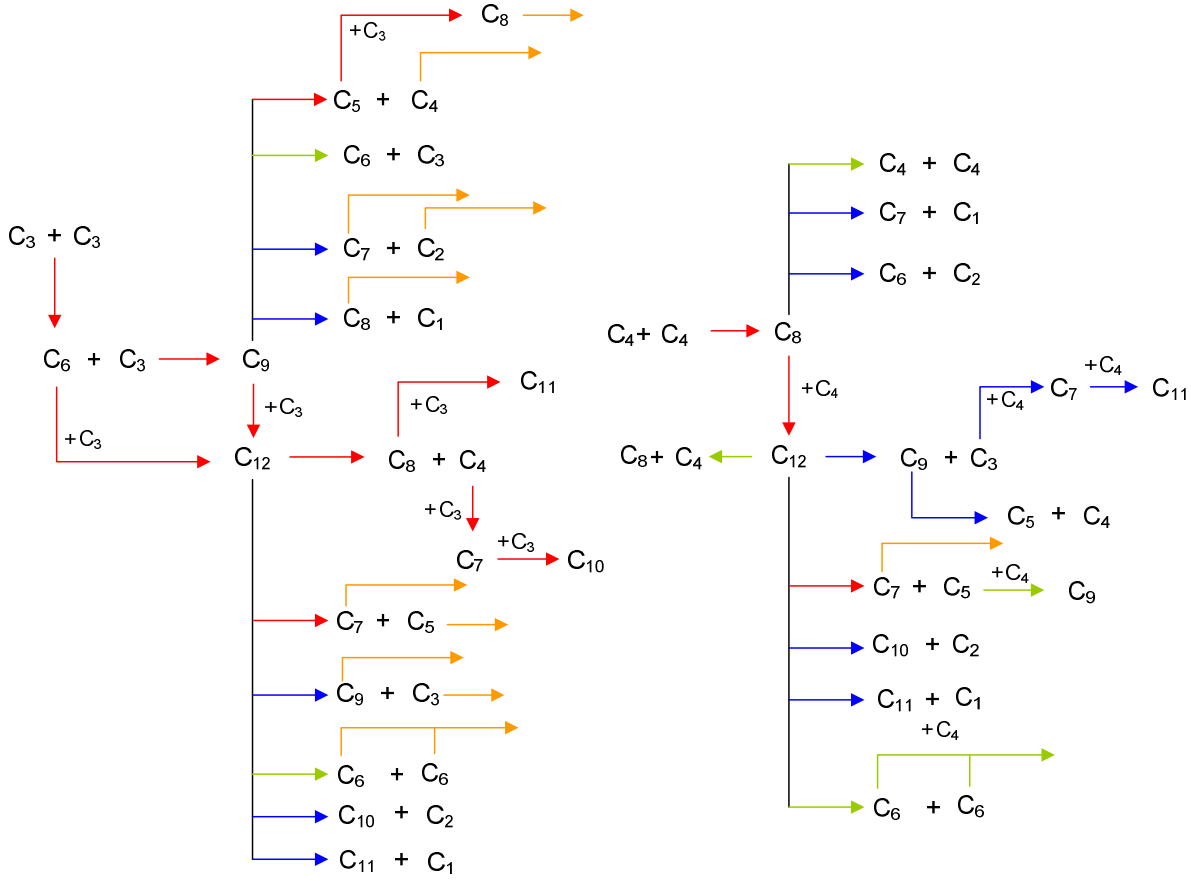

Figure 2-17: Reaction mechanism for McClean (1987). Reaction significance: → significant occurrence, → insignificant occurrence, → unknown occurrence, → normal route.

Modelling the oligomerisation over SPA is simplified by lumping all the carbon isomers under the same species (e.g. C_4 olefins would include 1-butene and iso-butene). This simplifies the possible reaction schemes by removing isomerisation and changing the varied amount of isomerised product to a single carbon number. This assumption would be adequate if the reactivates of varied isomers remained constant, which unfortunately is not always the case.

2.8 Closing remarks

Oligomerisation over SPA has been around since 1935 and extensive work has been done with various feeds over the catalyst. Many of these observations link directly to the reaction rate noticed over SPA. Firstly it has been shown that branched olefins of the same carbon length is more reactive than their linear counterparts, secondly the increased activity of the

catalyst has also been noticed where the acids strength of the catalyst has been increased. Although the articles listing these effects on the reaction rate over SPA are numerous, little has been done to include these effects in predicting the reaction rate over SPA. Where the reaction rate has been modelled (Paynter & Schuette, 1971; McClean, 1987; Coa *et al.*, 1988) these aspects of the oligomerisation over SPA has not been included in the proposed reaction kinetics. Not only has the increased reactivity of branched olefins been ignored when modelling the reaction rate, the propensity of SPA to skeletal isomerisation has also not been included in modelling the reaction progression over SPA.

This thesis investigates the oligomerisation of 1-hexene with regard to the reaction progression from 1-hexene to oligomerised and cracked products over a wide temperature range. Since it has been shown that branched olefins have a higher reactivity over the catalyst, the current research will attempt to incorporate the reactivity differences of linear (1-hexene) and branched olefins (2,3-dimethyl-2-butene) together with skeletal isomerisation in the proposed kinetic model (Chapter 3). The link between activity and acid strength on the reaction rate will be investigated in Chapter 4 by altering the acid content of the catalyst as well as the addition of water to the reaction mixture.

3 Reaction Kinetics for 1-Hexene Dimerisation

3.1 Background

A kinetic model poses a simplistic means of optimising a preferred reaction to the desired product without the need of excessive experiments. A good kinetic model simplifies and encapsulates the important steps in the reaction mechanism. Literature is however limited on the reaction kinetics over SPA. The work has focused mainly on examining the product spread at a constant space velocity (Ipatieff, 1938; De Klerk, 2004; De Klerk *et al.*, 2004) rather than focusing on trend differences when a single parameter is varied.

Where the reaction rate has been measured over SPA grouping of components is inevitably assumed, especially for components of identical length (Paynter & Schuette, 1971; McClean, 1987; Coa *et al.* 1988). It has been shown for butene oligomerisation, that the reactivity of the olefins is connected to the position of the double bond as well as the degree of branching. Even though isomerisation is known to occur over SPA, the rate of isomerisation (both double bond and skeletal isomerisation) has been ignored during the modelling of the reaction rate (McClean, 1987). Paynter & Schuette (1971) did accommodate for the difference in the reactivity observed fro 1-butene and 2-butene but no allowances was made for the differences in the reactivity of iso-butene. Coa *et al.* (1988) incorporated isomerisation but only in modelling the formation of a non-reactive isomer, which could easily have been a pseudo equilibrium. If the feed isomer composition is not varied, lumping these isomers together would not alter the modelling of the reaction rate. Large differences in the reactivity of isomers have been measured in the literature, suggesting the need for the addition of extra parameters in modelling the rate description.

Since little is known about the dimerisation of 1-hexene over SPA, 1-hexene can be used as a model light naphtha feed for the production of distillate (diesel and jet fuel). Measuring the reaction progression will give insight into the reaction over SPA in terms of *1)* the formation of hexene isomers and the dimerised product, as well as *2)* the effect of temperature on the product spectrum, especially with regard to cracking and secondary dimerisation. To decouple the rate of dimerisation for linear and branched hexenes (and their respective isomers), in this investigation the reaction rate for the dimerisation of 1-hexene and 2,3-dimethyl-1-butene (DMB) was measured in a batch reactor from 100 to 250 °C at 6 MPa.

3.2 Experimental

3.2.1 Materials

The SPA catalyst used during this investigation was obtained from Süd-Chemie Sasolburg (properties listed in Table 3-1). Due to the hydrophilic nature of the catalyst, the catalyst was dried at 200 ^{o}C overnight before each run.

Table 3-1: SPA C84/3 Properties

Free acid (%)	25
Total acid (%)	76
Ortho:pyro silicon phosphates ratio	2.2:1
Pore volume ($cm^3.g^{-1}$)	0.12
Main metal impurities	
Fe (mass %)	0.4
Al (mass %)	0.1

The dimerisation of hexenes was completed with two different hexene isomers, namely 1-hexene (97%) and 2,3-dimethyl-2-butene (DMB) (98%). Tetradecane (99%) was used as solvent to ensure that the reaction remained in the liquid phase. All the chemicals were supplied by Sigma-Aldrich.

3.2.2 Experimental setup and method

All the experiments were conducted in a 200-ml stainless steel batch reactor setup, illustrated in Figure 3-1.

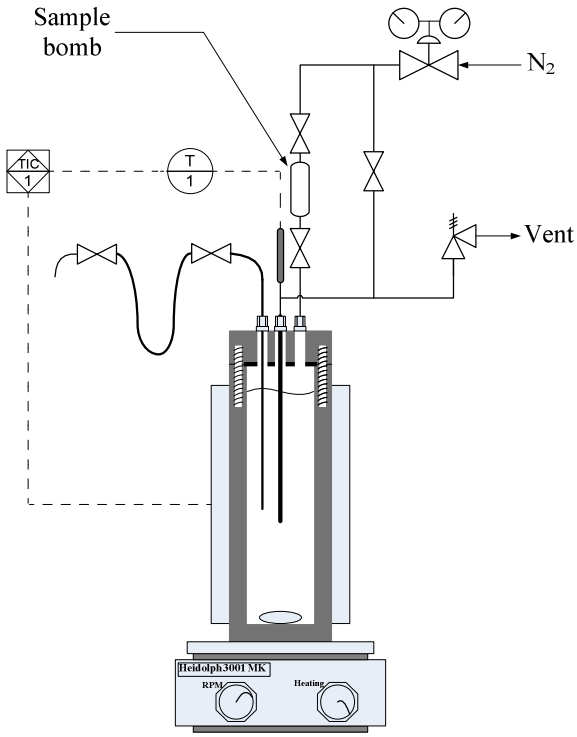

Figure 3-1: Experimental setup

The reactor pressure was controlled by a pressure regulator using a N_2 blanket. Approximately 5 g of the milled catalyst was loaded in the reactor vessel together with 75 g of solvent. This solvent/catalyst mixture was then heated to the desired reaction temperature at a pressure of 1 MPa. Once the required temperature had been reached, 35 g of the chosen hexene isomer was charged to the reactor from a sample bomb by increasing the pressure to 6 MPa – where it was maintained for the remainder of the reaction. This was taken as the start of the reaction and a sample was taken at this point to determine the exact composition of the initial mixture. Although a slight drop in temperature (less than 5% of the set point temperature, meaning if the set point temperature was 200 °C the temperature drop was to 190 °C) was observed after the addition of the hexene reactant, the temperature was re-established before the next sample was taken, where it was controlled within 1 °C of the desired set point, using a heating jacket fitted with a temperature controller. The reaction mixture was agitated with a Heidolph 3001 MK magnetic stirrer at a rate of 1000 rpm after establishing that this would be sufficient to eliminate any external mass transfer effects (Figure 3-2). A further experiment was done whereby the catalyst was milled to 150 µm and 300 µm to determine if internal mass transfer was limiting (Figure 3-3).

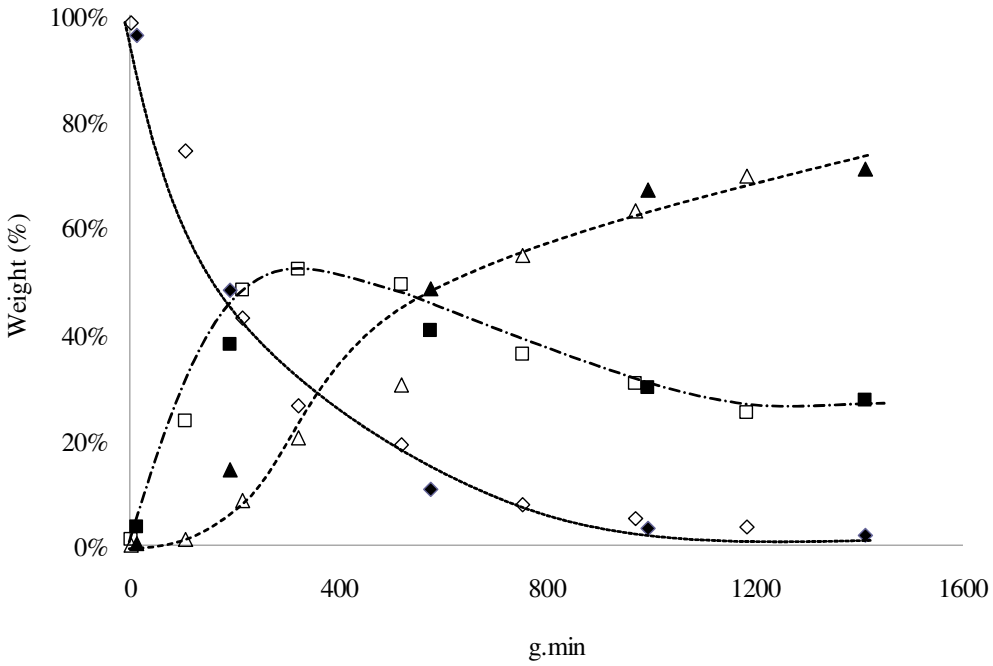

Figure 3-2: 1-Hexene reaction progression at 250 °C versus weight time (g_{cat}.min). Weight fraction of: ◊ = Linear hexene isomers; □ = skeletal hexene isomers and △ = overall hexene depletion (D). The stirrer speed is indicated by the open (500 rpm) and solid (1000 rpm) data points.

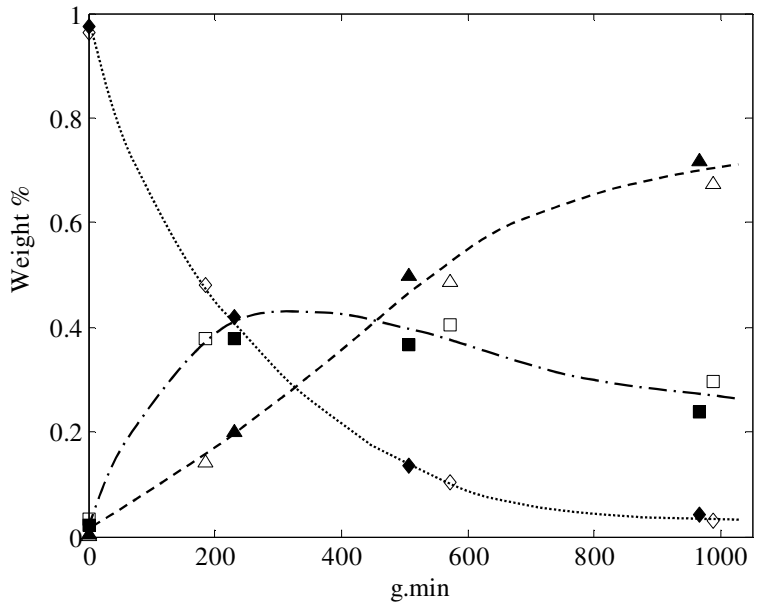

Figure 3-3: The reaction rate of 1-hexene at 250 °C (1000 rpm), where the catalyst was ground to 150 µm (open points) and 300 µm (closed points). Weight fraction of: ◊ = Linear hexene isomers; □ = skeletal hexene isomers and △ = overall hexene depletion.

Therefore all experiments were completed at 1000 ppm with the catalyst ground to less than 150 µm to eliminate the effect of both internal and external mass transfer. The reaction progression was measured for 1-hexene and DMB respectively at 100, 150, 200 and 250 °C. A list of all the experiments that were completed to evaluate the kinetics for the dimerisation of hexene is shown in Table 3-2.

Table 3-2: Kinetic experiments completed.

T	m_{cat} (g)	V (L)
	DMB	
100 °C	5.0	0.15
150°C	7.7	0.17
200°C	6.0	0.19
250°C	5.7	0.22
	1-Hexene	
100 °C	5.1	0.16
150°C	7.2	0.18
	5.6	0.17
200°C	4.3	0.19
	5.1	0.21
	5.3	0.19
250°C	6.4	0.25
	8.0	0.25

3.2.3 Analysis

Samples were analysed by means of an Agilent Technologies 6890 gas chromatograph (GC) fitted with a flame ionisation detector (FID). Elutriation was established on a 50-m long Pona column with a 0.2 mm inner diameter and a 0.5 mm film thickness with N_2 as carrier gas at a flow rate of 25 ml/min. A split ratio of 100:1 was used. The initial column temperature was 40 ^{o}C, where it was held for 5 minutes, after which the temperature was ramped up to 300 ^{o}C at increments of 8 ^{o}C/min, where it was finally held constant for 5 minutes. The retention times of various hexene isomers were determined by injecting analytical grade standards from Sigma Aldrich: cis & trans 2-hexene (85%), 3,3-dimethyl-1-

butene (95%), 2-methyl-2-pentene (98%), 2,3-dimethyl-1-butene (97%), 2,3-dimethyl-2-butene (98%) and 2-ethyl-1-butene (95%). The hexene isomers were also confirmed using GC-MS, the possibility does however exist that some isomers are hidden due to overlapping.

The dimerised product cracked in a wide range of products, and C_4 to C_{13} olefins were detected. All the components elutriated before the tetradecane solvent, suggesting that the formation of trimer product was insignificant over the entire temperature range investigated. Overlapping with the tetradecane solvent which could mask the formation of oligomerised product was eliminated by the fact that the tetradecane weight fraction remained constant throughout all the experimental runs.

To differentiate between the cracked products, a GC-FID analysis was compared to the elutriation of the carbon numbers identified from a GC-MS (MS – mass spectrometry). The GC-MS was set to identify products from 20-300. Significant overlapping occurred for carbon numbers larger than C_9. Since the GC-MS could not be used for the analysis of every sample, the peak carbon numbers were related to the GC-FID residence times and from this a carbon number could be attributed, depending on the residence time of the peak through the column. A conservative residence estimate was used to identify each carbon number. The carbon distribution that resulted for the GC-FID analysis is shown in Table 3-3.

Table 3-3: Carbon analysis.

	GC Residence time (min)	
	Lower boundary	Upper boundary
C_4	0.00	2.04
C_5	2.04	3.03
C_6	3.03	4.45
C_7	4.45	8.00
C_8	8.00	10.50
C_9	10.50	12.50
C_{10}	12.50	14.30
C_{11}	14.30	15.70
C_{12}	15.70	18.60
C_{13}	18.60	22.50
C_{Other}	22.50	t_{end}

Due to the excessive overlapping of peaks, the GC-MS could not be used to distinguish between olefins, cyclics or aromatic molecules. Each one of these molecules could form from the dimerisation of 1-hexene over an acid catalyst (Figure 2-10). For this reason 1-hexene was dimerised to 80% total conversion of the hexene isomers and the product (boiling higher than 170 °C) was distilled and analysed, using GCxGC to determine the fraction of olefins, cyclics and/or aromatics. The GCxGC was done using a Pegasus 4D GCxGC system, supplied by Leco, Co. (St. Joseph, MI, USA), equipped with both TOF-MS and an FID detector. The primary column was a 50-m FFAP capillary column (0.20 mm internal diameter, *i.d.*, and 0.30-µm film thickness, *df*). The secondary column was a 2-m Rtx-5 column (0.1 mm *i.d.*, 0.1 µm *df*). The primary oven was programmed as follows: 35 °C for 1 min, ramped at 3 °C/min to 240 °C. The second oven followed the first oven program with a 10 °C offset. A duel jet thermal modulation system was used with an 8-second modulation period; 0.5 mL was injected using an Agilent Technologies 7683 auto injector. Hydrogen carrier gas was used at a constant flow of 1.3 mL/min. The split ratio was 400:1. Data collection for the TOF-MS and FID was at 100 spectra/sec.

3.3 Results & Discussion

3.3.1 Double bond and skeletal isomerisation

During oligomerisation, isomerisation and cracking occur simultaneously (Quann *et al.,* 1988). Since it has been shown that SPA is more prone to the oligomerisation of branched olefins (de Klerk, 2008), the rate of isomerisation is critical to describing the reaction rate. Previous work on the isomerisation of 1-hexene in the vapour phase indicated that isomerisation appeared to be step-wise: 1-hexene → methyl pentenes → dimethyl butenes (Hay *et al.*, 1945). If the hexene isomers identified throughout the progression of the reaction are plotted, a clear stepwise progression is seen in the formation of the isomers, shown in Figure 3-4. Initially only 1-hexene is present which disappears almost instantaneously from the bulk reaction mixture to form linear double bond isomers. Shortly after the appearance of double bond isomers, skeletal isomers are seen in the reaction mixture.

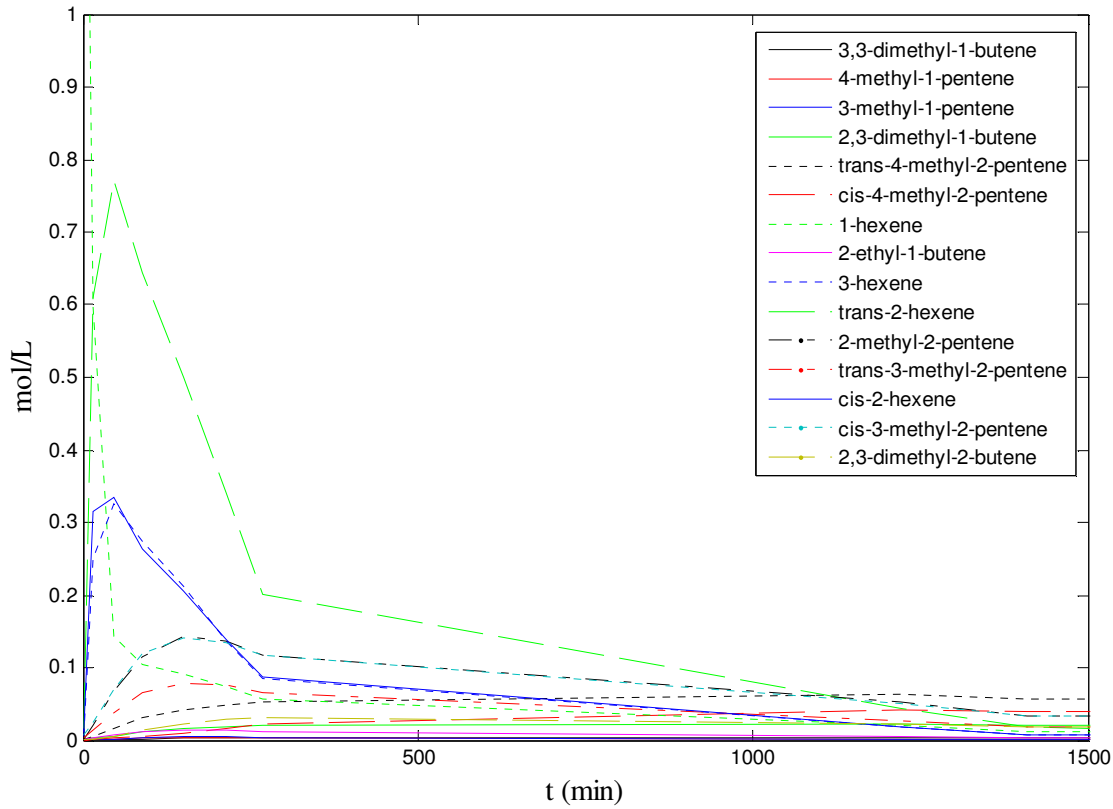

Figure 3-4: Hexene isomers identified by GC-FID during the dimerisation of 1-hexene at 200 °C.

The hexene isomers were further divided according to the degree of branching and the position of the double bond to identify differences in the reactivity of the different isomers. The grouping of the hexene isomers were done as described in Table 3-4.

Table 3-4: Groupings of hexene isomers

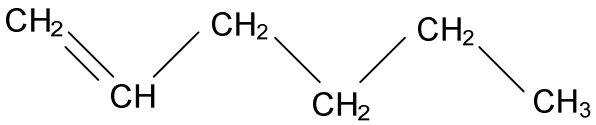	Linear hexenes, Figure 3-5 a)
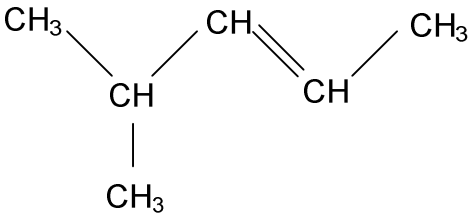	Beta disubstituted olefins (group A); where the double bond is located between two secondary carbons, e.g. trans-4-methyl-2-pentene, Figure 3-5 *b*).
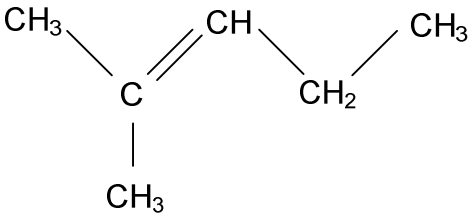	Tetra- and Trisubstituted olefins (group B); with the double bond between a secondary and tertiary carbon or situated between two tertiary carbons, e.g. 2-methyl-2-pentene; cis- and trans-3-methyl-2-pentene; 2,3 dimethyl-2-butene, Figure 3-5 *c*).
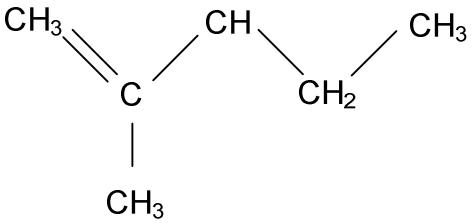	Mono substituted and alpha disubstituted olefins (group C); where the double bond is situated between a primary and tertiary carbon, e.g. 2,3-dimethyl-1-butene; 2-ethyl-1-butene, 3-methyl-1-pentene, Figure 3-5 *d*).

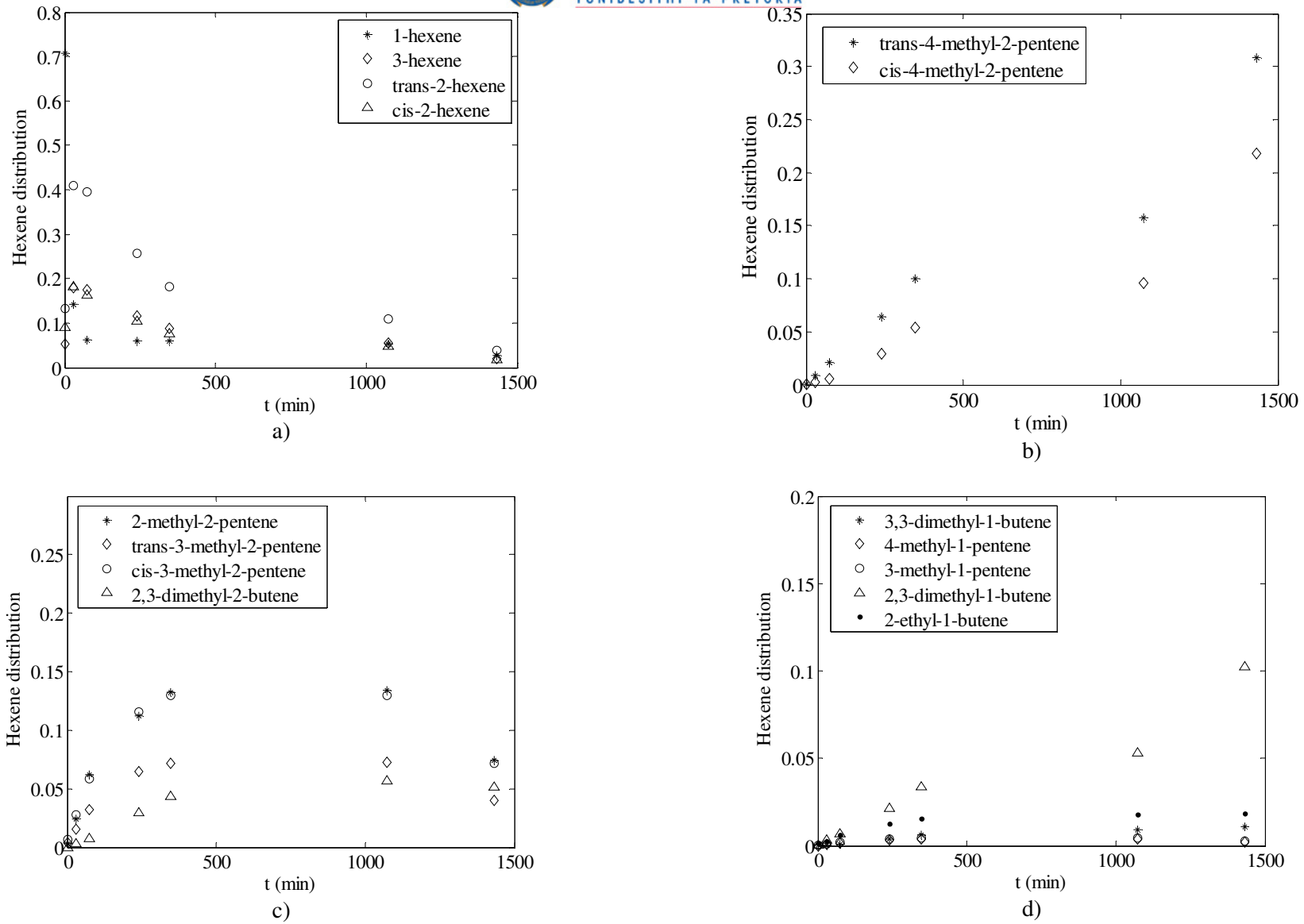

Figure 3-5: Isomers identified for 1-hexene dimerisation at 200 °C divided into *a)* linear hexenes, *b)* group A branched h*e*xenes, *c)* group B branched hexenes and *d)* group C branched hexenes.

As can be seen from Figure 3-5 linear hexenes are initially present to a much more significant extent than the branched hexenes, also the formation and subsequent depletion of branched hexenes is mostly localised with the formation of group B branched hexenes. Whereas group A and C skeletal isomers form to a lesser extent with little depletion afterwards. Skeletal isomerisation of olefins can either occur by methyl shift (Figure 2-11 *b))* or by the cracking of dimerised product (*isomerisation cracking*). The latter of the two was not seen in the early stages of the reaction. Branched hexenes were identified before the formation of C_{12}s for all experiments, indicating that the isomerisation of linear hexenes occurs by methyl shift. This is not to say that the dimerisation of linear hexenes does not occur, but rather that isomerisation occurs faster. It should also be noted that before a branched product can form from isomerisation cracking of two linear hexenes, skeletal isomerisation of the C_{12} product would first need to occur. From this work it is more evident that isomerisation occurs through methyl shift and not isomerisation cracking.

Throughout the investigation, linear hexenes seemed to convert irreversibly to skeletal isomers, with branched hexenes being more prominent toward the latter stages of the experiment. This indicates that the cracking of C_{12}s, to hexenes, results in the formation of branched hexenes, which indicates an equilibrium distribution between the dimerised product (C_{12}s) and the branched hexenes. If the dimerisation of linear hexenes occurs, the dimerised product will first need to isomerise before cracking to a branched product can be possible, Figure 3-6. This indicates that either linear hexene did not dimerise significantly or that the dimerised product can easily isomerise.

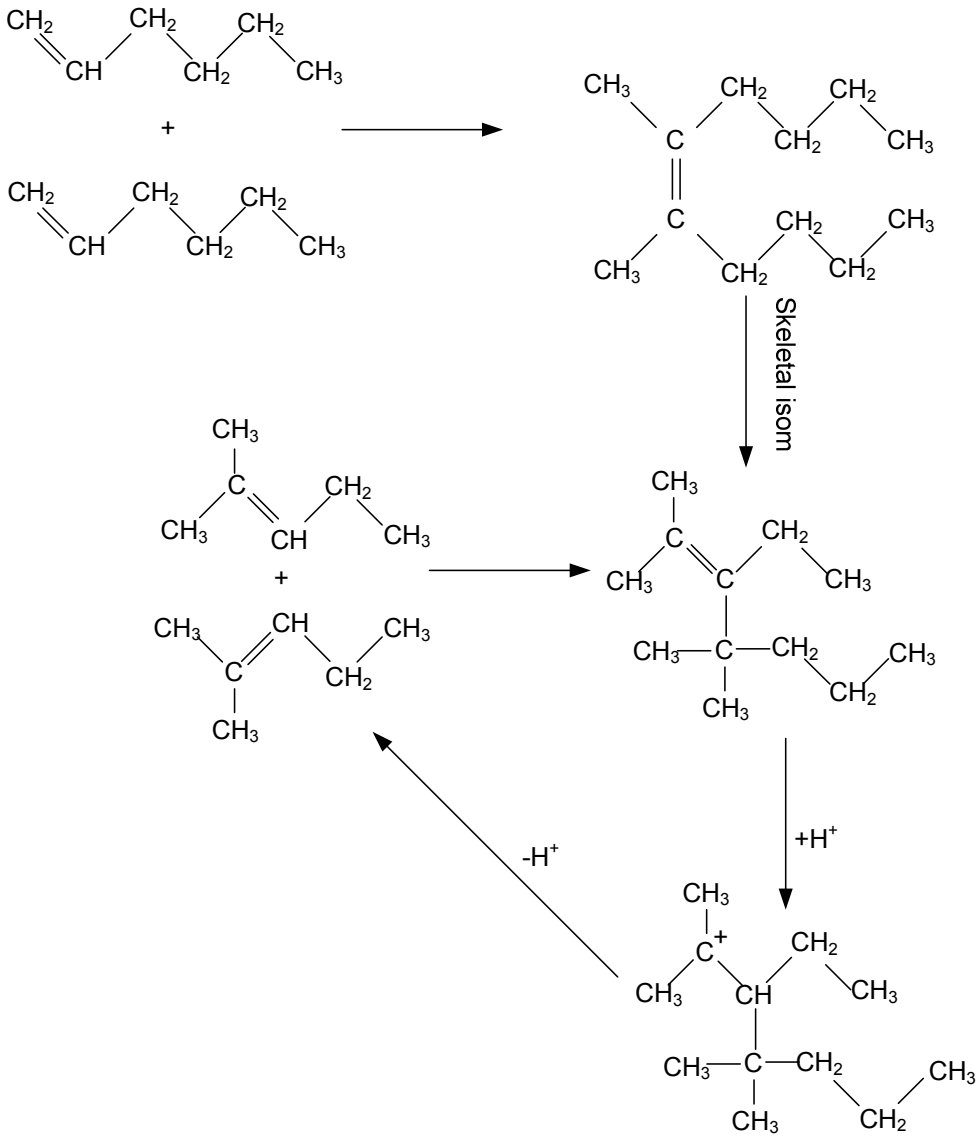

Figure 3-6: Cracking route of C_{12} product.

To determine whether the disappearance of the linear hexenes is due to the formation of skeletal isomers or due to the conversion to dimerised product, the depletion of all hexene isomers relative to the formation and depletion of linear hexenes and branched hexenes was studied, Figure 3-7. Since 1-hexene disappears quickly to the other linear isomers, all the linear hexenes were lumped together. The depletion of the hexenes was assumed to occur toward the formation of C_{12} dimers, merely to illustrate the rate of reaction, not the product selectivity. Linear hexenes in this instance are a grouping of all linear hexenes, 1-hexene included. Initially little depletion of hexene isomers was seen, with an inflection point evident for the depletion of hexenes where the formation of branched hexenes reached a maximum

(Figure 3-7, with the dotted line indicating the inflection point). This indicates that the depletion of hexenes to dimerised product occurs to a greater extent once skeletal isomers have been formed.

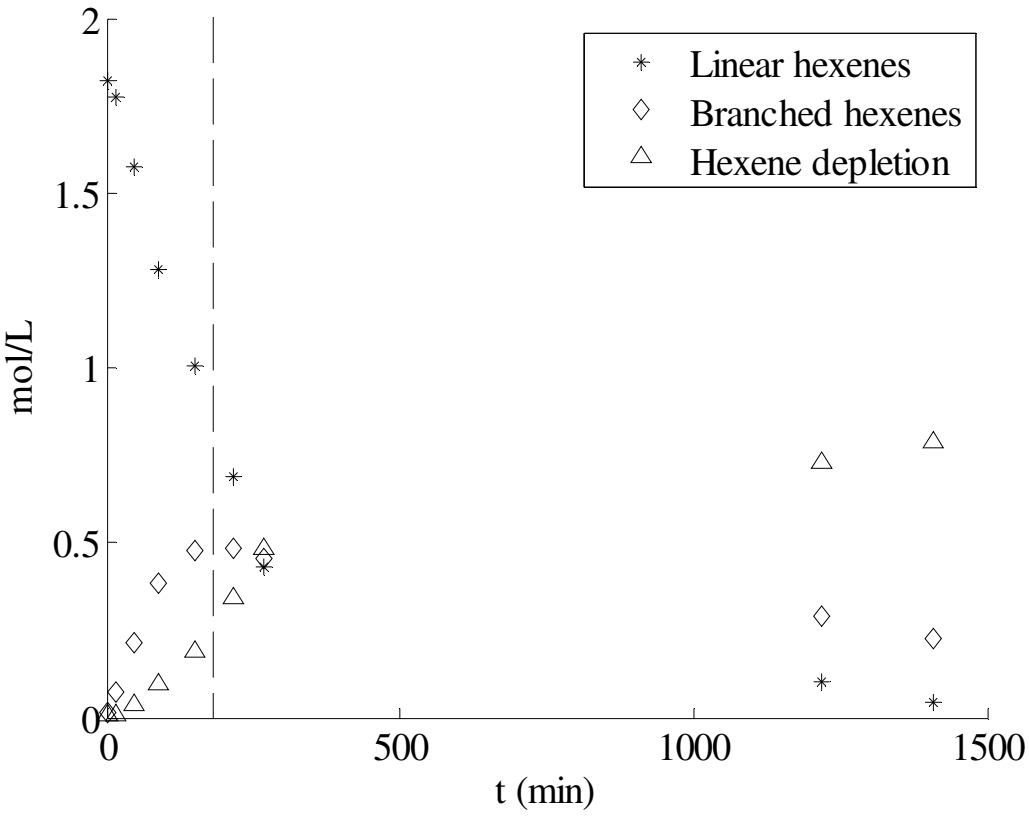

Figure 3-7: The reaction progression for 1-hexene dimerisation with reference to linear hexenes, branched hexenes and hexene depletion (dimerisation) at 200 °C.

If 1-hexene is fed into the reactor, the interaction between linear hexenes, branched hexenes and dimerised product is convoluted. It is not simple to determine whether the oligomerised product is formed from the dimerisation of branched hexenes or the co-dimerisation between the linear and branched isomers. For this reason, new insights into the dimerisation of hexene were gained from the dimerisation of 2,3-dimethyl-2-butene (DMB) with reference to 1-hexene dimerisation (especially while using a reaction model). The relative formation of hexene isomers and dimerised product can be correlated to give a clearer indication of the isomers that are most reactive. Figure 3-8 shows the formation of hexene isomers seen during the dimerisation of DMB over SPA. The hexenes isomers identified are dominated by two isomers: *1)* DMB and *2)* 2,3-dimethyl-1-butene (DM1B, double bond isomers).

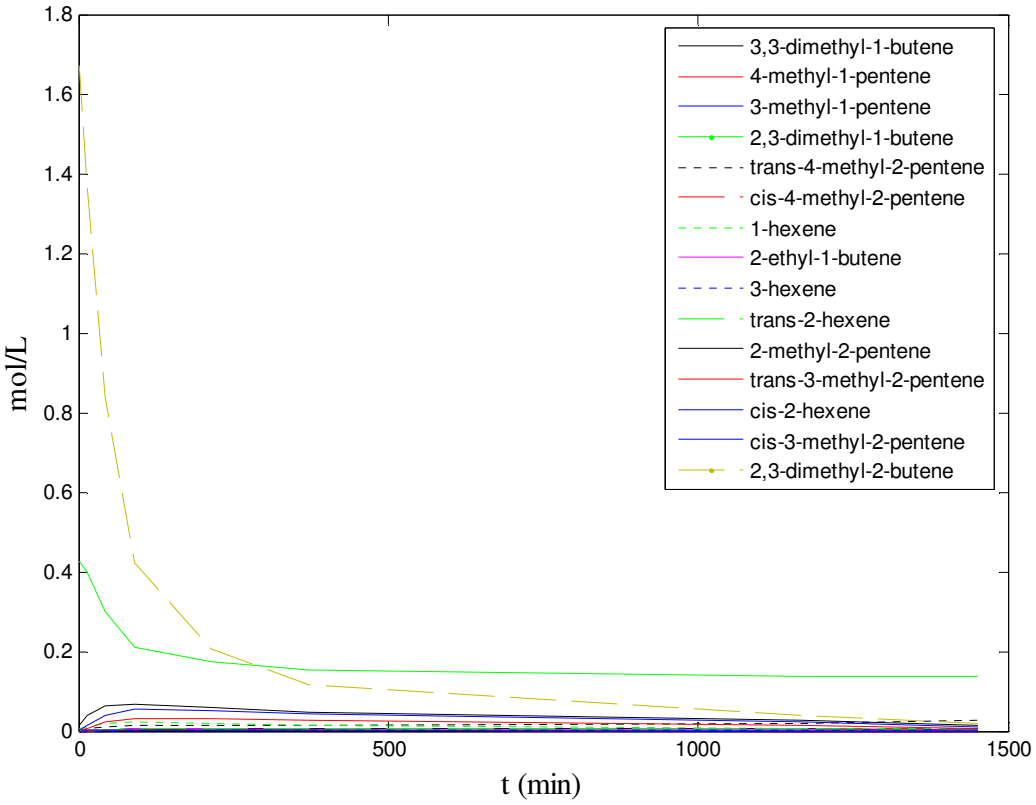

Figure 3-8: Hexene isomers identified for the dimerisation of DMB at 200 °C.

The distribution of hexene isomers is again separated based on the position of the double-bond and is shown in Figure 3-9. It can be seen that linear hexenes are formed to an insignificant extent. Not only is the formation of linear hexenes limited but also the formation of other skeletal hexene isomers does not occur significantly. This indicates that methyl shift occurs irreversibly and that the formation of other hexene isomers, when dimerising DMB, only results from the cracking of oligomerised product.

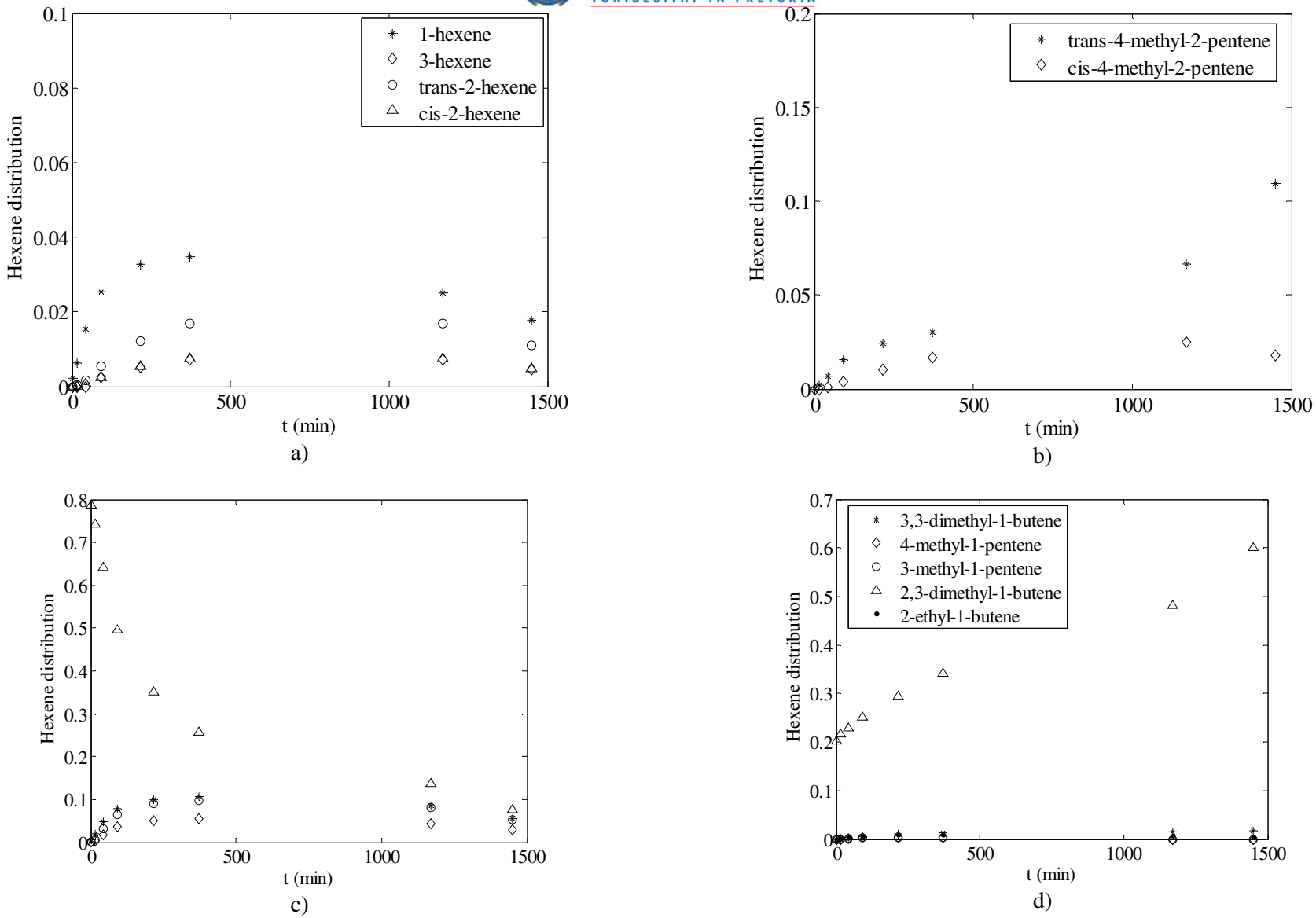

Figure 3-9: Isomers identified for DMB dimerisation at 200 °C divided into *a)* linear hexenes, *b)* group A branched hexenes, *c)* group B branched hexenes *d)* group C branched hexenes.

If the depletion of hexene isomers for the dimerisation of DMB is plotted, a steadier depletion of the hexene isomers to dimerised product is observed. It is also evident that there is no inflection point in the depletion of hexenes, indicating a single-step depletion of hexenes. The formation of linear hexenes is also seen to be insignificant with respect to the other hexene isomers and dimerised product; these trends were observed over the entire temperature range.

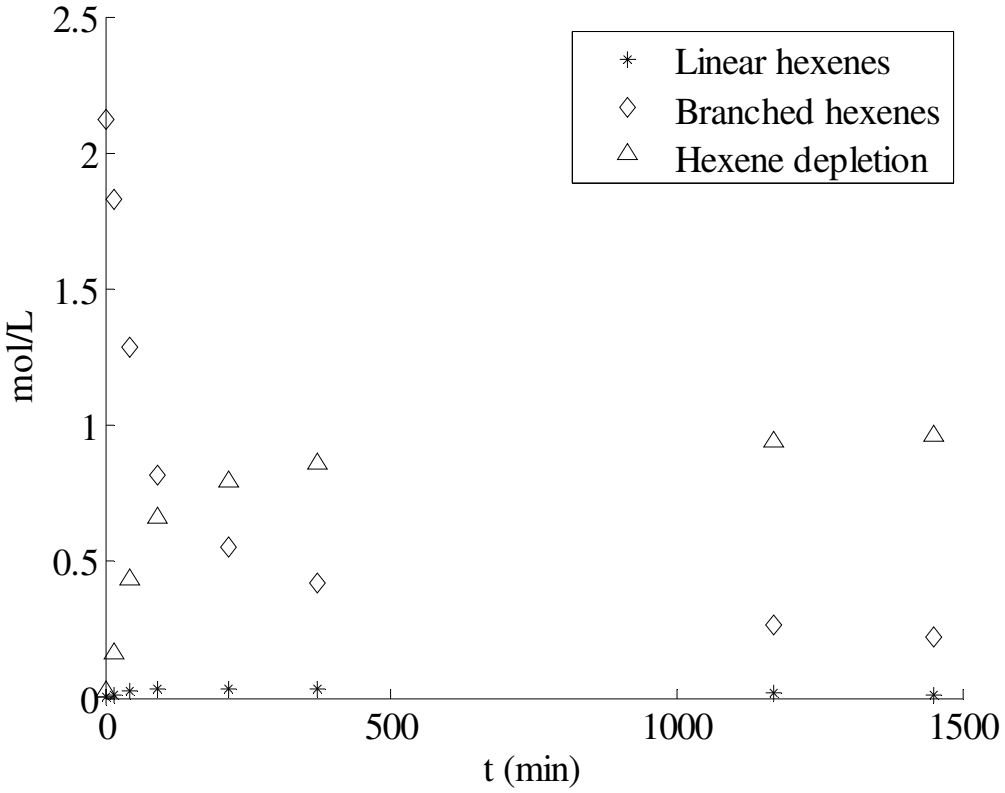

Figure 3-10: The reaction progression for DMB dimerisation with reference to linear hexenes, branched hexenes and hexene depletion (dimerisation) at 200 °C.

From Figure 3-8 and Figure 3-9 it seems that the double bond isomer of DMB, DM1B, forms quickly and the then remains constant. This might indicate that the isomer is non-reactive, or that an equilibrium distribution prevails. If the equilibrium distribution of hexene isomers are determined using an RGIBS reactor from Aspen^{TM}, the distribution in Table 3-5 is obtained. This shows that at 200 °C the equilibrium distribution of DMB and DM1B favours DM1B, whereas at lower temperatures DMB is favoured.

Table 3-5: Equilibrium distribution of hexene isomers from RGIBS reactor (Aspen™)

	100 °C	150 °C	200 °C	250 °C
1-hexene	0.1%	0.2%	0.3%	0.5%
cis-2-hexene	0.6%	1.0%	1.5%	2.1%
trans-2-hexene	1.6%	2.3%	3.1%	3.8%
cis-3-hexene	0.2%	0.4%	0.6%	0.8%
trans-3-hexene	1.0%	1.5%	2.0%	2.4%
2-methyl-1-pentene	4.6%	5.7%	6.6%	7.2%
3-methyl-1-pentene	0.3%	0.5%	0.8%	1.1%
4-methyl-1-pentene	0.2%	0.3%	0.4%	0.5%
2-methyl-2-pentene	15.0%	13.4%	11.8%	10.5%
3-methyl-cis-2-pentene	18.9%	20.1%	20.5%	20.3%
4-methyl-cis-2-pentene	1.2%	1.7%	2.2%	2.6%
4-methyl-trans-2-pentene	2.6%	3.2%	3.7%	4.2%
2-ethyl-1-butene	2.1%	2.9%	3.7%	4.4%
2,3-dimethyl-1-butene	22.9%	23.5%	23.7%	23.7%
3,3-dimethyl-1-butene	0.1%	0.1%	0.2%	0.2%
2,3-dimethyl-2-butene	28.6%	23.3%	19.0%	15.6%

To determine if the DM1B is unreactive or if an equilibrium distribution is present, more data is required. If the distribution of DMB and DM1B is plotted for the reaction rate of DMB of SPA at 150 °C, Figure 3-11, it is evident that DMB is favoured. As such the distribution of the DMB and DM1B can be attributed to the equilibrium distribution of isomers.

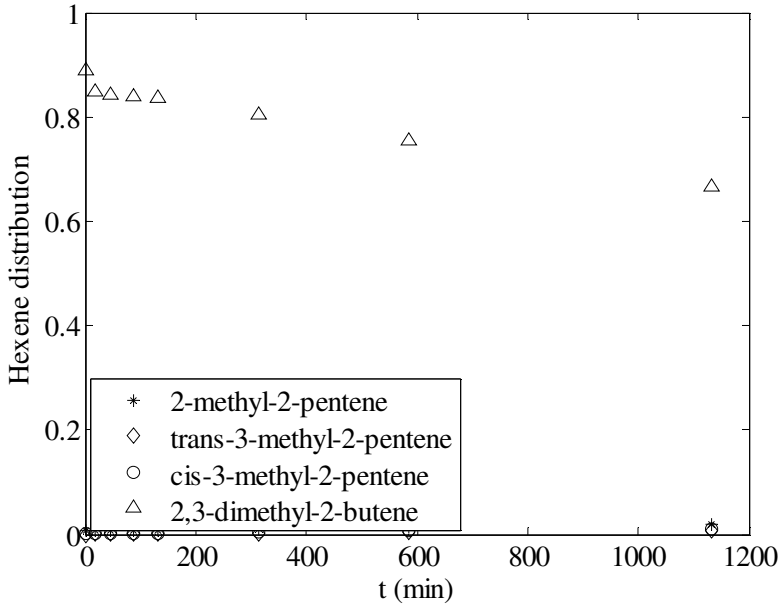

a)

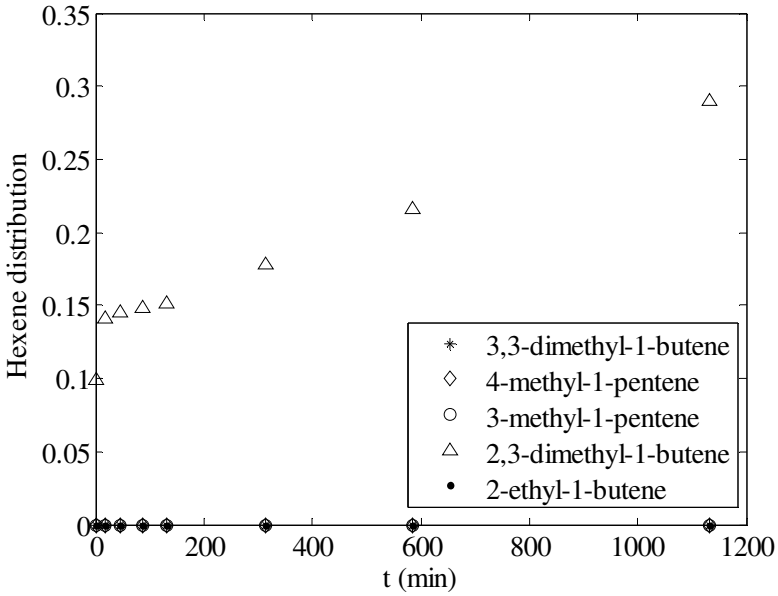

b)

Figure 3-11: Distribution of DMB at 150 °C for *a*) group B branched hexenes and *b)* group C branched hexenes (an insignificant amount of linear hexenes and group A hexenes was observed at 150 °C for the dimerisation of DMB over SPA).

3.3.2 Dimerised and cracked products

In the previous section the emphasis was placed on the formation of hexene isomers with little emphasis on the product spread. As cracking is prominent over SPA, the chain length of the resulting product is important to quantifying the quality of the produced fuel, Section 2.1. The formation of the different carbon numbers identified from GC-MS/FID is shown in Figure 3-12. For each carbon number a bar graph is shown; each bar indicates the chronological formation of the product from the onset of the reaction (first bar) to the end of the experiment (last bar).

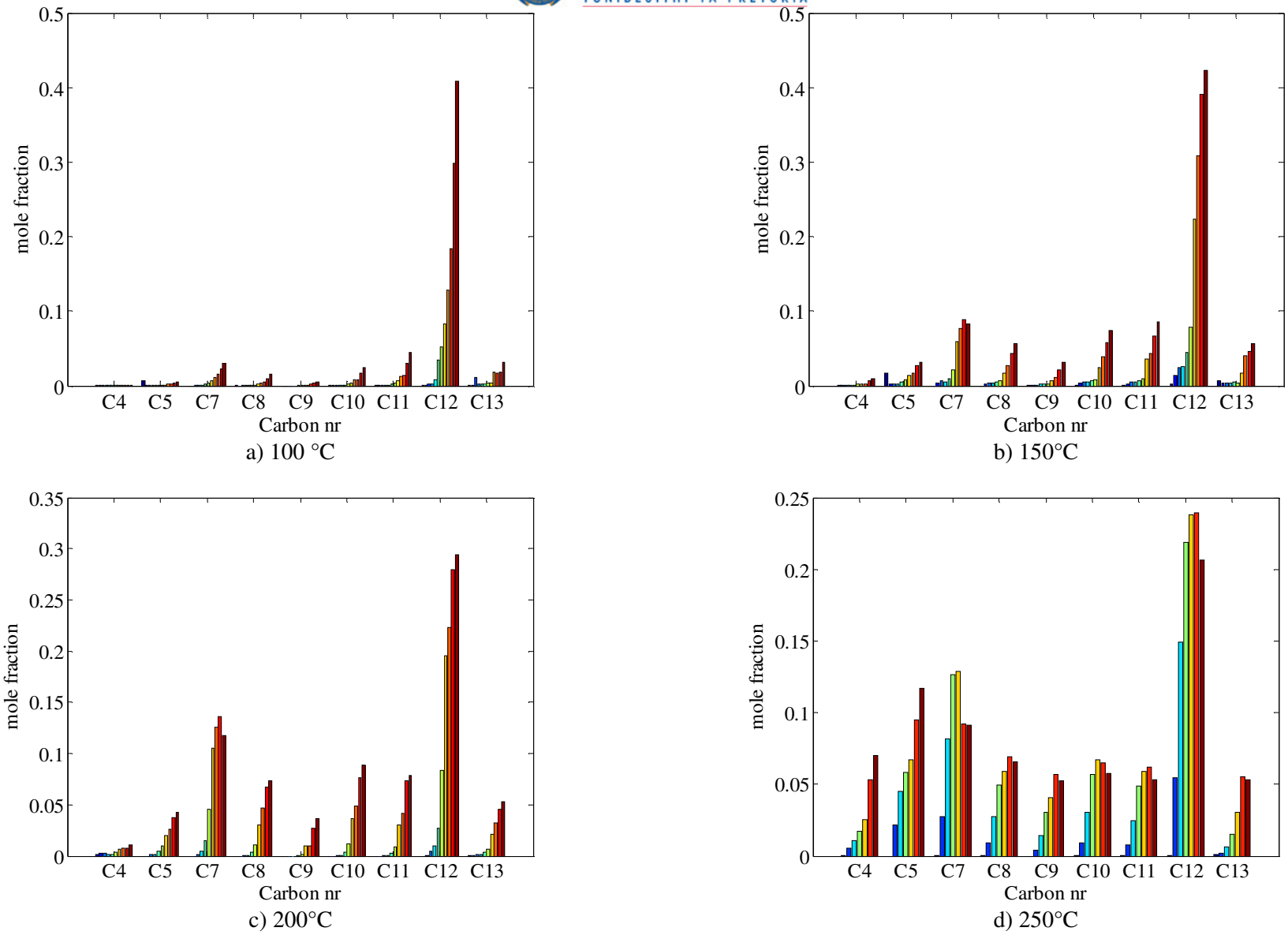

Figure 3-12: Formation of oligomerised and cracked products for 1-hexene dimerisation.

It is notable from the GC-MS analysis of the product that the reaction of 1-hexene over SPA is limited to the formation of dimerised product, with no trimerised product identified. It is clear from Figure 3-12 that a much higher selectivity toward the formation of dimers is seen at lower temperatures, with little cracking observed. As the temperature increases, the carbon number distribution evens out. A simplistic method of evaluating the distribution of the cracked product at each interval is to evaluate the concentration of each carbon number with respect to the total hexene depletion to C_{12}s, D, as shown in Equation 3-1.

$$K_{eq} = \frac{C_x}{D} \qquad 3\text{-}1$$

where C_x is the concentration of carbon number x and D is the total hexene depletion expressed as C_{12} formation.

This assumes that cracking occurs after dimerisation, which is in line with the work of De Klerk (2005b) who states that the cracking of hexenes will only become significant above 275 °C. Therefore in this investigation, only the cracking of olefins heavier than C_6 should occur. For this reason, cracking will only occur once dimerisation has occurred. The resulting distribution of each carbon number, from the start to the end of each experiment, is shown in Figure 3-13. Both Figure 3-12 and Figure 3-13 indicate a higher selectivity toward cracked products at higher temperatures, with lower temperatures being more selective toward the dimerisation of hexene. Interestingly, the distributions of dimerised and cracked products are relatively flat for each carbon number from the onset of the reaction. This indicates that once dimerisation has occurred, the cracking and co-dimerisation that follow are essentially instantaneous with an *equilibrium* distribution. Similar trends are evident for the dimerisation of DMB, shown in Appendix 8.1 (Figure 8-1 and Figure 8-2).

The observation that the carbon number distribution evens out quickly suggests that it is not possible to isolate the formation of dimerised product at a minimal formation of cracked products. This indicates that the gasoline to diesel/jet fuel distribution (due to both cracking and co-dimerisation) for the dimerisation of hexenes will depend on the reaction temperature, not on the residence time in the reactor.

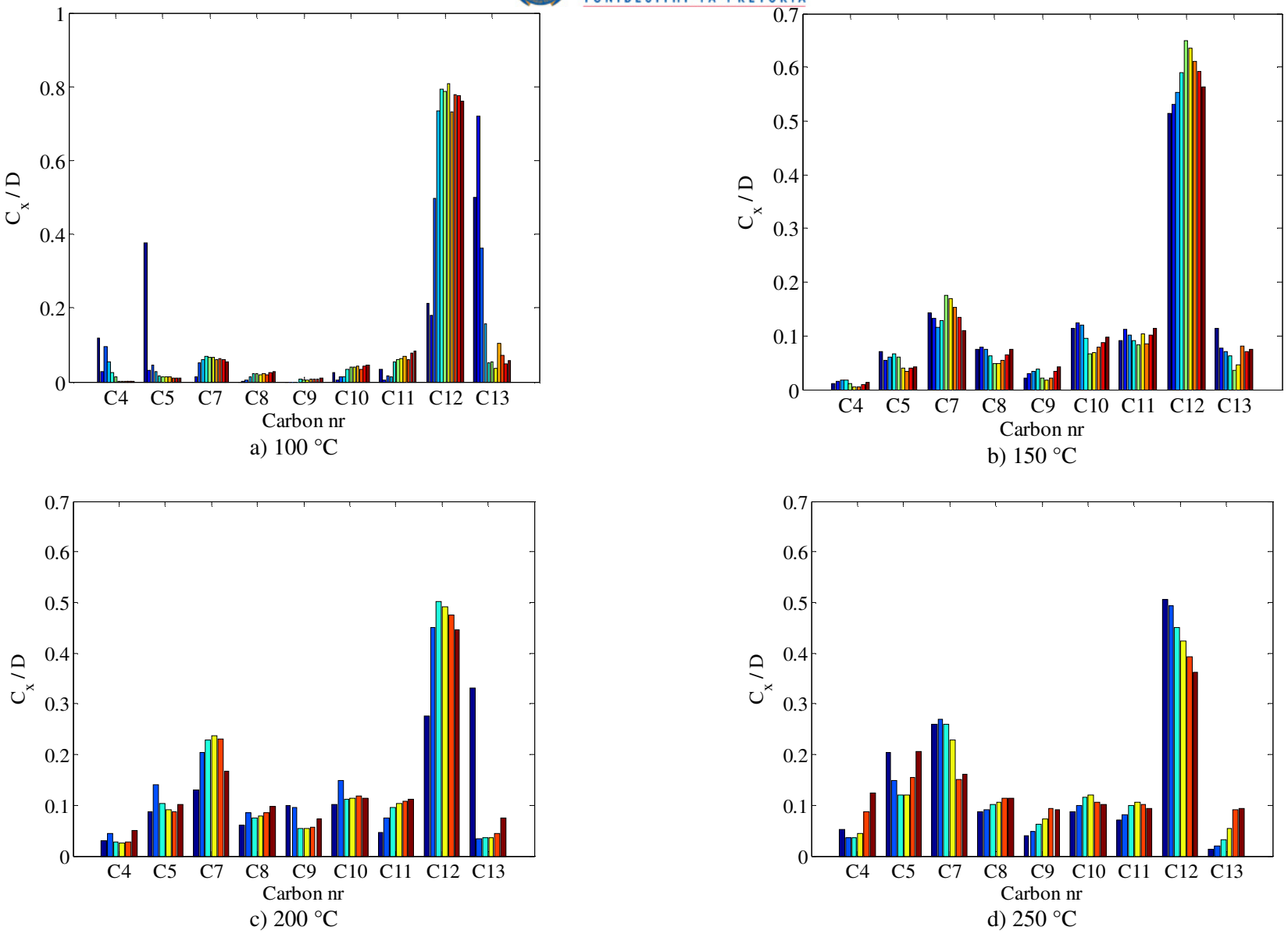

Figure 3-13: Distribution of cracked and dimerised product for 1-hexene dimerisation.

To assess the product spread further, a GCxGC analysis was done on the product from 1-hexene dimerised product (boiling above 170 °C) at 100, 150 and 250 °C (unfortunately, data could not be collected at 200 °C). The GCxGC analysis indicated that even at 100 °C the formation of cyclics and aromatics was evident, increasing as the temperature increased (Table 3-6 and Figure 8-3 in the appendix). Due to the increased cracking at higher temperatures, the distribution of observed carbon numbers expanded at higher temperatures. It was not possible, to analyse each sample using the GCxGC, so the formation of cyclics/aromatics could not be incorporated into the kinetic evaluation of 1-hexene dimerisation.

The formation of cyclic and aromatic compounds over SPA is by no means a new occurrence and has been noted by Ipatieff (1935) and Ipatieff and Corson (1936) for the oligomerisation of propylene and ethylene respectively. The formation of aromatics for the oligomerisation of short chain olefins over SPA is however not so conclusive. A GC x GC analysis that was completed for the oligomerised product from the oligomerisation of C_3 and C_4 olefins over SPA showed that cyclic molecules was present in the product (Van der Westhuizen *et al.*, 2010). Although cyclics is a precursor to the formation of aromatics, no aromatics was observed in the investigation. These investigations focused on the oligomerisation of short chain olefins, whereas 1-hexene was oligomerised in this instance. An investigation that observed aromatics while oligomerising 1-hexene, however using USY Zeolite, was Anderson *et al.* (1991). No other reference could be found to the formation of aromatics over SPA for 1-hexene oligomerisation. It is however not within the scope of this research to investigate the formation of aromatics from 1-hexene, but rather focus on the oligomerisation of 1-hexene.

Table 3-6: Product spread for GCxGC at different temperatures.

Carbon Number	Olefins	Cyclic Olefins	Total
	W %	W %	W %
C_9	0.03	0.00	0.03
C_{10}	5.71	0.02	5.73
C_{11}	4.54	0.18	4.72
C_{12}	64.42	1.86	66.28
C_{13}	7.88	0.27	8.15
C_{14}	1.27	0.32	1.60
C_{15}	0.12	0.09	0.21
C_{16}	0.34	0.09	0.43
C_{17}	0.44	0.40	0.85
C_{18}	2.16	3.80	5.96
C_{19}	0.13	0.52	0.65
C_{20}	0.00	0.06	0.06
C_{21}	0.00	0.00	0.00
		Light material < C_8	0.05
		Aromatics	5.29
Total	87.04	7.62	100.0

a) 100 °C

Carbon Number	Olefins	Cyclic Olefins	Total
	W %	W %	W %
C_9	0.00	0.04	0.04
C_{10}	1.32	0.05	1.37
C_{11}	13.22	0.53	13.74
C_{12}	45.35	0.41	45.75
C_{13}	14.59	1.94	16.53
C_{14}	3.06	0.70	3.75
C_{15}	1.42	0.36	1.78
C_{16}	1.42	0.80	2.22
C_{17}	3.44	0.67	4.11
C_{18}	2.40	3.52	5.92
C_{19}	0.00	0.68	0.68
C_{20}	0.00	0.89	0.89
C_{21}	0.00	0.00	0.00
		Light material < C_8	0.03
		Aromatics	3.18
Total	86.21	10.58	100.0

b) 150 °C

Carbon Number	Olefins	Cyclic Olefins	Total
	W %	W %	W %
C_9	0.03	0.00	0.03
C_{10}	0.70	0.05	0.74
C_{11}	7.45	0.71	8.16
C_{12}	32.62	4.49	37.12
C_{13}	9.66	2.38	12.04
C_{14}	4.26	5.88	10.14
C_{15}	1.31	3.39	4.71
C_{16}	1.08	2.34	3.41
C_{17}	0.40	2.61	3.01
C_{18}	0.36	4.01	4.37
C_{19}	0.00	0.97	0.97
C_{20}	0.00	0.36	0.36
C_{21}	0.00	0.08	0.08
		Light material < C_8	0.08
		Aromatics	14.78
Total	57.86	27.28	100.0

c) 250 °C

3.4 Kinetic model

To extract the reaction progression of the dimerisation of 1-hexene further, a kinetic model can be used to compensate for reactivity differences between hexene isomers. To model the reaction kinetics for the dimerisation of 1-hexene, the reaction sequence was depicted with respect to linear hexenes (A), branched hexenes (B) and hexene depletion to dimerised product (D) as shown in Figure 3-14. For the determination of the reaction progression various groupings and routes were evaluated to determine which gave the most successful prediction of the reaction rate, the reaction route depicted in Figure 3-14 gave the best description of the oligomerisation kinetics.

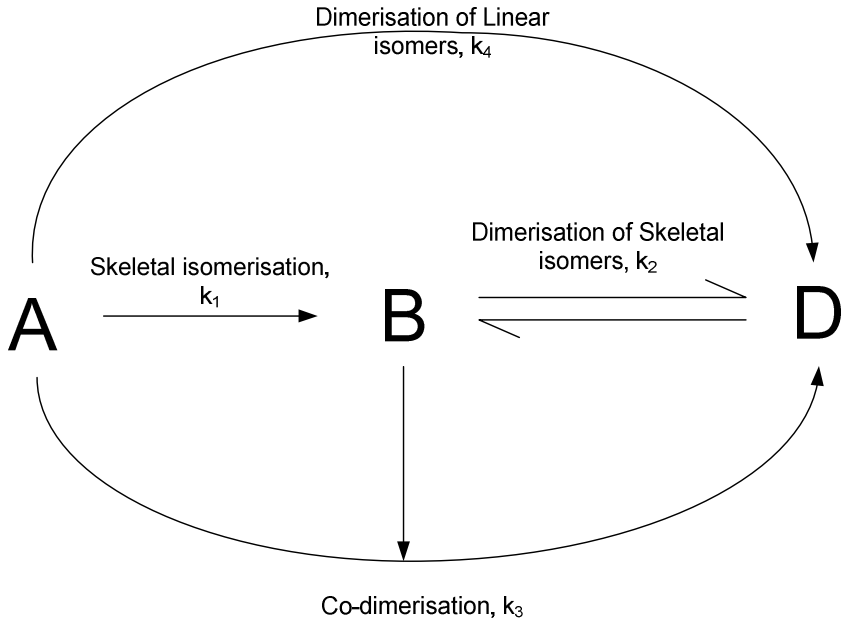

Figure 3-14: Reaction mechanism for hexene dimerisation.

Due to the almost instantaneous disappearance of 1-hexene by double bond isomerisation, all the linear hexenes could be successfully incorporated into a kinetic model as only linear hexenes (A). Even though some of the hexene isomers formed during the dimerisation of DMB seemed non-reactive (especially the group C isomers that formed to an insignificant extent), the incorporation of extra parameters to model this occurrence would only be justified if the simplified model shown in Figure 3-14 could not describe the rate of dimerisation of 1-hexene/DMB for all reaction conditions.

If double bond isomerisation is incorporated in the reaction path it is evident that the rate of double bond isomerisation far outweighed the other rate constants (Schwarzer *et al.*, 2009).

Essentially only an equilibrium constant is needed to predict the distribution of linear hexenes, as such to simplify the amount of kinetic parameters fitted to the experimental data the linear hexenes were lumped together. It is important to note that the reaction mechanism proposed in Section 2.6.2 focused extensively on the phosphoric acid ester forming with an alpha olefin, the literature focused on short chain olefins where the ester will only form with regards to an alpha olefin. For hexene oligomerisation this is not necessarily true, especially if the reaction rate of DMB is to be accounted for Figure 3-10.

Another possibility is that the rate of sorption limits the reaction rate, the first attempt at modelling the reaction rate was assuming a first order rate constant ($r_a = -kC_a$) as would be the case for sorption into another phase (Schwarzer *et al.*, 2009). This method of did not give a poor description of the reaction progression. To however reconcile all the reaction data (100 - 250 °C) the use of an elementary reaction order (second order kinetics), as would be true for a rate controlled reaction rate, improved the achieved fitting.

As such the reaction rate was modelled by using an elementary kinetic model shown in Equations 3-2 to 3-4, where k_1 is the rate of skeletal isomerisation, k_2 the dimerisation of skeletal/branched isomers (DBH), k_3 the co-dimerisation of linear and branched hexenes (CD) and k_4 the dimerisation of linear hexenes (DLH).

$$\frac{dC_A}{dt} = m_{cat}\left(-k_1 C_A - k_3 C_A C_B - k_4 C_A^2\right) \qquad 3\text{-}2$$

$$\frac{dC_B}{dt} = m_{cat}\left(k_1 C_A - k_2 C_B^2 + \frac{k_2}{K_{eq}} C_D - k_3 C_A C_B\right) \qquad 3\text{-}3$$

$$\frac{dC_D}{dt} = m_{cat}\left(k_2 C_B^2 - \frac{k_2}{K_{eq}} C_D + k_3 C_A C_B + k_4 C_A^2\right) \qquad 3\text{-}4$$

Where C is the concentration of A, B and D respectively; t is the time in min; m_{cat} is the weight concentration of catalyst; k_x is the rate constant and K_{eq} is the equilibrium distribution constant between branched hexenes and dimerised product. The optimisation of the kinetic parameter proved troublesome, particularly in view of the play-off between the CD, DLH and DBH with respect to the dimerisation of either 1-hexene or DMB. For this reason the kinetic

parameters were fitted for all the experimental data at one temperature, i.e. both the 1-hexene and DMB experimental data at a fixed temperature were used to fit the kinetic parameters, by minimising the absolute average relative error (AARE) for all the data gathered at that temperature (Equation 3-5).

$$AARE = \sum_{l} \sum_{n}^{A-D} \sum_{m} \left(\frac{\left| C_{\Pr edicted,l,n,m} - C_{Experimental,l,n,m} \right|}{C_{Experimental,l,n,m}} \right) \qquad 3\text{-}5$$

where *l* is the experiments completed at each temperature; *n* is A, B and D respectively and *m* is the data measured at each time interval.

After the optimisation of the kinetic parameters it became clear that DLH did not occur to a significant extent, and that only DBH and CD had to compensated for in order to model the experimental data. The resulting kinetic description for the experiments that were completed from 100-250 °C is shown for both 1-hexene and DMB in Figure 3-15 *a) - h)*. The kinetic fit of the experimental data allowed a good prediction of the formation and depletion of linear and branched hexenes and the resulting total depletion of hexenes for both 1-hexene and DMB dimerisation, especially taking into account that the same kinetic parameters were used to describe the reaction rate for both 1-hexene and DMB as the initial reagent. This also corroborates the inclusion of group C skeletal isomers into B.

With an increase in temperature, a more pronounced formation is seen in branched hexenes for 1-hexene dimerisation. A distinct maximum is also seen in the formation of branched hexenes at higher temperatures (Figure 3-15 *d)*), suggesting that the rate of formation of branched hexenes is more pronounced at higher temperatures.

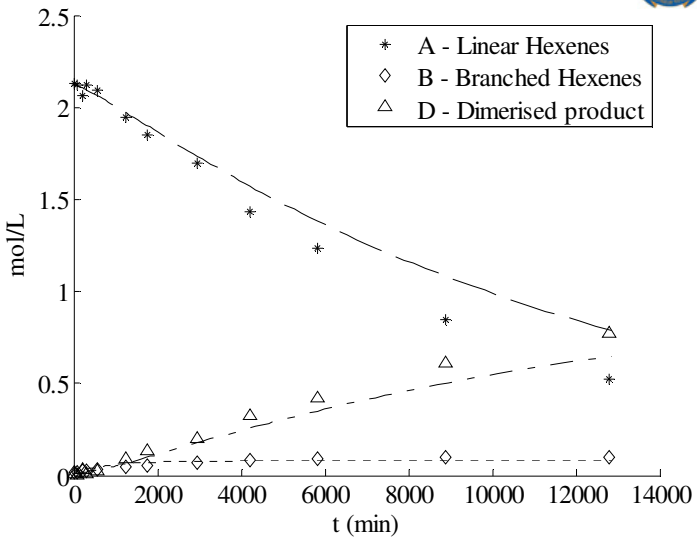

a) 1-Hexene, 100 °C

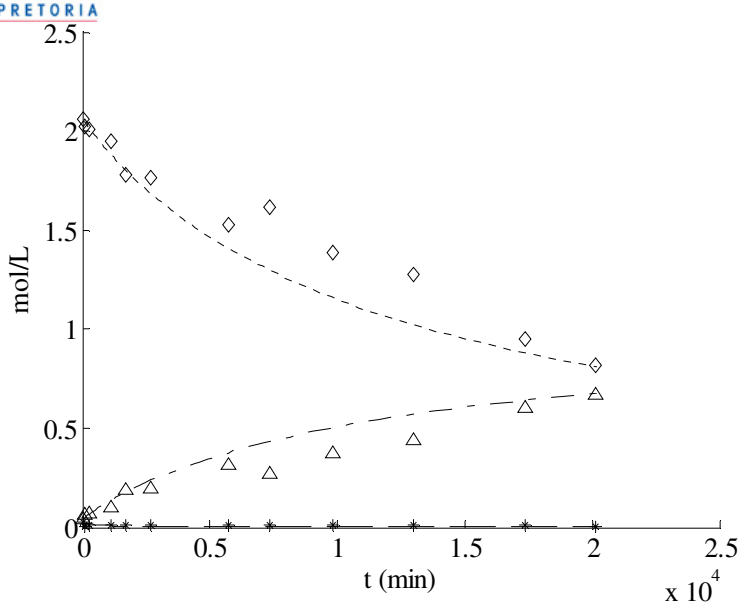

e) DMB, 100 °C

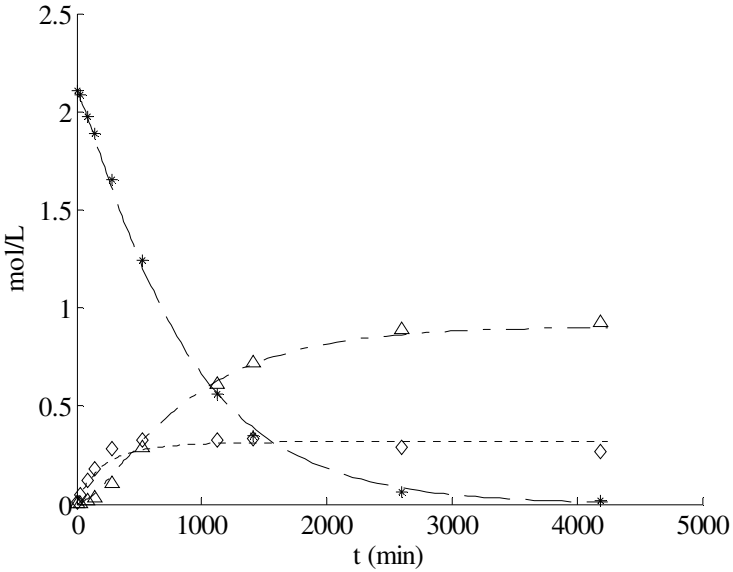

b) 1-Hexene, 150 °C

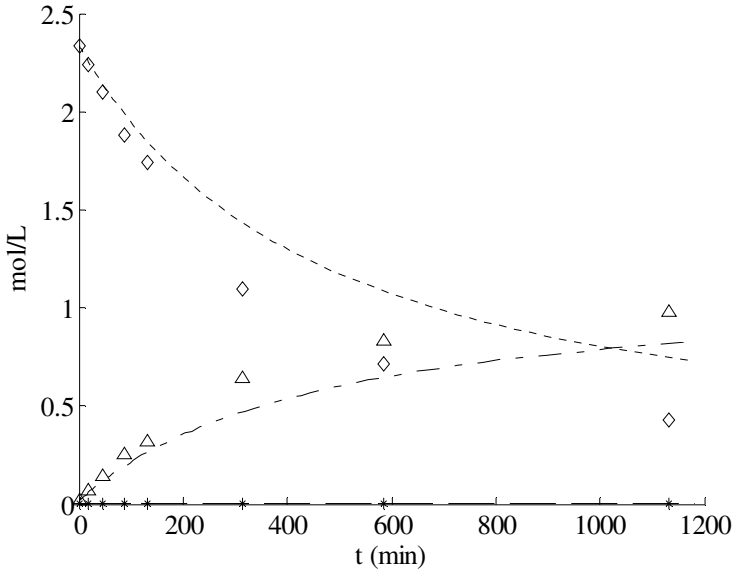

f) DMB, 150 °C

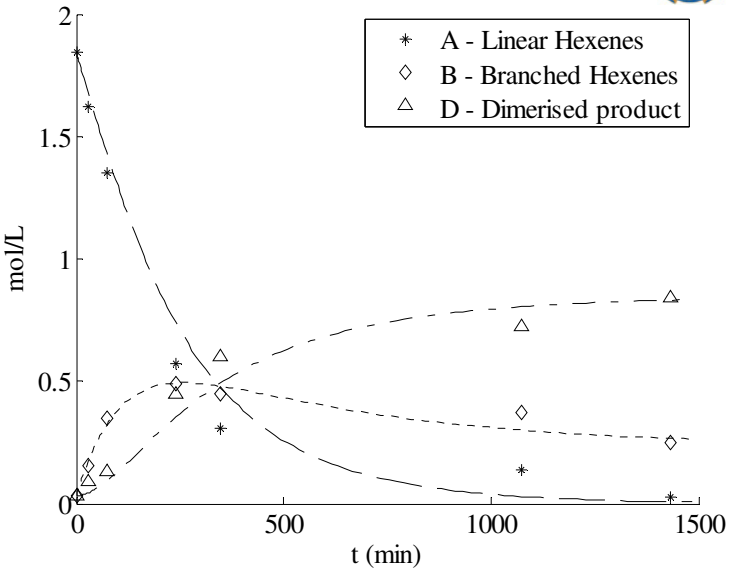

c) 1-Hexene, 200 °C

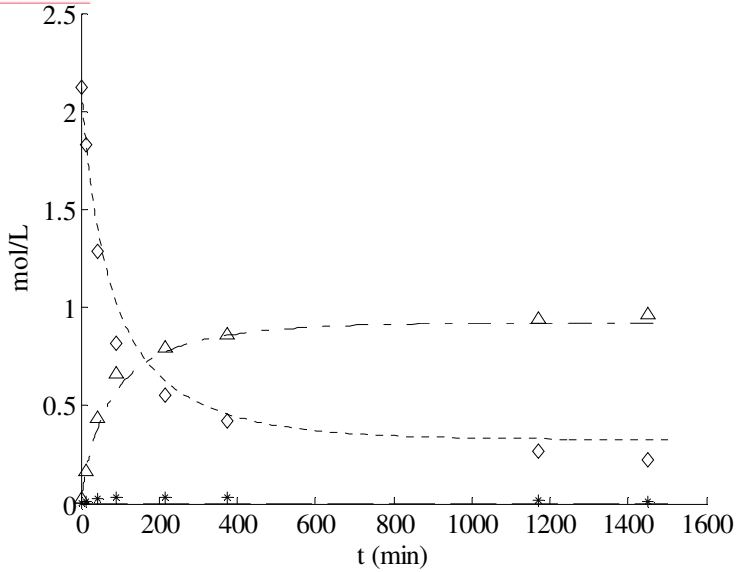

g) DMB, 200 °C

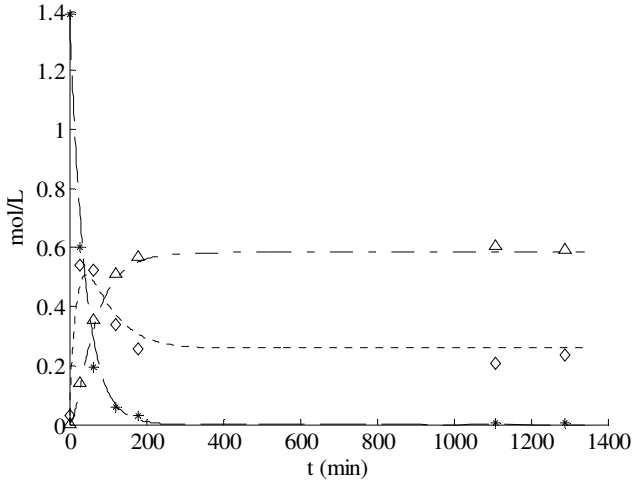

d) 1-Hexene, 250 °C

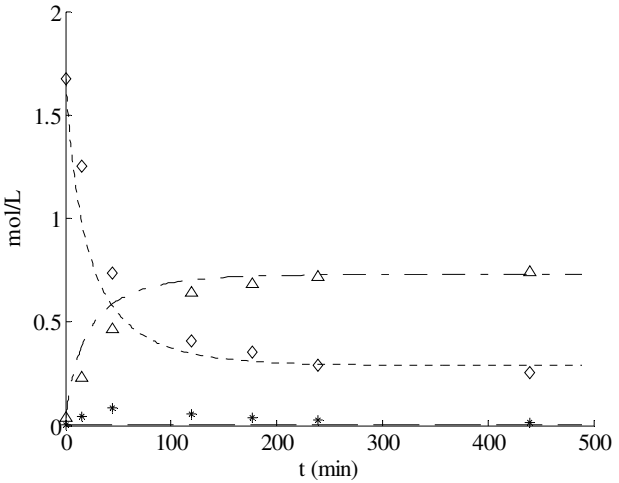

h) DMB, 250 °C

Figure 3-15: Kinetic fit of the dimerisation of 1-hexene, a) – d), and DMB, e) – h), with * - linear hexenes, ◊ - branched hexenes and △ - total hexene depletion.

To account for the temperature dependence of the rate constant, an Arrhenius relationship (Equation 3-6) can be used.

$$\ln(k_x) = \ln(k_{x,o}) + \frac{E_a}{RT} \qquad 3\text{-}6$$

where $k_{x,o}$ is the pre-exponential constant; T is the temperature in K and E_a is the activation energy.

The resulting temperature dependence of the kinetic parameters is shown in Figure 3-16.

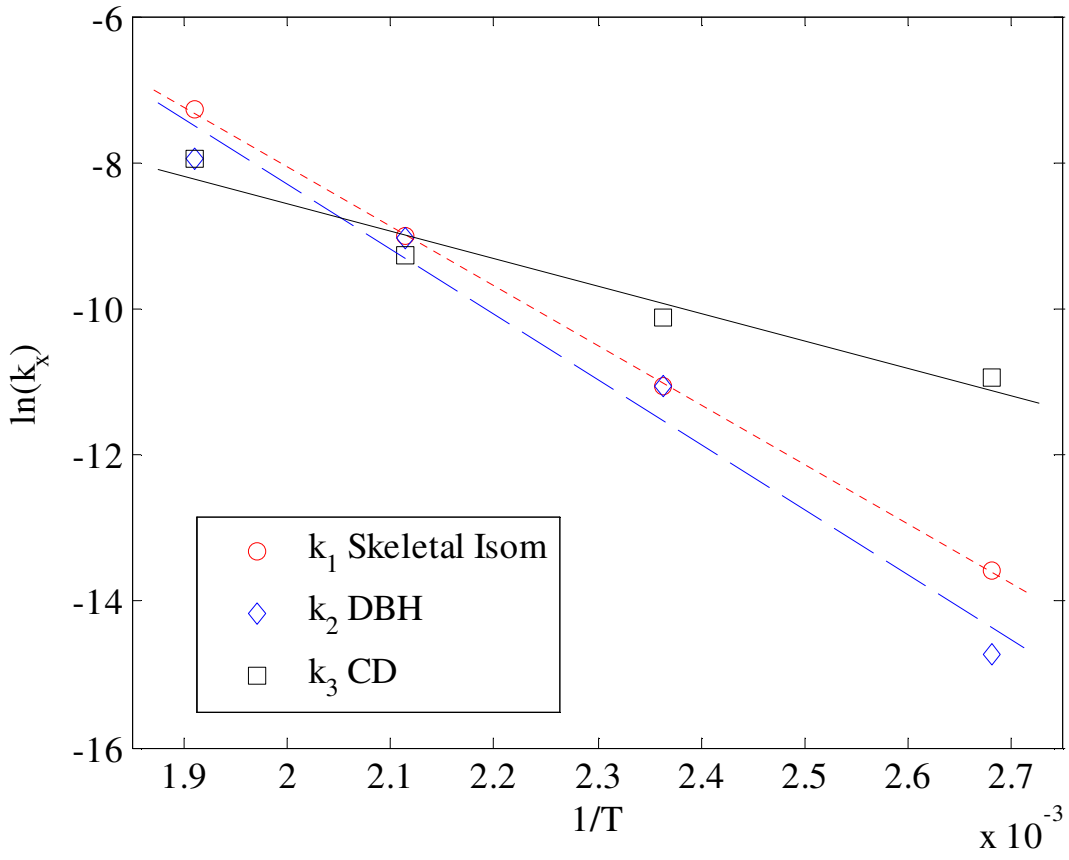

Figure 3-16: Arrhenius relationship of fitted kinetic parameters, where the rate constant is for the various steps given in Figure 3-14, k_1 – skeletal isomerisation, k_2 – DBH and k_3 – CD.

It is evident from the Arrhenius relationship that at low temperatures (100 – 150 °C), dimerisation (either by DBH or CD) is limited by the rate of skeletal isomerisation. The large activation energy for skeletal isomerisation has the result that at higher temperatures (200 – 250 °C) the dimerisation of hexenes can occur more freely.

The modelling of the reaction rate does not cover what transpires in the product after dimerisation, i.e. cracking and secondary dimerisation. It is clear from Figure 3-13 that the product ratio evens out quickly, irrespective of the reaction temperature or the residence time. Therefore, to correlate the product distribution with regard to the amount of dimerised hexene (D), the cracking distribution can be defined as specified by K_{eq} (Equation 3-1). The determined K_{eq} values can be represented by a Van't Hoff relationship, Figure 3-17. The straight-line relationship is not perfect over the entire temperature range, although the general trend obeys the Van't Hoff relationship.

It is clear that the formation of longer chain olefins (C_{12} and C_{13}) is favoured at low temperatures whereas the formation of cracked (and secondary dimerised) product is favoured at higher temperatures.

If the predicted temperature relationship is compared to the product distribution observed for the dimerisation of DMB (Figure 3-18), a large divergence in the resulting formation of cracked products is evident. There is a greater selectivity to the formation of secondary cracked products (C_8, C_9 and C_{10}) from the dimerisation of shorter chain olefins (C_4, C_5 and C_7), for DMB. DMB will form predominantly branched products in comparison to 1-hexene, especially at lower temperatures, as such more cracking will occur more readily to lower chain olefins which will then convert quickly due to the increased reaction rate of shorter chain olefins. By contrast, the formation of longer chain olefins (C_{11}, C_{12} and C_{13}) correlate well with the 1-hexene product spread, especially at higher temperatures. The differences seen in the product formation from DMB dimerisation and 1-hexene dimerisation can be linked to the lack of CD for the dimerisation of DMB. Since it is not possible to distinguish which products (carbon length) originate from CD or from the DBH, the comparison of the product distribution between 1-hexene and DMB is mute.

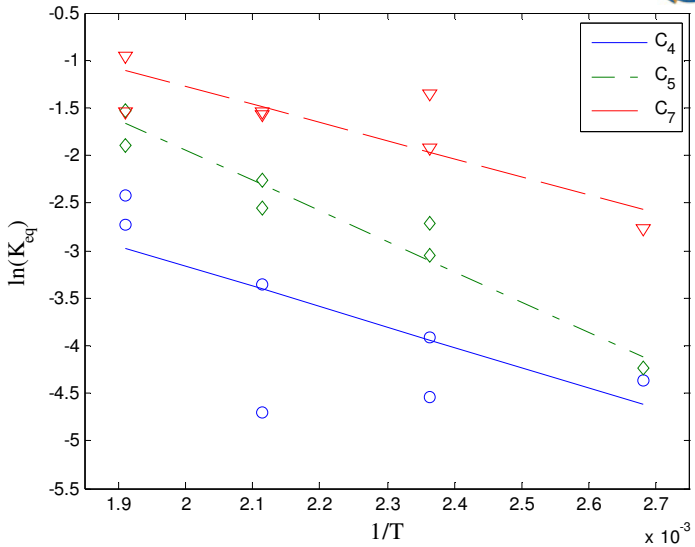

a) ○ - C_4, ◊ - C_5 and ▽ - C_7

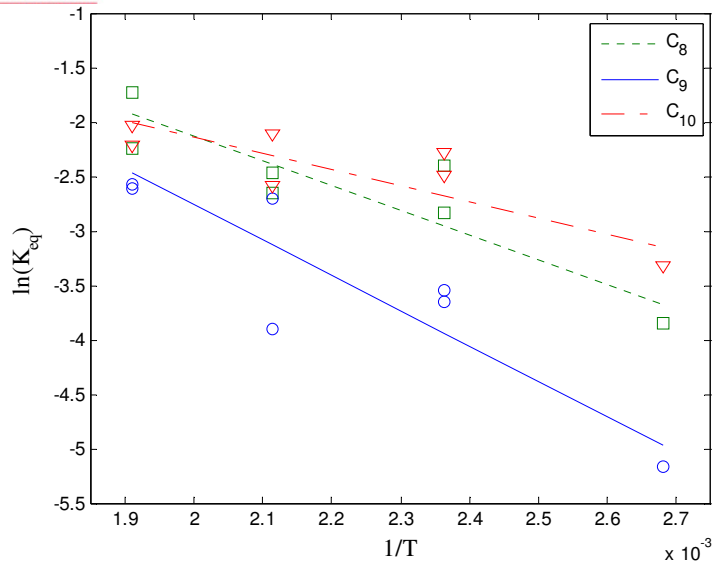

b) □ - C_8, ○ – C_9 and ▽ - C_{10}

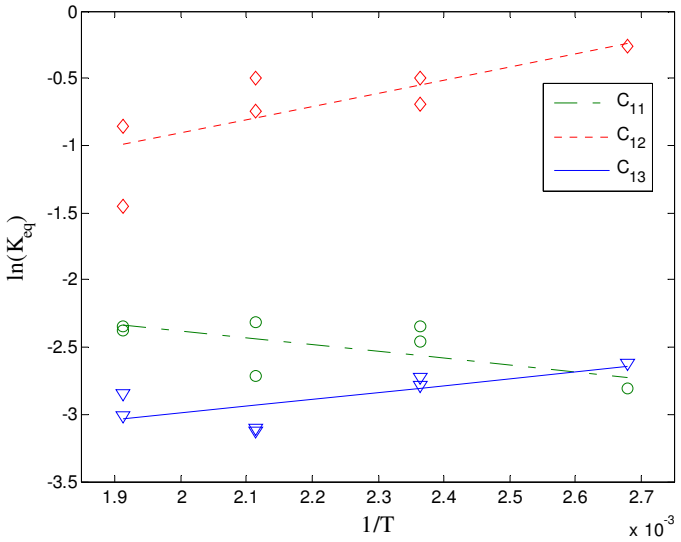

c) ○ - C_{11}, ◊ - C_{12} and ▽ - C_{13}

Figure 3-17: $\ln(K_{eq})$ for each carbon number versus 1/T for 1-hexene dimerisation (excluding C_6) *a)* C_4, C_5 and C_7, *b)* C_8, C_9 and C_{10} and *c)* C_{11}, C_{12} and C_{13}.

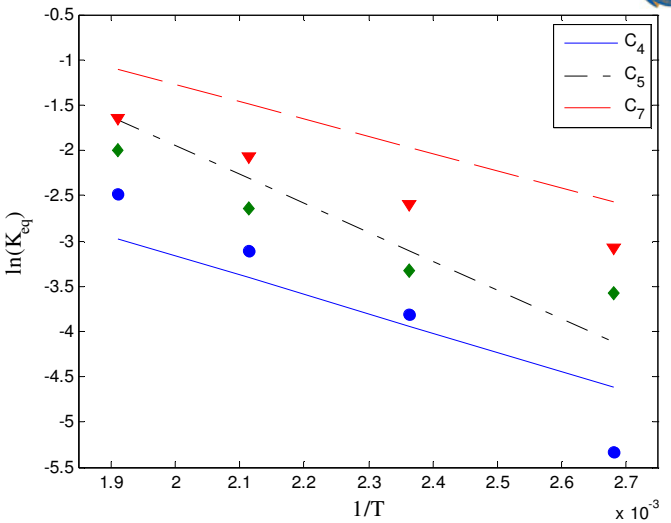

a) ○ - C_4, ◊ - C_5 and ▽- C_7

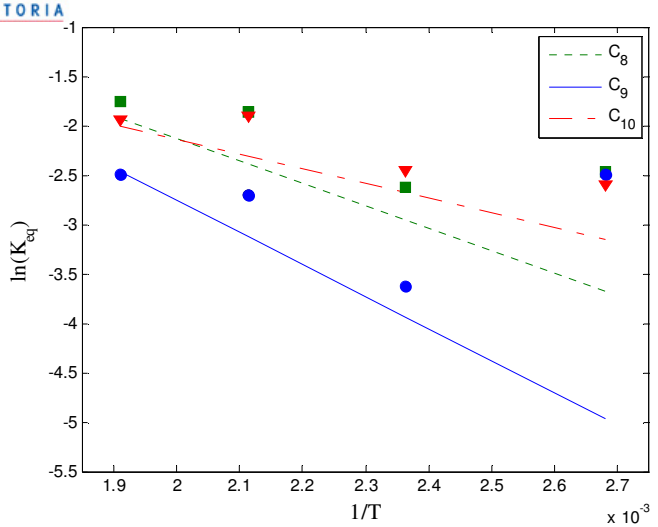

b) □ - C_8, ○ - C_9 and ▽- C_{10}

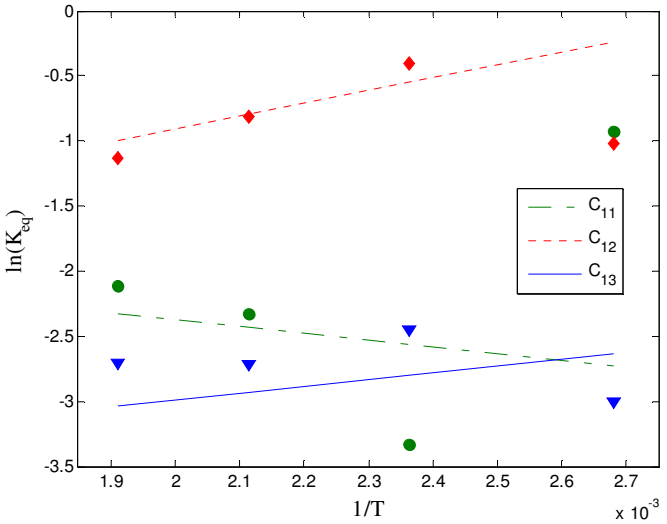

c) ○ - C_{11}, ◊ - C_{12} and ▽- C_{13}

Figure 3-18: $\ln(K_{eq})$ for each carbon number versus 1/T for DMB dimerisation a) C_4, C_5 and C_7, b) C_8, C_9 and C_{10}, and c) C_{11}, C_{12} and C_{13}, the solid lines representing the carbon distribution observed for 1-hexene dimerisation (Figure 3-17).

3.5 Conclusions

A reaction mechanism was proposed for the dimerisation of 1-hexene whereby dimerisation can occur by the dimerisation of linear hexenes (DLH) or, after skeletal isomerisation has occurred, by the co-dimerisation of linear and branched hexenes (CD) as well as the dimerisation of branched hexenes (DBH). To determine the kinetic parameters, kinetic experimental data was obtained, using a batch reactor from 100 – 250 °C for both 1-hexene and DMB as reagents.

The reaction rate was described, using a simple elementary kinetic model which resulted in a good description of the dimerisation of DMB and of 1-hexene. When modelling the reaction rate, it was found that the rate of DLH was negligible. Indicating that skeletal isomerisation needs to take place before oligomerisation of the hexenes will occur. Only the DBH and CD were needed to model the reaction rate, with CD taking place mainly at lower temperatures and DBH mainly at higher temperatures.

It was shown from the analysis of the reaction product that the carbon number distribution reached an equilibrium distribution almost instantaneously. Therefore the extent of cracking is solely a function of temperature. The resulting carbon number distribution from the cracking of dimerised product could be described, using a simple equilibrium distribution which resulted in an adequate prediction of the carbon number distribution for 1-hexene dimerisation.

The oligomerised product also contained high fractions of aromatics, even at lower temperatures, which increased with temperature. Aromatic formation has been shown to occur for propene oligomerisation by Ipatieff (1935) and Ipatieff and Corson (1936) although at much higher temperatures. Van der Westhuizen *et al.* (2010) showed the presence of aromatic precursors at lower temperatures, for light olefin oligomerisation. Therefore it is concluded that the aromatic formation is propagated with the addition of 1-hexene to the reaction mixture.

4 Effect of Acid Strength on 1-Hexene Dimerisation

It is usually assumed for an acid-catalysed reaction that the rate of reaction is proportional to the acid strength of the catalyst. The literature review covering the effect of hydration on the oligomerisation of olefins summarises the importance of acid strength on the resulting products (Section 2.5). Investigations in the literature focused on the effect of acid strength on the oligomerisation of short chain olefins at a constant space velocity, but there is little in the literature to link the effect of acid strength to the reaction kinetics, especially when oligomerising/dimerising longer chain olefins.

Due to the hydrophilic nature of SPA, the addition of water to the reaction system would result in the adsorption of water to "*free acid*", altering the acid strength of the catalyst and presumably resulting in an inhibited reaction rate. This allowed the opportunity of investigating the reaction rate at various acid strengths of the free acid by the addition of water or by the pre-treatment of the catalyst.

4.1 Experimental

To investigate the effect of the acid strength of SPA on the reaction rate of hexene dimerisation, batch experiments were completed at 150, 200 and 250 °C for various hydration levels within the catalyst. The acid strength of the catalyst was altered either by the addition of water or by the pre-treatment of the catalyst.

4.1.1 Acid strength characterisation

The literature abounds with different methods to describe the acid strength of phosphoric acid, e.g. *% H_3PO_4* or *% P_2O_5*. For consistency, in this chapter the acid strength of the SPA is expressed as the fraction of phosphoric pentoxide (P_2O_5) in water. Since the active phase of SPA is the supported liquid phosphoric acid (free acid), when the acid strength is discussed it is with reference to the strength of the free acid. Determining the activity of the catalyst requires that certain parameters of the catalyst should be known:

- Firstly, the free acid content. This is the weight fraction of free acid that is supported on the catalyst, expressed as weight percentage H_3PO_4 per gram of catalyst.
- Secondly, the acid strength of the free acid. This is determined by the pre-treatment of the catalyst.

The acid strength of the phosphoric acid is fixed by the pre-treatment of the catalyst. Before any experiments were run as discussed in Chapter 3, the catalyst was first dried at 200 °C to ensure a constant hydration of the catalyst. This defines the base acid strength for this investigation; since the catalyst was left in the oven overnight it can be assumed that an equilibrium distribution of water and phosphoric acid is present for the acid. From the investigation of Ohtsuka & Aomura (1962) it was shown that heating of SPA at 200 °C stabilises at either 74.5%, 73% and 72% dependent on the type of kiezelguhr support used for the preparation of the SPA. Since a Celite support, from America, was used for the SPA in this investigation the acid strength was taken as 72%. From Figure 2-5 it is evident that the acid distribution of the Celite SPA did not yet stabilise after 10 hours of pre-treatment at 200 °C. The difference between 72% (Celite) to 74.5% (Makkari kiezelguhr, for which the acid distribution did stabilise) would however not influence the modelling of the reaction kinetics but only alter the base line acid strength. As such for all experiments completed in Chapter 3 the base line acid strength of the supported liquid phosphoric acid will be assumed to be 72% P_2O_5 as well as further experimental work completed where the catalyst is pre-treated at 200 °C.

To determine the free acid content present on the dried catalyst, the technique described by Cavani *et al.* (1993) was used whereby the catalyst is washed with water at room temperature for 10 min – leaching off the supported liquid phosphoric acid. The acid concentration is then calculated from the quantity of acid neutralised by the titration of the leached acid with a 0.2 Molar solution NaOH to a pH of 4.62 (Coetzee *et al.*, 2006). The free acid content of the catalyst pre-treated at 200 °C was determined to be 21.6% (on a weight basis), which is similar to the values reported in the literature (Table 3-1).

This defined the free acid content of the catalyst as well as the acid strength of the SPA before the experiment started (as used in Chapter 3). Two sets of experiments were completed: firstly, to investigate the effect of free acid content at a constant temperature and secondly, to investigate the effect of the acid strength at various temperatures.

The effect of acid strength was investigated by altering the initial hydration of the catalyst. This was accomplished by the addition of water (up to 2000 ppm) to the solvent (and reagent) or by drying the tetradecane and solvent with a molecular sieve. The effect of hydrating/drying the catalyst at 150, 200 and 250 °C could then be determined with reference to the reaction kinetics of SPA baked at 200 °C (Chapter 3). Water was added to the solvent before the mixture was heated; meaning that once the reaction temperature was reached and the 1-hexene injected, the SPA had already adsorbed the added water and reached the desired

acid strength. The rest of the experimental procedure was kept similar as described in Section 3.2.2. For each experiment the P_2O_5 percentage (acid strength) was subsequently calculated with reference to the base acid strength of 72% P_2O_5 using Equation 4-1.

$$P_2O_5(W\%) = \frac{P_2O_5{}^{o} * W_{Free\ acid}}{W_{Free\ acid} + W_{H_2O}} \qquad 4\text{-}1$$

where $W_{Free\ acid}$ is the weight free acid content, as determined from the titration of the catalyst with NaOH, $P_2O_5°$ is defined as the base catalyst phosphoric acid strength and W_{H20} is defined as the quantity of grams of water added to the reaction mixture. The experiments that were completed to investigate the effect of hydration are shown in Table 4-1.

Table 4-1: Experiments completed where the catalyst was hydrated/dried at various temperatures.

T (°C)	State	m_{cat} (g)	V (L)	Free acid content (W %)	Acid strength (% P_2O_5)
150	Hydrated	5.4	0.17	21.6%	60.5%
	Normal	7.2	0.18	21.6%	71.3%
		5.6	0.17	21.6%	71.3%
	Excess catalyst/drying	21.4	0.15	21.6%	71.8%
200	Hydrated	5.0	0.20	21.6%	59.6%
	Normal	4.3	0.19	21.6%	70.8%
		5.1	0.21	21.6%	70.9%
		5.3	0.19	21.6%	71.0%
	Excess catalyst/drying	5.1	0.20	21.6%	71.5%
		15.1	0.18	21.6%	71.8%
250	Hydrated	5.8	0.29	21.6%	56.9%
	Normal	6.4	0.25	21.6%	70.9%
		8.0	0.25	21.6%	71.1%
	Excess catalyst/drying	15.3	0.22	21.6%	71.8%

The effect of altering the free acid content was investigated on the reaction rate at 200 °C. The free acid content of the catalyst was manipulated by pre-treating the catalyst in one of two ways: *1)* the catalyst was washed for 10 min in water and then dried at 200 °C; *2)* the

catalyst was baked overnight in an oven at 600 °C (in an attempt to remove most of the free acid from the catalyst (Cavani *et al.*, 1993)). A reference point is needed to correlate the acid strength at this increased pre-treatment temperature. Since the acid strength for pre-treatment at 200 °C was close equilibrated value for acid strength, therefore the acid strength value was chosen as 86% P_2O_5 (Brown and Whitt, 1952).

The methods described above can be used to give a complete overview of acid strength on the rate of 1-hexene dimerisation over SPA. Accordingly, to formulate the effect of acid strength and free acid content on the reaction rate, the experiments completed at 200 °C (shown in Table 4-1) could then be supplemented by the experiments where the free acid content was altered at 200 °C (listed in Table 4-2) to give an indication of the effect of free acid and acid strength on the reaction rates.

Table 4-2: Experiments completed to investigate the effect of acid strength on the reaction rate at 200 °C by altering the free acid content.

T (°C)	State	m_{cat} (g)	V (L)	Free acid content (W %)	Acid strength (% P_2O_5)
200	*Baked 600 °C*	5.5	0.20	0.4%	49.8%
	SPA washed and dried	6.3	0.20	5.7%	66.4%
	SPA washed and dried	3.3	0.20	5.7%	66.4%

Two experiments were also completed with homogeneous ortho phosphoric acid (Sigma-Aldrich, 345245, ortho phosphoric acid 99.999%) and pyro phosphoric acid (Sigma-Aldrich, 43314, ≤ 80% pyro phosphoric acid) to gain an idea of the difference in the reactivity of the two acids. The experiments were completed by using a glass insert to protect the stainless steel reactor from the liquid phosphoric acid.

4.2 Results and discussion

The reaction kinetics was modelled as described in Section 3.4 for the experiments completed that were dependent on acid strength. The reaction rate was modelled by using an elementary kinetic model, shown in Equation 3-2 to 3-4 The AARE was minimised by optimising the rate constant applicable to a specific acid strength and temperature.

$$\frac{dC_A}{dt} = m_{cat}\left(-k_1 C_A - k_3 C_A C_B\right) \qquad 3\text{-}2$$

$$\frac{dC_B}{dt} = m_{cat}\left(k_1 C_A - k_2 C_B^2 + \frac{k_2}{K_{eq}} C_D - k_3 C_A C_B\right) \qquad 3\text{-}3$$

$$\frac{dC_D}{dt} = m_{cat}\left(k_2 C_B^2 - \frac{k_2}{K_{eq}} C_D + k_3 C_A C_B\right) \qquad 3\text{-}4$$

4.2.1 Reaction rate for liquid ortho and pyro phosphoric acid

It has been shown that the acid strength of liquid phosphoric acid affects the rate of oligomerisation of short chain olefins (Bethea & Karchmer, 1956), Section 2.5. By contrast, this investigation was for liquid phosphoric acid with reference to propene, where no isomerisation can occur. To gain a preliminary idea of how the reaction rate of 1-hexene dimerisation changes, depending on the acid strength, 1-hexene was dimerised at 200 °C using both ortho and pyro phosphoric acid. Ortho phosphoric acid dehydrates to form pyro phosphoric acid (Equation 2-6):

$$2H_3PO_4 \leftrightarrow H_4P_2O_7 + H_2O \qquad 2\text{-}6$$

From the phosphoric acid distribution (ortho, pyro, tri phosphoric acid, etc.) measured by Jameson (1959) for various acid strengths of phosphoric acid (Figure 2-2), both ortho and pyro phosphoric acid will be present on the free acid on SPA. For low acid strengths (<68% P_2O_5), only ortho phosphoric acid should be present, whereas pyro phosphoric acid peaks at about 78% P_2O_5. One easy measure of the activity of the two acids is the dissociation constant of the acids (Section 2.4): the first dissociation constant for ortho phosphoric acid is 7.5×10^{-3} whereas pyro phosphoric acid has a first dissociation constant of 1.4×10^{-1}, indicating that pyro phosphoric acid is a much stronger acid. For this reason, the difference in the kinetics seen for ortho and pyro phosphoric acid is crucial to understanding how the reaction rate is affected by acid strength.

The kinetic parameters obtained from the optimisation are shown in Table 4-3, with the resulting description of the kinetic data shown in Figure 4-1 a) and b). Even though the kinetic parameters shown in Table 4-3 are based on the mass of the acid added, the comparison by mass will give a good indication of the difference in reactivity between the two acids due to dissociation. It is evident from Table 4-3 that pyro phosphoric acid is far more active toward the dimerisation of 1-hexenes. It can also be seen when comparing Figure 4-1 *a)* and *b)* that skeletal isomers form faster when pyro phosphoric acid is the catalyst (which is supported by the kinetic parameters).

The increased in reaction rate with the increase in acid strength is to be expected. It is though intriguing that skeletal isomerisation and the dimerisation of branched hexenes (DBH) is affected to a much more significant extent than the rate of co-dimerisation (CD) of linear and branched hexenes. The change is due to skeletal isomerisation occurring more readily which results that CD occurs to a much lesser extent.

Table 4-3: Kinetic parameters obtained for the dimerisation of 1-hexene over liquid ortho and pyro phosphoric acid. Where the rate constants are for the various steps given in Figure 3-14, namely k_1 – skeletal isomerisation, k_2 – dimerisation of branched hexenes (DBH) and k_3 – the co-dimerisation of linear and branched hexenes (CD).

	Pyro phosphoric acid	Ortho phosphoric acid
k_1 (L/min.g)	30.6×10^{-6}	4.1×10^{-6}
k_2 (L^2/mol.min.g)	107.6×10^{-6}	27.6×10^{-15}
k_3 (L^2/mol.min.g)	27.0×10^{-6}	7.9×10^{-6}

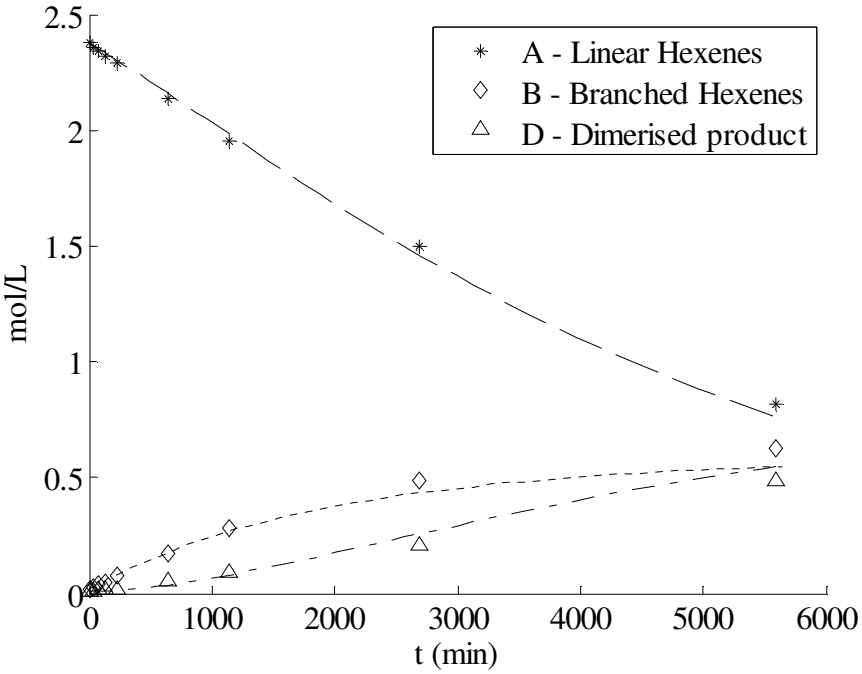

a) Ortho phosphoric acid

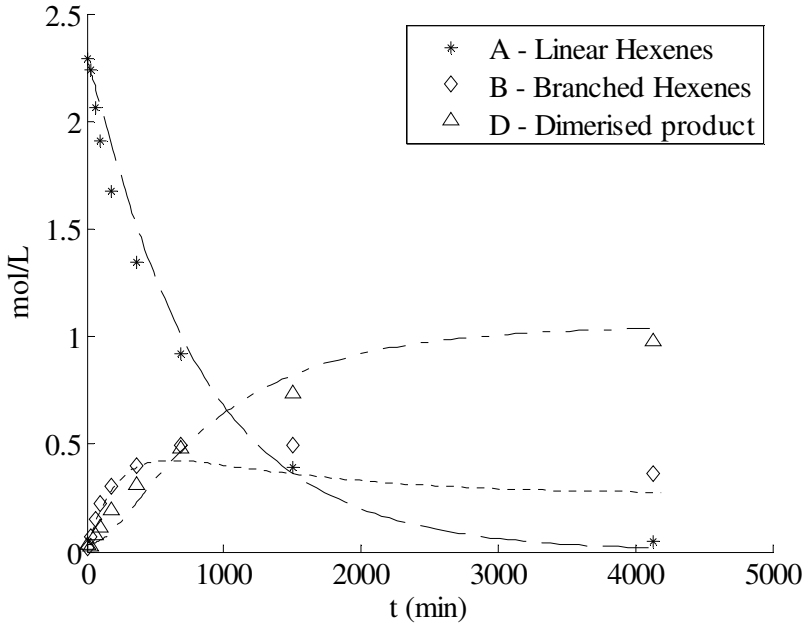

b) Pyro phosphoric acid

Figure 4-1: Dimerisation of 1-hexene at 200 °C over a) ortho phosphoric acid and b) pyro phosphoric acid where * - linear hexenes, ◊ - branched hexenes and △ - total hexene depletion.

4.2.2 Reaction kinetics for various acid strengths of SPA

Since the active phase for SPA is the free layer of phosphoric acid, the difference in reactivity between ortho and pyro phosphoric acid indicates that the activity of SPA should depend on the acid strength of the catalyst, especially taking into account that the variation in the acid strength will shift the free acid from completely ortho phosphoric acid to a mixture of ortho and pyro phosphoric acid (Figure 2-2). To estimate the effect of the acid strength of SPA, the rate of 1-hexene dimerisation was measured at a constant temperature (200 °C) for various acid strengths and acid loadings by pre-treating the reaction mixture and the catalyst. The resulting acid strength was expressed using Equation 4-1. The kinetic model expressed in Equation 3-3 to 3-4 was fitted to each individual experiment. The resulting prediction of the data is shown on each figure, Figure 4-2 and Figure 4-3. The end goal of the optimisation is to investigate the effect of acid strength on the rate constants.

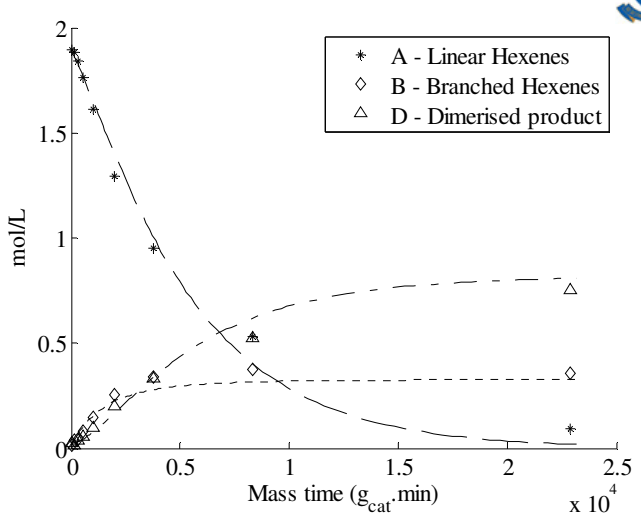

a) 49.8%

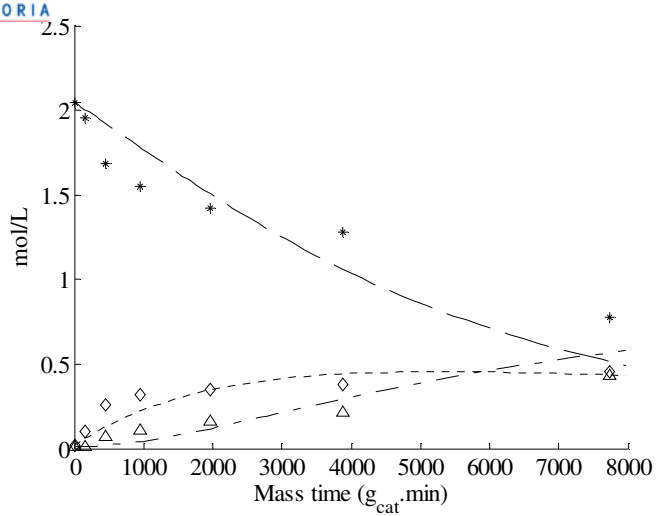

b) 59.6%

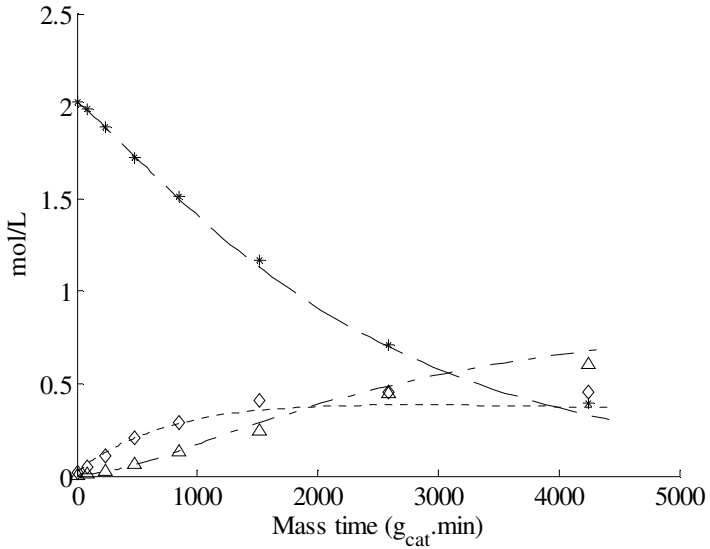

c) 66.4%

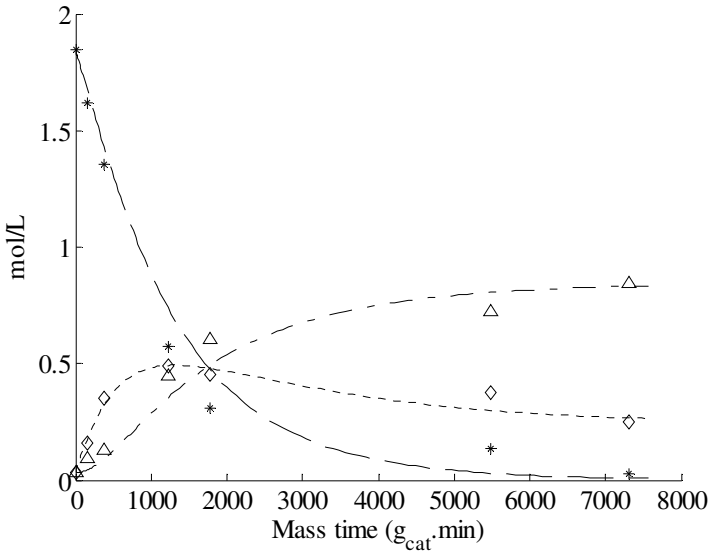

d) 70.8%

Figure 4-2: Reaction progression for the dimerisation of 1-hexene at 200 °C for acid strengths of 49.8% - 70.8% P_2O_5 , with * - linear hexenes, ◊ - branched hexenes and △ - total hexene depletion.

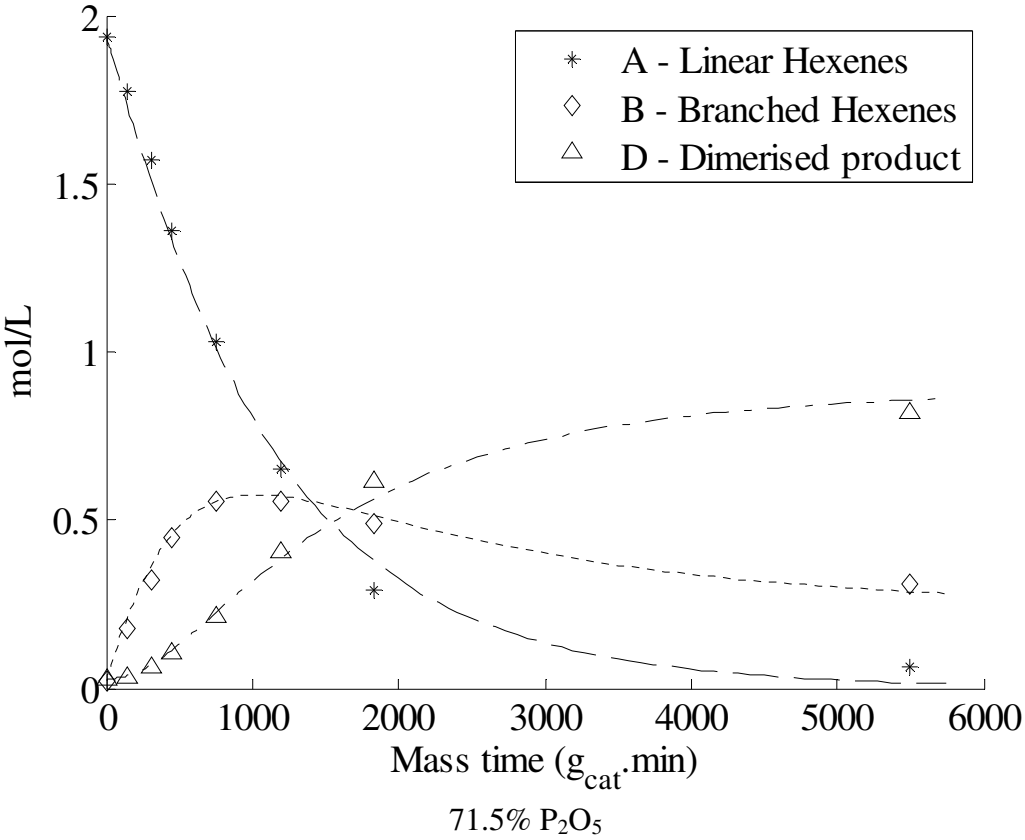

Figure 4-3: Reaction progression for the dimerisation of 1-hexene at 200 °C for an acid strength of 70.3% P_2O_5, with * - linear hexenes, ◊ - branched hexenes and △ - total hexene depletion.

For the case where the catalyst was baked at 600 °C, Figure 4-2 *a),* there was still some catalytic activity. It could be plausible that the activity is due to silicon phosphates and the presence of trace amounts of water in the feed (<50 ppm water in the reaction mixture). It is not possible to eliminate the non-reactivity of the silicon phosphates. However, if the catalytic activity is attributed to the residual acid strength present in the catalyst (either due to un-evaporated phosphoric acid or due to hydration of silicon phosphates to free acid), the acid strength of the reaction would be 49.8%. The reaction rate of the dried catalyst is though nearly negligible in comparison to the normal untreated catalyst.

When looking at Figure 4-2 *a) – d)* and Figure 4-3, the effect of acid strength is noticeable on the rate of 1-hexene dimerisation. The total rate of hexene depletion increases from an acid strength of 49.8% P_2O_5 to 71.5% P_2O_5. The reaction rate is therefore dependent on the acid strength. It is also evident that with an increase in the acid strength the formation of branched hexenes is also more significant. This suggests an increased propensity toward

skeletal isomerisation at higher acid strengths, which is beneficial for the total rate of hexene depletion. This corresponds to what was seen previously for ortho and pyro phosphoric acid (Table 4-3) and the findings of De Klerk (2004) for the oligomerisation of butenes over SPA. A more detailed analysis of the reaction rate is needed to distinguish how each reaction step is influenced by acid strength.

The resultant rate constants versus the acid strength of the catalyst are shown in Figure 4-4. An exponential growth is observed in the rate of constants for the formation of skeletal hexene isomers (k_1, Figure 4-4 *a)*) and the subsequent rate of dimerisation of branched hexenes (DBH) (k_2, Figure 4-4 c*)*). This corresponds to the increase in the first order rate constant predicted by Bethea & Karchmer (1956) for the oligomerisation of short chain olefins.

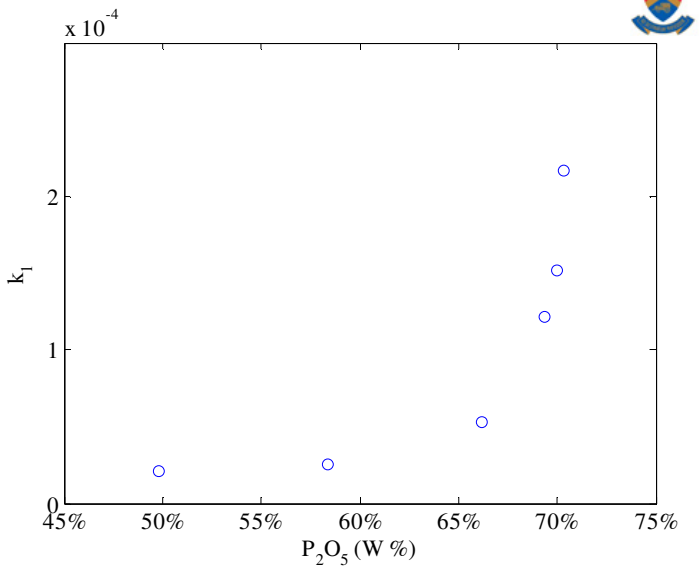

a) k_1 Skeletal isomerisation (L/min.g)

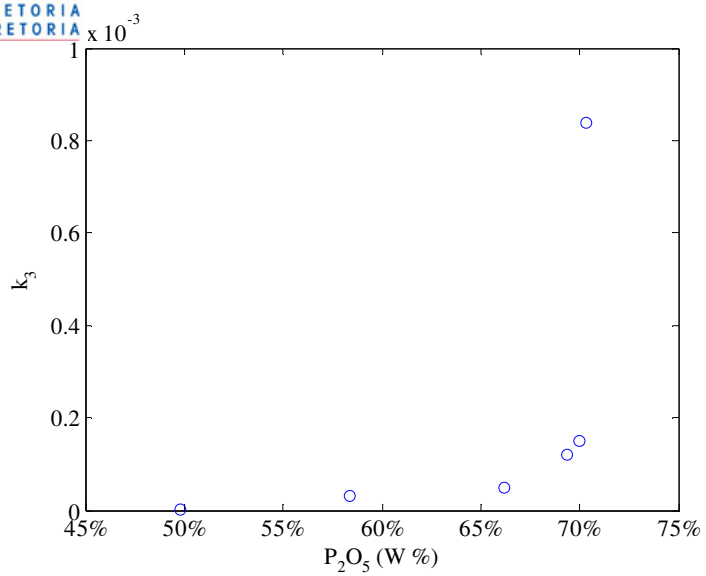

c) k_2 BHD (L^2/mol.min.g)

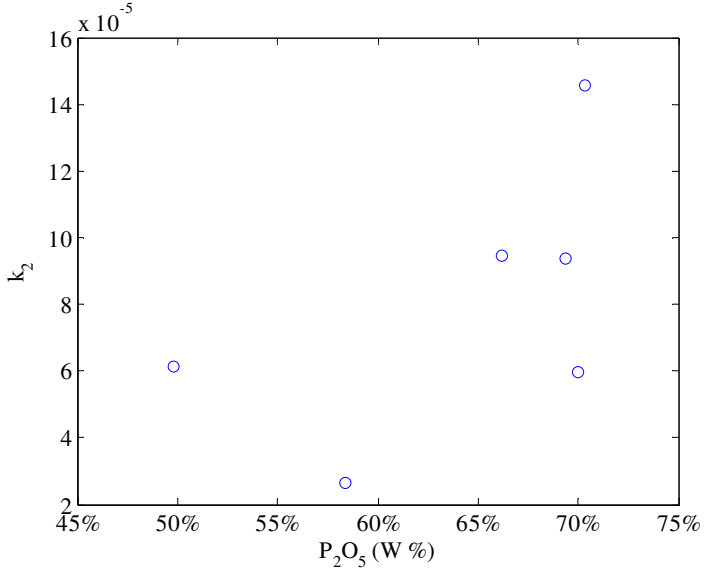

b) k_3 CD (L^2/mol.min.g)

Figure 4-4: Rate constants versus acid strength on the rate constants at 200 °C, k_1 – skeletal isomerisation, k_2 – DBH and k_3 – CD.

At low acid strengths the rate of co-dimerisation of linear and branched hexenes (CD) (k_3, Figure 4-4 b)) is similar to the rate of DBH (k_2, Figure 4-4 b)). As the acid strength increases the rate of isomerisation of branched hexenes increases significantly, which promotes the rate of DBH until the rate of CD becomes insignificant. This complicates the modelling of the rate of CD. Since the other rate constants are affected to an exponential extent by acid strength, it is plausible that the same trend would suffice for the rate of CD.

It can be seen from the dependence of the rate on acid strength for the rate of skeletal isomerisation (k_1) and DBH (k_2) that the reaction rate escalates suddenly at an acid strength of 68% P_2O_5. This is the phosphoric acid strength where the acid distribution shifts from predominantly ortho phosphoric acid to pyro phosphoric acid (Figure 2-2), indicating that pyro phosphoric acid is more active toward the dimerisation of hexenes. This corroborates the conclusion of Zhirong *et al.* (2000) that pyro phosphoric acid affects activity toward oligomerisation.

Experiments were also completed at 150, 200 and 250 °C for acid strengths of 60%, 70.5% and 71.8% P_2O_5 respectively. The reaction rate was evaluated for each individual experiment, the experimental data and the resulting fits are shown in Figure 4-5 and Figure 4-6. The dependency of each rate constant on temperature, for a specific acid strength, can then be evaluated using the Arrhenius relationship, shown in Figure 4-7.

A negative activation energy is seen for the dimerisation of branched hexenes (Figure 4-7 *c)*), because the rate of BHD is dominated by CD at lower temperatures (150 °C). The exponential relationship with acid strength is clear, however, for the rate of skeletal isomerisation (Figure 4-7 *a)*) and the CD (Figure 4-7 *b)*). Typically the reaction rate increases with an increase in the acid strength of the catalyst. This is contrary to the finding by McClean (1987) that there is an inverse dependency of some rate constants with acid strength.

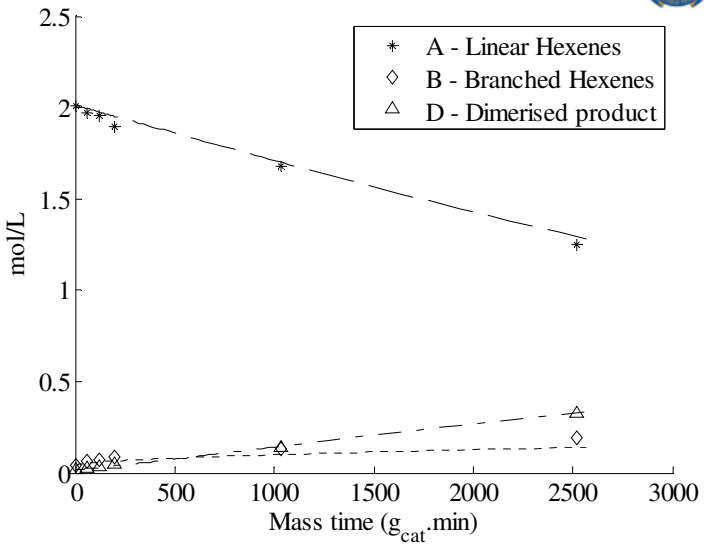

a) 60.5% P_2O_5, 150 °C

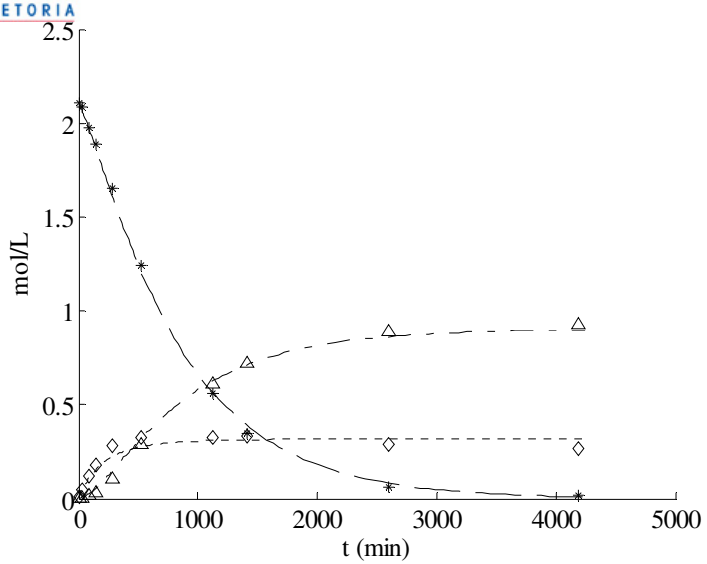

b) 71.3% P_2O_5, 150 °C

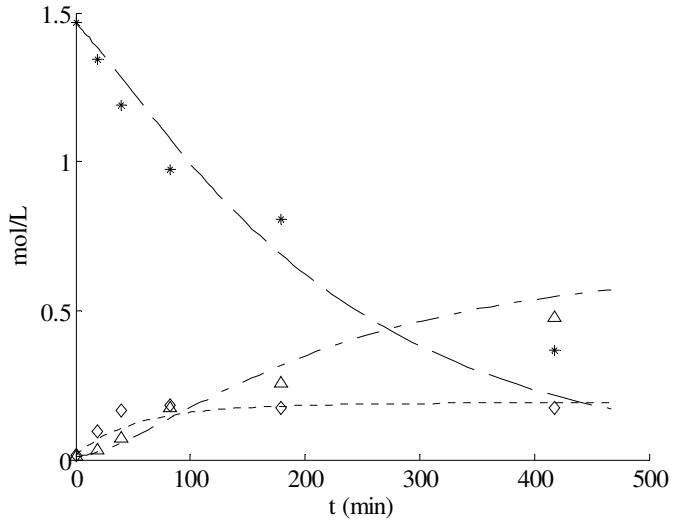

c) 71.8% P_2O_5, 150 °C

Figure 4-5: Rate of 1-hexene dimerisation for various acid strengths *a)* 60.5%, *b)* 71.3% and - *c)* 71.8% at 150 °C, with * - linear hexenes, ◊ - branched hexenes and △ - total hexene depletion.

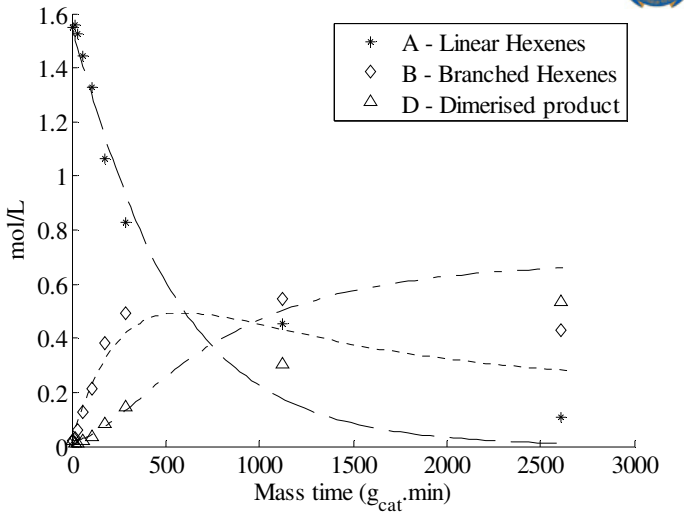

a) 59.6% P_2O_5, 250 °C

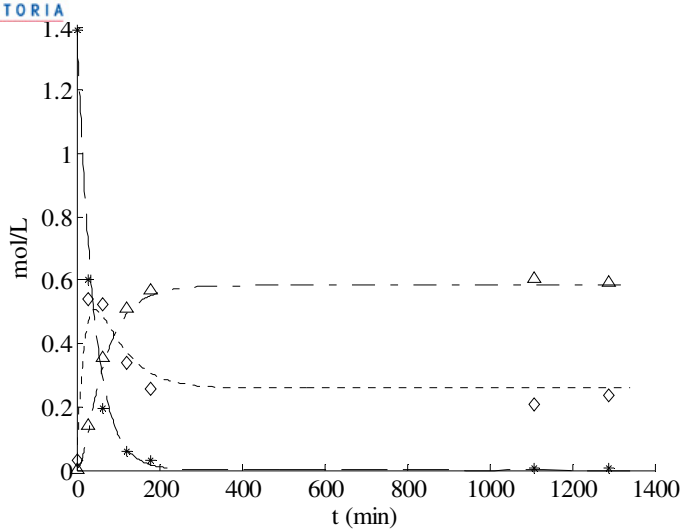

b) 70.8% P_2O_5, 250 °C

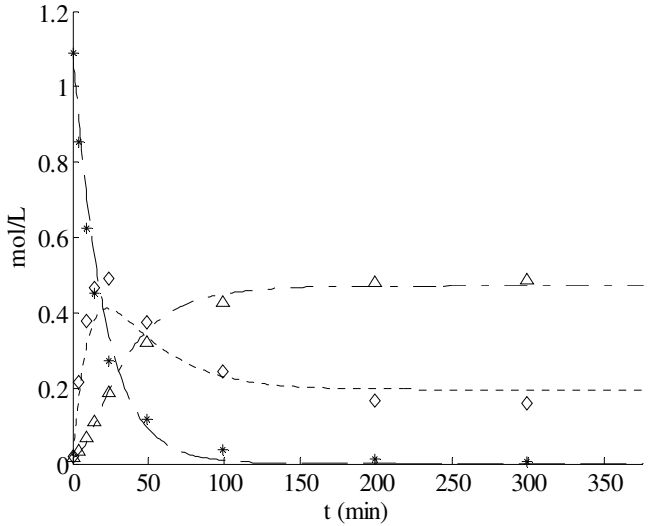

c) 71.5%, 250 °C

Figure 4-6: Rate of 1-hexene dimerisation for various acid strengths *a)* 58.4%, *b)* 73.1% - *c)* 73.7% at 250 °C, with * - linear hexenes, ◊ - branched hexenes and △ - total hexene depletion.

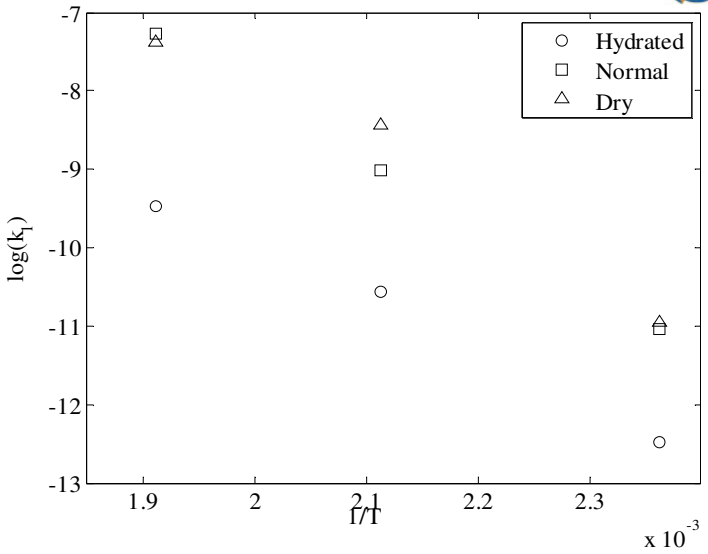

a) k_1 Skeletal isomerisation (L/min.g)

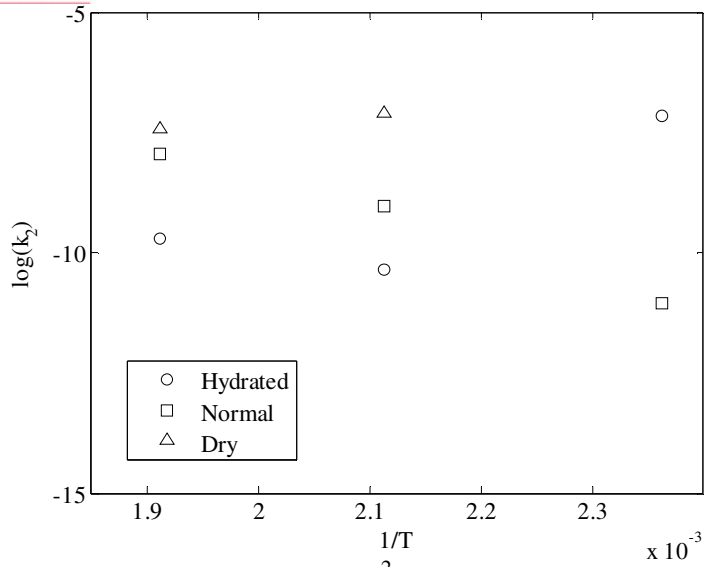

c) BHD k_2 (L^2/mol.min.g)

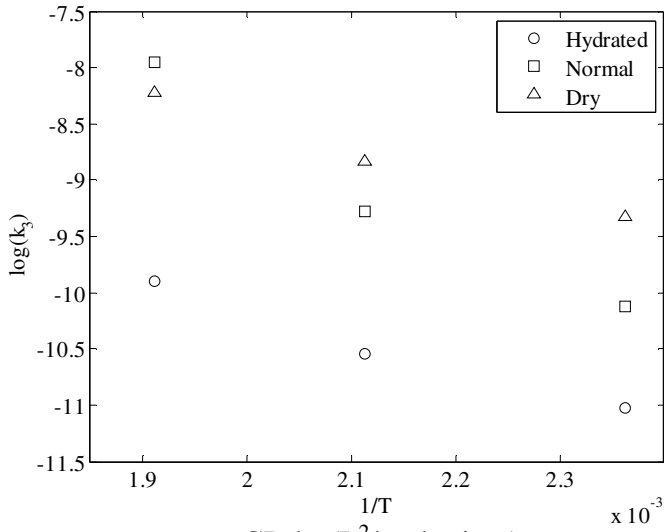

b) CD k_3 (L^2/mol.min.g)

Figure 4-7: Effect of the hydration of SPA on the rate constants, k_1 – skeletal isomerisation, k_2 – DBH and k_3 – CD.

The trends seen in the dimerisation of hexenes at various acid strengths (Figure 4-4) and temperatures (Figure 4-7) indicate that an exponential dependency persists for both temperature and acid strength. The activation energy appears constant for both k_1, k_3 with some deviation in k_2, suggesting that the activation energy for the reaction is not affected by the acid strength and that the activation energies determined previously will still hold (Figure 3-16). It would therefore be appropriate to model the reaction rate in a similar fashion as that proposed by McClean (1987), Equation 2-9, but using an exponential dependency with acid strength on the rate constant.

To describe how the rate constants for the dimerisation of hexene are affected by the acid strength, Equation 4-2 was fitted to all the kinetic data gathered (Table 3-2 and Table 4-2) by minimising the AARE between the experimental and predicted concentrations by altering the pre-exponential constant, $k_{x,o}$, and the acid strength dependency, k_{x,A_A} (where A_A is the P_2O_5 weight %). The activation energy was taken as predicted in Section 3.4.

$$k_x = k_{x,o} e^{-\frac{H_a}{RT} + k_{x,A} A_A} \qquad 4\text{-}2$$

The resulting fitted parameters are shown in Table 4-4. It is evident that the rate of skeletal isomerisation and the DBH are more dependent on the acid strength than the CD. The model's predicted rate constants (Equation 4-2) correlate well with the rate constants derived from the fitting of the individual experiments. Previously the rate constants were fitted for each individual acid strength at a specific temperature (Figure 4-4 and Figure 4-7) whereas Equation 4-2 would allow for the regression of all data simultaneously. The parity plot between the resulting rate constants is shown in Figure 4-8, and the AARE was calculated to be 29%. This was expected, since some of the previously fitted parameters showed a negative activation energy (the dry reaction rate constant, Figure 4-7 *c)*), which was not allowed for in Equation 4-2.

Table 4-4: Pre-exponential constant and acid strength dependency of rate constants

	$k_{x,o}$	k_{x,A_A}
k_1 Skeletal isomerisation (L/min.g)	1.21	11.42
k_2 BHD (L^2/mol.min.g)	3.59×10^{-3}	21.47
k_3 CD (L^2/mol.min.g)	8.79×10^{-4}	8.39

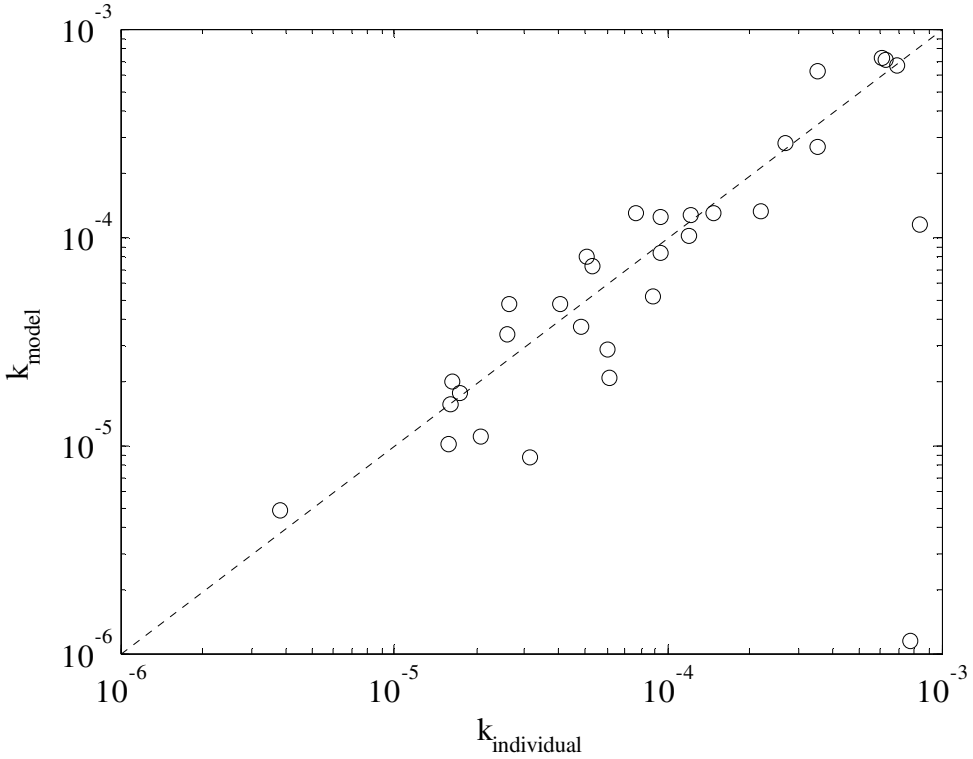

Figure 4-8: Comparison between the kinetic parameters modelled individually and the parameters of the model given in Equation 4-2.

4.2.3 Effect of acid strength on the product spectrum

If the product spectrum of the various acid strengths investigated is compared, the effect is not as obvious as it is with the reaction rate. The product distribution for various acid strengths was expressed as described in Section 3.3.2. The resulting product distribution for various acid strengths at 200 °C is shown in Figure 4-9 *a) -d)* and Figure 4-10.

From the product spectrum of the catalyst where the acid was pre-treated at 600 °C, a higher selectivity toward dimerised product was evident (Figure 4-9 *a)*). This indicates that cracking is inhibited at lower acid strengths. However, when there is an increase in acid strength from 58.4% P_2O_5 to 70.3% P_2O_5, this trend does not hold (Figure 4-9 *b)-d)*), as less cracking was seen in the case where the catalyst was washed and dried at 200 °C (Figure 4-9 *b)*) than in the cases where the catalyst was hydrated and dried (Figure 4-9 c*) & d)*). There is however a large jump in the free acid strength from the baked catalyst (600 °C, free acid = 0.4%), to the washed catalyst (free acid = 5.7%) and the hydrated/dried/untreated catalyst (free acid = 21.6%). This suggests that the free acid content affects the degree of cracking seen (i.e. less cracking is seen with lower free acid contents).

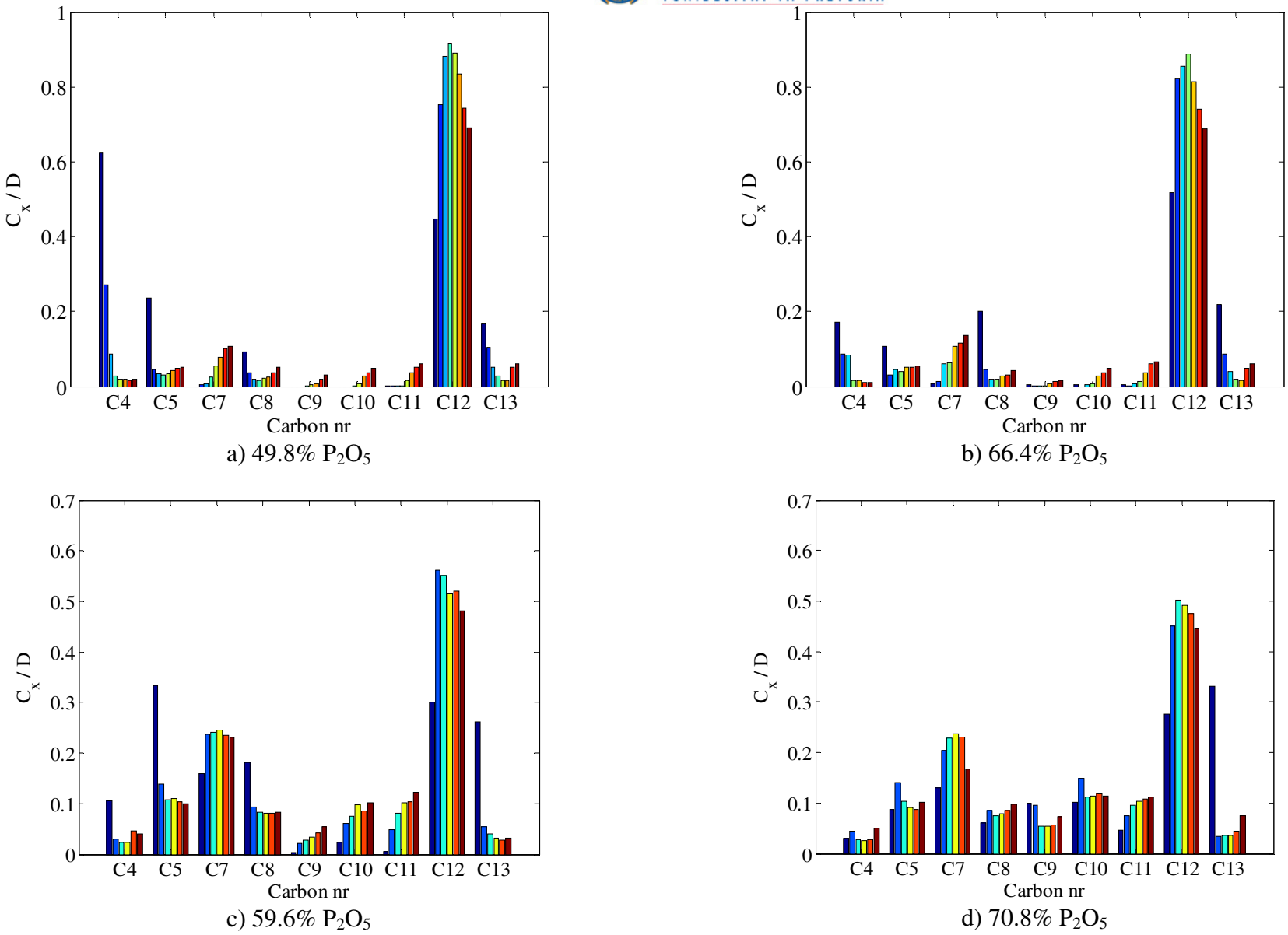

Figure 4-9: Effect of acid strength on the product spread at 200 °C, a) 49.8% to d) 69.4% P_2O_5.

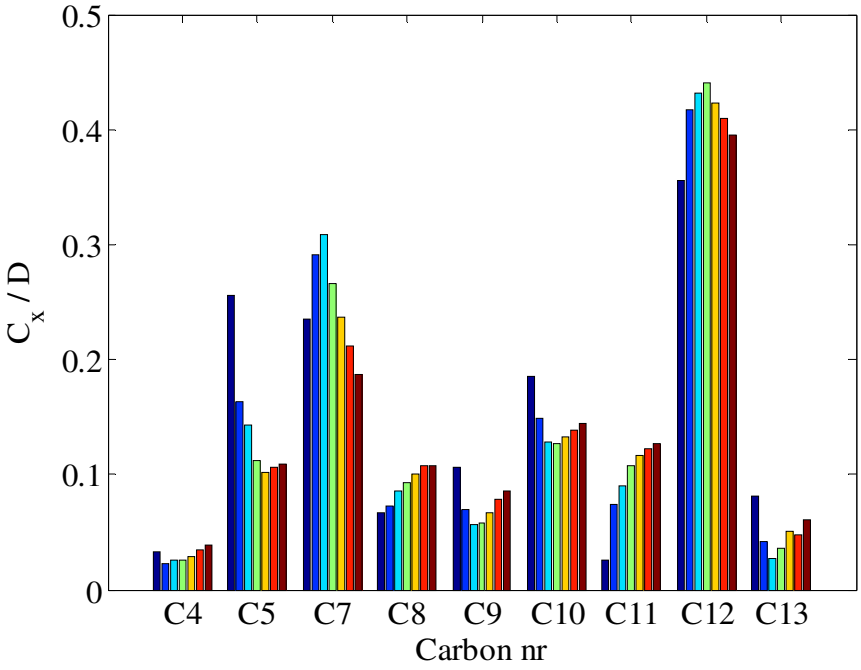

Figure 4-10: Effect of acid strength on the product at 200 °C, 71.5% P_2O_5.

The reactions where the acid strength was altered by changing the hydration of the catalyst, with the same quantity of free acid, showed little deviation in the observed product spectrum obtained in Section 3.3.2 as seen in Figure 4-11. The deviation observed is similar to the deviation seen for the dimerisation of 1-hexene (±70.8% P_2O_5). This suggests that the degree of cracking observed during the dimerisation of 1-hexene is a function of the quantity of free acid on the catalyst and the reaction temperature, and is independent of the acid strength of the catalyst. The product distribution for 1-hexene oligomerisation over SPA is essentially controlled by two reaction rates: firstly, the rate of oligomerisation and secondly, the rate of cracking. The fact that the product distribution seems unaffected by acid strength indicates that the rate of oligomerisation is always the limiting reaction, even at high hydrations. Only by dramatically influencing the free acid content does the rate of cracking become prominent. Therefore the distribution of cracking products, at a specific temperature, can be seen to be always at a pre-determined equilibrium distribution.

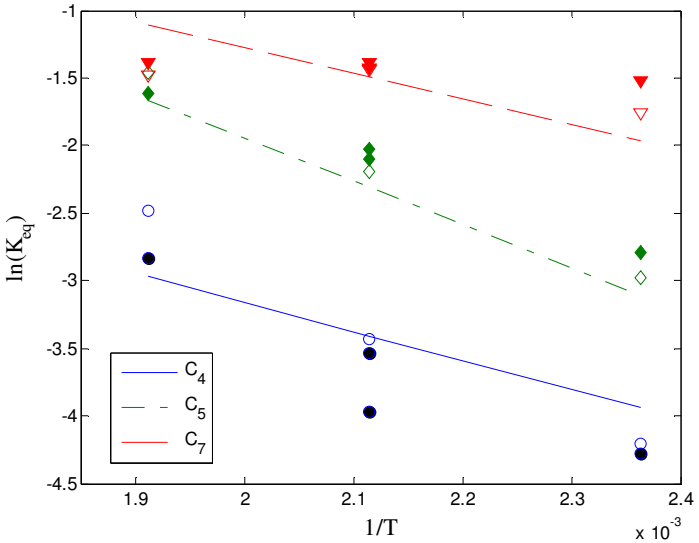

a) ○-C_4, ◊-C_5 and ▽-C_7

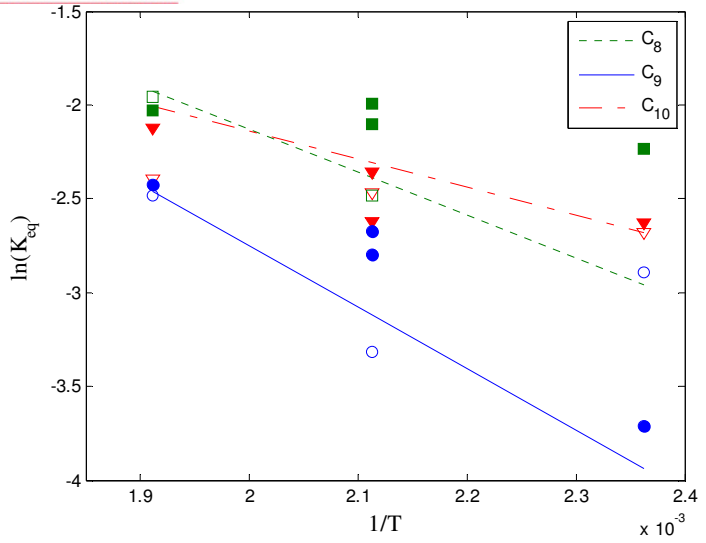

b) □ - C_8, ○ - C_9 and ▽- C_{10}

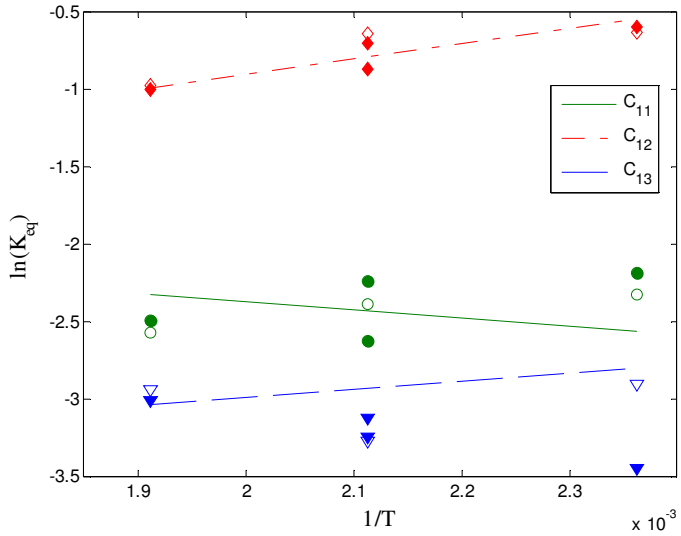

c) ○-C_{11}, ◊-C_{12} and ▽-C_{13}

Figure 4-11: The effect of acid strength on $\ln(K_{eq})$ versus the 1/T where: 59.6% P_2O_5 (open points), 71.8% P_2O_5 (solid points).

4.3 Conclusions

It was shown that the reaction rate is highly dependent on the acid strength. With a decrease in the acid strength, the reaction rate decreased considerably. An exponential dependence of the rate constant was established with acid strength, which was integrated with the temperature dependence of the reaction rate (Equation 4-2). The proposed equation enabled the prediction of the reaction rate at all the gathered temperatures and acid strengths investigated. The resulting optimisation showed that the rate of skeletal isomerisation and DBH increased to the greatest extent with an increase in acid strength.

The carbon number distribution seemed to be unaffected by the extent of hydration, but it was seen that less cracking occurred as the free acid content of the catalyst dropped. This indicated that the fraction of cracking observed was a function of the free acid content and the reaction temperature, and was not dependent on the acid strength. Where the free acid content did not vary, the product distribution remained unaffected by the acid strength of the catalyst, meaning that rate of oligomerisation is limiting when predicting the product distribution and an equilibrium distribution of cracked products can be assumed.

5 Product spectrum

The product formed from the oligomerisation of 1-hexene over SPA can be used as either lubricating oils, detergent production of fuel blending. Since it has previously been indicated that the 1-hexene does not form product longer than twenty the use for lubricating oils can directly be excluded. The degree of branching will however effect whether the product can be used for detergent production or petrol/jet/diesel blending.

Work done previously by De Klerk *et al.* (2006) indicated a difference between the degree of branching seen in the gasoline fraction that was dependent on the acid strength of the liquid phosphoric acid used when oligomerising C_4 olefins. These authors state that the acid strength of the phosphoric acid promotes skeletal isomerisation, oligomerisation as well as the cracking of oligomerised product. This makes it difficult to stipulate which reaction is promoted more significantly when influencing the degree of branching of the gasoline product. Trimerisation did not occur for the dimerisation of hexenes, indicating that only cracking will influence the degree of branching of the product. It was shown previously that the carbon distribution observed remained independent of the hydration/acid strength of the catalyst, and yet it was still shown that the rate of skeletal isomerisation and DBH was affected to a significant extent by the acid strength of the catalyst. This indicates that even though the carbon distribution remained unaffected, the degree of branching of the dimerised product might differ at various hydrations. Since this is an important measure of the quality of a fuel, the influence of the acid strength on the degree of branching of the dimerised product ought to be investigated. In previous chapters, the degree of branching of the dimerised product could not be measured owing to the significant overlapping in the GC analysis, therefore a more in-depth analysis of the sample would be needed to determine the impact of acid strength on the branching of the dimerised product.

5.1 Experimental

To determine whether the degree of branching of the dimerised product is affected by the acid strength of the catalyst, the degree of branching of the product was ascertained by proton nuclear magnetic resonance (H NMR) analysis for three different phosphoric acid strengths at 80% hexene conversion. The experiments were completed to obtain a degree of branching based on the hydration runs completed at 200 °C in Chapter 4 whereby the 1-hexene was dimerised with SPA pretreated at 200 °C for the following cases: *1)* with only the latent water

present in the 1-hexene, *2)* addition of 2000 ppm water to the reagent and *3)* increasing the catalyst loading, and drying the 1-hexene with a mole sieve thereby increasing the ratio of the latent water to catalyst ratio. The reaction conditions for these three runs are shown in Table 5-1.

Table 5-1: Three reactions completed at 200 °C for analysis of the dimerised product.

	Sample 1	Sample 2	Sample 3
P_2O_5 (W %)	62.0%	70.3%	71.4%
m_{cat} (g)	12.34	12.29	28.54
1-Hexene (g)	272.2	267.3	263.7
ppm H_2O	1461	150	80
Hexene conversion (%)	88.9%	80.3%	85.1%

To ensure that a clear indication of the product branching could be observed with the H NMR analysis, the dimerisation was completed without the addition of solvent. Since olefin content interferes with the branching measurement, the product was hydrogenated. The hydrogenation was done in a Parr autoclave reactor at 60 °C at a hydrogen pressure of 50 bars. The hydrogenation was completed using a 0.3% Pd Al_2O_3 catalyst with a particle size of 3 mm from Heraeus. The extent of the hydrogenation was determined from the Bromine number of the sample. A Mettler and Toledo DL 58, with the solvent and titrant prepared as specified by the manufacturer, were used for this purpose. The hydrogenation was found to be at least 97.8% complete, which was sufficient for H NMR testing.

After the hydrogenation it was necessary to separate the reagent from the products. A PiloDist 1000 was used to separate the mixture into two fractions for H NMR testing: *1)* the gasoline fraction, boiling higher than C_6 paraffins (75 °C – 174 °C); and *2)* the distillate, which was taken as the product boiling after n-decane (>174 °C) (De Klerk *et al.,* 2006).

5.2 Results and discussion

5.2.1 Acid strength

After the product was hydrogenated and fractionated into a gasoline and distillate fraction, both samples were sent for GC/MS analysis to gain an idea of the carbon number distribution. The resulting analysis is shown in Table 5-2 for the gasoline and the distillate fractions. The

GC/MS analysis shows no clear difference in the carbon number distribution dependent on the hydration of the catalyst (as indicated previously, Figure 4-11).

Table 5-2: Mole percentage carbon distribution from GC-MS for the a) gasoline and b) distillate cut.

a)	Gasoline cut		
Acid Strength	71.4%	70.3%	62.0%
$\leq C_5$	0%	0%	0%
C_6	1%	0%	0%
C_7	15%	5%	16%
C_8	15%	12%	17%
C_9	18%	16%	17%
C_{10}	37%	43%	35%
C_{11}	14%	22%	15%
C_{12}	0%	1%	0%
$\geq C_{13}$	0%	0%	0%

b)	Distillate cut		
Acid Strength	71.4%	70.3%	62.0%
$\leq C_9$	0%	0%	0%
C_{10}	3%	4%	5%
C_{11}	53%	53%	56%
C_{12}	35%	37%	35%
C_{13}	7%	4%	4%
C_{14}	1%	1%	0%
C_{15}	0%	0%	0%
C_{16}	1%	1%	0%
$\geq C_{17}$	0%	0%	0%

The gasoline and distillate fractions were sent for H NMR analysis to determine the fraction of CH_3 — bonds. An idea of the branching of the reaction products could then be determined from the average molecular weight of the sample (Table 5-3: a degree of branching of two indicates two methyl branches are present on the hydrocarbon).

Table 5-3: Degree of branching of fuel cut

Acid strength	Gasoline cut	Distillate cut
71.4%	2.35	2.95
70.3%	2.58	2.97
62.0%	2.35	3.00

This means that for the same conversion of hexenes the acid strength did not influence the product distribution for either the gasoline or diesel fraction (*i.e.* same extent of cracking) and that the acid strength also did not influence the degree of branching. This is similar to what was observed in Section 4.2.3 where the acid strength did not alter the carbon distribution obtained. This indicates that the only lever which will influence the carbon distribution is temperature (Section 3.3.2). This was however for a fairly small variance in the acid strength of SPA for this investigation.

One case in the literature where oligomerisation of naphtha range products have been calculated, is the thermal oligomerisation of a C_5/C_6 FT cut at 320 – 400 °C where the CH_3:CH_2 ratio was 0.4 to 1 (De Klerk, 2005b). The extent of oligomerisation was more severe than for this investigation, the final boiling point of the product was a 540 °C which if the normal boiling point of a hydrocarbon is assumed equates to a C_{48} paraffin. The cetane number measured for the distillate fraction was though found to be between 41 and 48. If the correlation of O'Conner *et al.* (1992) is used to estimate the cetane number of the diesel fraction for this investigation the cetane was found to be 29. The low cetane is due to the high degree of branching observed in the distillate fraction, as such the distillate would mostly be viable as a jet fuel.

As for the degree of branching of the gasoline, data is available for the oligomerisation of butenes over SPA (Bekker and Prinsloo, 2009). The degree of branching found for the dimerised product, the C_8 fraction, was found to be 2.3 at 210 °C. If it is assumed that C_4 and C_6 dimerisation occurs through a branched intermediate the degree of branching should be similar for two dimerised fractions (C_8 and C_{12} fractions respectively). During C_4 oligomerisation over SPA, trimerisation will occur to the distillate fraction (trimerisation) which was not observed for hexene. This would result that the degree of branching of the C_8 fraction is lower than observed for the C_{12} fraction of the hexene dimerisation product (which was on average 3.0).

The degree of branching of the C_8 fraction (2.3) for C_4 oligomerisation is quite similar to gasoline fractions degree of branching for hexene dimerisation (on average 2.4). There are however some distinct differences between the two products: the gasoline fraction for the hexene dimerisation contained C_7-C_{11} hydrocarbons formed predominantly from cracking and secondary oligomerisation whereas the C_8 fraction formed from dimerisation and is depleted by further oligomerisation as well as cracking to shorter chain olefins.

The quality of the hydrogenated gasoline fraction is highly dependent on the degree of branching and the carbon number. For a degree of branching between 2-3 the RON can vary between 50 to 101.8 over this carbon number, Table 5-4 (Daubert and Danner, 1987; Jones and Pujado, 2006). This states that the RON of the gasoline fraction is dependent on where the branching is positions. For a definitive description of the gasoline fractions quality, engine testing would be required.

Table 5-4: RON of C_7-C_{10} paraffin dependent on the branching

Component	RON
Dimethyl pentane	83.1-91.1
Trimethyl butane	101.8
Dimethyl hexane	72.5
Trimethyl pentane	100
Dimethyl heptane	50.3
Trimethyl hexane	91
Trimethyl heptane	86.4

5.3 Conclusion

The effect of acid strength was tested by comparing the degree of branching seen for three different acid strengths at the same conversion of hexenes. A large degree of branching was evident in both the gasoline and distillate fractions. As such the cetane number of the distillate fraction was found to be 29, indicating that the distillate would be more viable as a jet fuel than a diesel. Engine testing of the gasoline fraction would be needed for a more clear indication of the RON of the hydrogenated gasoline.

For the range of acid strength investigated it was found, that the acid strength of the catalyst did not influence the degree of branching or the carbon distribution of the product. Therefore temperature is the most viable means of altering the carbon distribution of the product.

6 Conclusions

Kinetic data was gathered for the dimerisation of 1-hexene between 100 – 250 °C. To compensate for the differences in reactivity between linear and branched hexenes, the dimerisation was also completed for DMB. Due to the increased reactivity of branched olefins, a reaction mechanism was proposed that allowed for the skeletal isomerisation of linear hexenes, after which dimerisation/co-dimerisation occurs. It was concluded from the optimisation of the kinetic model that the reaction kinetics could be adequately modelled using a simple elementary kinetic model. Only the co-dimerisation of linear and branched hexenes (CD) and the dimerisation of branched hexenes (BHD) were needed to model the reaction rate accurately (with linear dimerisation found to be negligible). At low reaction temperatures the co-dimerisation of linear and branched hexenes dominated the reaction rate whereas at higher temperatures, the reaction rate was dominated by the dimerisation of branched hexenes. The reaction progression was seen to be controlled by the rate of skeletal isomerisation.

It became evident from the dimerisation of hexene using liquid ortho and pyro phosphoric acid that the acid strength has a strong influence on the activity of the catalyst. Experiments were conducted for various acid strengths of the catalyst. The acid strength of the catalyst was altered by either the hydration of the catalyst or by altering the free acid content of the catalyst. An exponential dependency of the rate constants on acid strength was observed at each acid strength from the prediction of the experimental data with an elementary kinetic model. This was incorporated into the rate constant which resulted in a kinetic model that could be used to predict the reaction rate at various acid strengths and temperatures.

It was also clear from the observed carbon distribution that carbon distribution evens out as soon as dimerisation occurs. Cracking and secondary dimerisation therefore occur much faster than the dimerisation of hexene. Higher temperatures promoted cracking, resulting in a flat carbon number distribution, whereas lower temperatures resulted in the formation of longer carbon chains. It was also seen that the product distribution was not dependent on the acid strength of the catalyst but was dependent on the free acid concentration of the catalyst. Since the free acid strength of the commercial catalyst does not differ during operation, the carbon number distribution is effectively only dependent on the reaction temperature.

The possibility still remained that increasing the acid strength could affect the branching of the produced product. Data on the dimerised product was then gathered for three acid

strengths for a constant temperature of 200 °C at the same conversion. The product was hydrogenated and fractionated and the degree of branching determined. A large degree of branching was evident in both the gasoline and distillate fractions, indicating that the dimerisation of hexenes would result in the production of a gasoline and jet fuel. However, it became clear from the degree of branching observed at various hydration states of the catalyst that the acid strength did not influence the degree of branching or the carbon distribution for both the gasoline and distillate fractions.

7 Bibliography

Alcántara R., Alcántara E., Canoira L., Franco M.J., Herrera M. and Navarro A. (2000) Trimerization of isobutene over Amberlyst-15 catalyst, *Reactive & Functional Polymers*, 45, 19–27.

Anderson J.R., Chang Y.F. and Western R.J. (1991) The Effect of Acidity on the Formation of Retained Residue from 1-Hexene over USY Zeolite Catalysts, *Catalyst Deactivation,* 745-751.

Bekker R. and Prinsloo N.M. (2009) Butene Oligomerization over Phosphoric Acid: Structural Characterization of Products, *Ind. Eng. Chem. Res.*, 48, 10156–10162.

Bentley R.W. (2002) Global oil & gas depletion: an overview, *Energy Policy*, 30, 189–205.

Bercik P.G., Metzger K.J. and Swift H.E. (1978) Oligomerization of C3-C4 Olefins Using a Novel Nickel-Aluminosilicate Catalyst, *Ind. Eng. Chem. Prod. Res. Dev.,* 3, 17, 214-219.

Bethea S.R. and Karchmer J.H. (1956) Propylene Polymerization in Packed Reactor Liquid Phosphoric Acid Catalyst, *Industrial Engineering Chemistry*, 3, 48, 370-377.

Brown E. H. and Whitt C.D. (1952) Vapour Pressure of Phosphoric Acids, *Industrial Engineering Chemistry*, 3, 44, 615-618.

Cao G., Viola A, Barrati R. and Morbidelli M. (1988) Lumped Kinetic Model for Propene-Butene Mixtures Oligomerization on a Supported Phosphoric Acid Catalyst, *Applied Catalysis*, 41, 301-312.

Cavani C., Girotti G. and Terzoni G. (1993) Effect of water in the performance of the 'solid phosphoric acid' catalyst for alkylation of benzene to cumene and the oligomerization of propene, *Applied Catalysis A: General,*2, 97, 177-196.

Chen W.J., Cao Z.T., Hou B. and Wang H.Y. (2008) Oligomerizing Olefins in Light Coke Gasoline to Diesel, *Gasolineum Science and Technology,* 26, 473–480.

Coetzee J. H., Mashapa T.N., Prinsloo N.M. and Rademan J.D. (2006) An improved solid phosphoric catalyst for alkene oligomerization in a Fischer-Tropsch refinery, *Applied Catalysis A: General*, 308, 204-209.

Commereuc D., Chauvin Y., Leger G. and Gailard J. (1982) Chemical Aspects of the Dimersol Process for Dimerisation of Olefins, *Revue de I'Institut Francais du Petrole*, 37,5, 639-649.

Cowley M., De Klerk A., Nel R.J.J. and Rademan J.D. (2006) Alkylation of Benzene with 1-Pentene over Solid Phosphoric Acid, *Ind. Eng. Chem. Res.*, 45, 7399-7408.

Cruz V.J., Izquierdo J.F., Cunill F., Tejero J., Iborra M., Fité C. and Bringué R. (2007) Kinetic modelling of the liquid-phase dimerization of isoamylenes on Amberlyst 35, *Reactive & Functional Polymers*, 67, 210–224.

Dancuart L.P., De Haan R. and De Klerk A. (2004) Processing of Primary Ficher-Tropsch Products, *Studies in Surface Science Catalysis,* 152, 482-532.

Da Rosa R.G., De Souza M.O. and De Souza R.F. (1997) Oligomerization and co-oligomerization of α-olefins catalyzed by nickel (II)/alkylaluminum systems, *Journal of Molecular Catalysis A: Chemical*, 120, 55-62.

Dazeley G.H. (1948) The Preparation of Lubricating Oils from Hydrocarbon-Synthesis Products (1), *Petroleum,* January, 14-15/26.

Daubert T.E. and Danner R.P., *Physical Constants of Hydrocarbon and Non-Hydrocarbon Compounds,* ASTM Data Series DS 4B, 2nd edition, Philidephia, 1987.

Deeter, W.F. (1950) Propylene Polymerization for Motor Gasoline Production, *The Oil and Gas Journal*, March, 252-258

De Klerk A. (2004) Isomerization of 1-Butene to Isobutene at Low Temperature, *Ind. Eng. Chem. Res.*, 43, 6325-6330.

De Klerk A. (2005a) Oligomerization of 1-Hexene and 1-Octene over Solid Acid Catalyst, *Ind. Eng. Chem. Res.*, 44, 3887-3893.

De Klerk A. (2005b) Thermal Upgrading of Fischer-Tropsch Olefins, *Energy & Fuels*, 19, 1462-1467.

De Klerk A. (2006a) Distillate production by the oligomerization of Fischer-Tropsch olefins over solid phosphoric acid, *Energy & Fuels*, 2, 20, 439-445.

De Klerk A. (2006b) Reactivity differences of octenes over solid phosphoric acid, *Ind. Eng. Chem. Res.,* 2, 45, 578-584.

De Klerk A. (2007) Effect of Oxygenates on the Oligomerisation of Fischer-Tropsch Olefins over Amorphous Silica-Alumina, *Energy & Fuels,* 21, 625-632.

De Klerk A. (2007a) Properties of synthetic fuels from H-ZSM-5 oligomerization of Fischer–Tropsch type feed materials, *Energy & Fuels*, 6, 21, 3084-3089.

De Klerk A., Engelbrecht D. J. and Boikanyo H. (2004) Oligomerization of Fischer-Tropsch Olefins: Effect of Feed and Operating Conditions on Hydrogenated Motor-Gasoline Quality, *Ind. Eng. Chem. Res.*, 43, 7449-7455.

De Klerk A., Leckel D. O. and Prinsloo N. M. (2006) Butene Oligomerization by Phosphoric Acid Catalysis: Separating the Effects of Temperature and Catalyst Hydration on Product Selectivity, *Ind. Eng. Chem. Res.*, 18, 45, 6127-6136.

De Klerk A., Nel R.J.J and Schwarzer S. (2007) Oxygenate Conversion over Solid Phosphoric Acid, *Ind. Eng. Chem. Res.*, 46, 2377-2382.

Di Girolamo M., Lami M. and Marchionna M. Liquid-Phase Etherification/Dimerization of Isobutene over Sulfonic Acid Resins, *Ind. Eng. Chem. Res.*, 36, 4452-4458.

Egloff G. (1936) Polymer Gasoline, *Industrial and Engineering Chemistry,* 28, 12, 1461-1467.

Egloff, G. and Welnert, P.C. (1951) Polymerisation with Solid Phosphoric Acid Catalyst, *Proceedings Third World Petroleum Congress,* Section IV, 201-214.

Escola J. M., Van Grieken R., Moreno J. and Rodríguez R. (2006) Liquid Phase Oligomerisation of 1-Hexene Using Al-MTS Catalysts, *Ind. Eng. Chem. Res.*, 45, 7409-7414.

Farkas, A. and Farkas, L. (1942) Catalytic Polymerization of Olefins in the Presence of Phosphoric Acid, *Industrial and Engineering Chemistry,34, 6, 716-721.*

Fortini E. M., González Bóveda M.C. and Löffler, D.G. (1997) Kinetics of 1-hexene dimerization catalyzed by a liquid-phase nickel complex, *React. Kinet. Catal. Lett.*, 2, 61, 281-287.

Friedman P. and Pinder K. L. (1971) Kinetics of Polymerization of Olefins in Production of Polymer Gasoline, *Ind. Eng. Chem. Process Der. Develop.*, 4, 10, 548-551.

Garwood W. E. Conversion of C_2 -C_{10} to Higher Olefins over Synthetic Zeolite ZSM-5, *ACS Symp. Ser.*, 218, 383-396.

Golombok M. and de Bruijn J. (2000) Dimerization of n-Butenes for High Octane Gasoline Components, *Ind. Eng. Chem. Res*, 39, 267-271.

Handlos, A.E. and Nixon, A.C. (1956) Vapor Pressure of Phosphoric Acid at High Temperature and Pressure, *Industrial and Engineering Chemistry,* 48,10, 1960-1962.

Hay R.G., Montgomery C.W. and Coull J. (1954) Catalytic isomerization of 1-hexene, *Industrial and Engineering Chemistry*, 4, 37, 335-339.

Heveling J., Nicolaides C.P. and Scurrell M.S. (2003) Activity and selectivity of nickel-exchanged silica-alumina catalysts for the oligomerization of propene and 1-butene into distillate-range products, *Applied Catalysis A: General*, 248, 239–248.

Honkela M.L. and Krause A. O. (2004) Kinetic Modeling of the Dimerization of Isobutene, *Ind. Eng. Chem. Res.*, 43, 3251-3260.

Honkela M.L. and Krause A.O.I. (2003) Influence of polar components in the dimerization of isobutene, *Catalysis Letters*, 3-4, 87, 113-119.

Ipatieff V.N. (1935) Catalytic Polymerization of Gaseous Olefins by Liquid Phosphoric Acid I. Propylene, *Industrial and Engineering Chemistry*, 9, 27, 1067-1069.

Ipatieff V.N. and Corson, B.B. (1935) Gasoline from ethylene by catalytic polymerisation, *Ind. Eng. Chem.*, 7, 28, 860-863.

Ipatieff V.N., Corson B.B. and Egloff G. (1935) Polymerization, a New Source of Gasoline, *Industrial and Engineering Chemistry,* 9, 27, 1077-1081.

Ipatieff V.N. and Pines H. (1936) Propylene Polymerisation Under High Pressure and Temperature with and without Phosphoric Acid, *Industrial and Engineering Chemistry,* 684-686

Ipatieff V.N. and Schaad, R.E. (1938) Mixed Polymerization of Butenes by Solid Phosphoric Acid Catalyst, *Ind. Eng. Chem.*, 5, 30, 596-599.

Ipatieff V.N. and Schaad, R.E. (1948) Polymerization of Pentenes, *Industrial and Engineering Chemistry,* 40, 1, 78-80

Jameson R.F. (1959) The Composition of the 'Strong' Phosphoric Acids, *J. Chem. Soc.*, 752–759.

Jones D.S.T and Pujado P.R., *Handbook of Petroleum Processing,* Springer, The Netherlands, 2006.

Jones E. K. (1956) Polymerization of Olefins from Cracked Gasses, *Advances in Catalysis,* 8, 219 -238.

Kotsarenko N.S., Shmachkova V.P., Mudrakovskii I.L. and Mastkhin V.M. (1989) Study of the Nature of the Active Component of the H3PO4/SiO2 Catalyst, *Kinetika i Kataliz,* 30, 5, 1117 -1122.

Kotz J.C. and Treichel P., *Chemistry and Chemical Reactivity,* New York, Saunders College Publishing, Volume 4, 1999.

Krawietz T.R., Lin P., Lotterhos K.E., Torres P.D., Barich D.H., Clearfield A. and Haw J.F. (1998) Solid Phosphoric Acid Catalyst: A Multinuclear NMR and Theoretical Study, *J. Am. Chem. Soc.*, 33, 120, 8502-8511.

Langlois G. E. and Walkey J. E. *Proceedings of the Third World Petroleum Congress*, The Hague, Netherlands, Vol 5, 1951.

Langlois G. E. and Walkey J. E. (1952) Improved Process Polymerizes Olefins for High Quality Gasoline, *Petroleum Refiner,* 31, 8, 79-83.

Makatun, V.N., Solovei, O.M., Polyakova, V.P. and Bachilo, B.A. (1985) Influence of Water in Phosphoric Acid Catalysts on the Rates of Reaction Accompanied by Proton Transport, *Kinetics and Catalysis*, 26, 1225-1229.

Mashapa T. N. and De Klerk A. (2007) Solid phosphoric acid catalysed conversion of oxygenate containing Fischer–Tropsch naphtha, *Applied Catalysis A: General*, 2, 332, 200–208.

McClean D.M., *A Kinetic Study of the Oligomerisation of Propene, Butene and Various Hexenes over Solid Phosphoric Acid,* Department of Chemical Engineering, University of Cape Town, 1987.

McMurry J., *Organic Chemistry,* Pacific Grove, Brooks & Cole Thompson Learning, Fifth Edition, 2000.

Monroe L.A. and Gilliland E.R. (1938) Polymerization of Propylene by Dilute Phosphoric Acid, *Industrial Engineering Chemistry,* 30,1, 58-63.

Montanari L., Montani E., Corno C. and Fattori S. (1998) NMR Molecular Characterization of Lubricating Base Oils: Correlation with their Preformance, *Applied Magnetic Resonance,* 14, 345-356.

Morrell J.C. [Patent], 3,132,109, US Patent, 1964.

Morrell J.C. [Patent], 3,050,472, US Patent, 1962a.

Morrell J.C. [Patent], 3,050,473, US Patent, 1962b.

Naworski J.S. and Harriott P. (1969) Oligomerization of 1-Butene in Sulfuric Acid. Mechanisms and Rates. *Ind. Eng. Chem. Fundamen*, 3, 8, 397-401.

Nel J.J.N. and de Klerk A. (2007) Selectivity Differences of Hexene Isomers in the Alkylation of Benzene over Solid Phosphoric Acid, *Ind. Eng. Chem. Res.*, 46, 2902-2906.

O'Connor C.T., Kojima M. and W.K. Schumann (1985) The Oligomerization of C4 Alkenes over Cationic Exchange Resins, *Applied Catalysis*, 16, 193-207.

O'Connor C.T., Forrester R.D. and Scurrell M.S. (1992) Cetane number determination of synthetic diesel fuels, *Fuel*, 71, 1323-1327.

Ohtsuka, H. and Aomura K. (1962) Activation of Solid Phosphoric Acid by Heat Treatment, *Bulletin of the Japan Petroleum Institute,* 4, 3-14.

Okuhara T. (2002) Water-Tolerant Solid Acid Catalyst, *Chem. Rev.*, 102, 3641-366.

Pater J. P. G., Jacobs P. A. and Martens J. A. (1998) 1-Hexene Oligomerization in Liquid, Vapor, and Supercritical Phases over Beidellite and Ultrastable Y Zeolite Catalysts, *Journal of Catalysis*, 179, 477-482.

Pater J. P. G., Jacobs P. A. and Martens J. A. (1999) Oligomerisation of Hex-1-ene over Acidic Aluminosilicate Zeolites, MCM-41, and Silica-Alumina Co-gel Catalysts: A Comparative Study, *Journal of Catalysis*, 184, 262-267.

Paynter J.D. and Schuette W.L. (1971) Development of a model for kinetics of olefin co-dimerisation, *Ind. Eng. Chem. Process Des. Develop*, 1, 19, 250-257.

Prinsloo N. M. (2006) Solid phosphoric acid oligomerisation: Manipulating diesel selectivity by controlling catalyst hydration, *Fuel Processing Technology*, 2, 87, 437-442.

Prinsloo N.M. (2007) Preparation of a Solid Phosphoric Acid Catalyst from Low-Quality Kieselguhrs Parameters Controlling Catalyst Quality and Performance, *Ind. Eng. Chem. Res*, 46, 7838-7843.

Quan R. J., Green L.A., Tabak S.A. and Krambeck F.J. (1988) Chemistry of Olefin Oligomerization over ZSM-5 Catalyst, *Ind. Eng. Chem. Res.*,27, 565-570.

Sarin R., Tuli D.K., Sinharay S., Rai M.M., Ghosh S. and Bhatnagar A.K. (1996) Higher Olefin Oligomerization Catalyzed by Sulphated Zirconia, *212th Meeting of the American Chemical Society,* 625-627.

Schmidt R., Welch, M. B. and Randolph B. B. (2008) Oligomerization of C5 olefins in light catalytic naphtha, *Energy & Fuels*, 2, 22, 1148-1155.

Schultz R.G. (1967) Olefin Dimerization over Cobalt-Oxide-on-Carbon Catalysts III (1967) Oligomerization of Ethylene, *Journal of Catalysis*, 3, 7, 286-290.

Schmerling, L. and Ipatieff, V.N. (1950) The Mechanism of the Polymerization of Alkenes, *Advances in Catalysis,* 2, 21-79.

Schwarzer R.B., du Toit E. and Nicol W. (2008) Kinetic model for the dimerisation of 1-hexene over a solid phosphoric acid catalyst, *Applied Catalysis A: General*, 340, 119-124.

Schwarzer R.B., du Toit E. and Nicol W. (2009) Solid phosphoric acid catalysts: The effect of free acid composition on selectivity and activity for 1-hexene dimerisation, *Applied Catalysis A: General*, 369, 83-89.

Shepard F.E., Rooney J.J. and Kemball C. (1962) The Polymerization of Propylene on Silica-Alumina, *Journal of Catalysis,* 1, 379-388.

Skupińska J. (1991) Oligomerization of α-Olefins to Higher Oligomers, *Chem. Rev.*, 91, 613-648.

Tabak S.A., F.J. Krambeck. and Garwood W.E. (1986) Conversion of Propylene and Butylene over ZSM-5 Catalyst, *AIChE J.*, 9, 32, 1526-1531.

Van der Westhuizen R. Potgieter H., Prinsloo N., de Villiers A. and Sandra, P. (2010) Fractionation by liquid chromatography combined with comprehensive two-dimensional gas chromatography–mass spectrometry for analysis of cyclics in oligomerisation products of Fischer–Tropsch derived light alkenes, *Journal of Chromatography A*, doi: 10.1016/j.chroma.2010.10.009

Van Grieken R., Escola, J. M., Moreno, J. and Rodríguez R. (2006) Liquid phase oligomerization of 1-hexene over different mesoporous aluminosilicates (Al-MTS, Al-MCL-41, Al-SBA-15) and micrometer/nanometer HZSM-5 zeolites, *Applied Catalysis A: General,* 2, 305, 176-188.

Vinnik M.I. and Obraztsov P.A. (1983) Determination of Water Vaporization Rate from Phosphoric Acid Catalyst According to the Change in its Catalytic Activity, *Kinetika I Kataliz,* 24, 4, 887-889.

Weast R. C., *CRC Handbook of Chemistry and Physics*, Boca Raton, CRC Press, p. D 103, 1988.

Weinert, P.C. and Egloff, G. (1948) Catalytic Polymerization And Its Commercial Application, *Petroleum Processing*, 585-593

Zhirong Z., Zaiko X., Yongfu C., Refeng W. and Yaping Y. (2000) Free phosphoric acid of diatomite–phosphate solid acid and its catalytic performance for propylene oligomerisation, *React. Kinet. Catal. Lett.*, 2, 70, 379–388.

8 Appendix

8.1 Product formation for the oligomerisation of DMB

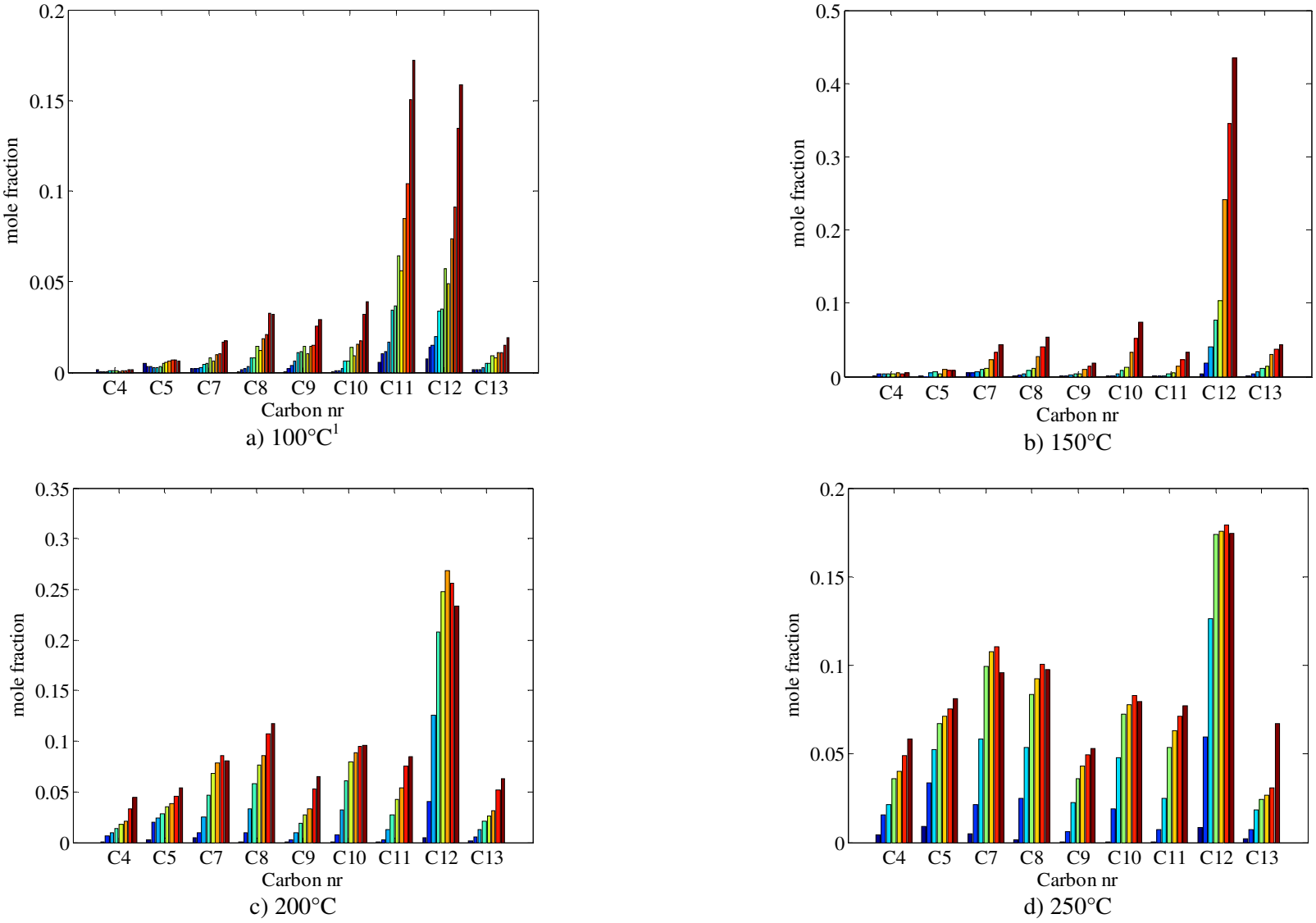

Figure 8-1: Formation of oligomerised and cracked products for DMB oligomerisation.

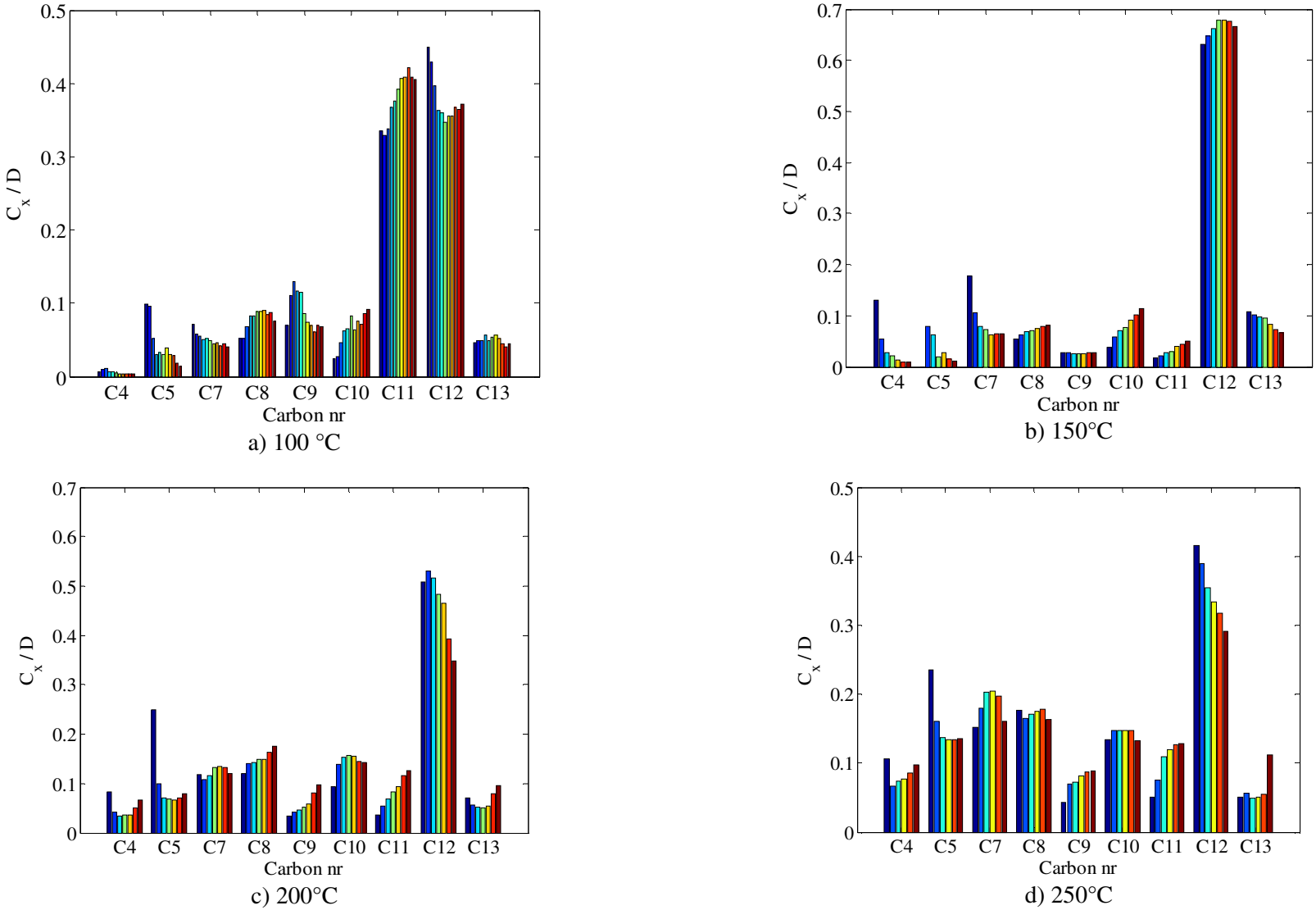

Figure 8-2: Distribution of cracked and oligomerised product for DMB oligomerisation.

[1] The large spike in the formation of C_{11} olefins is due to branched C_{12} product overlapping, this was not noted for 1-hexene oligomerisation.

8.2 GCxGC results

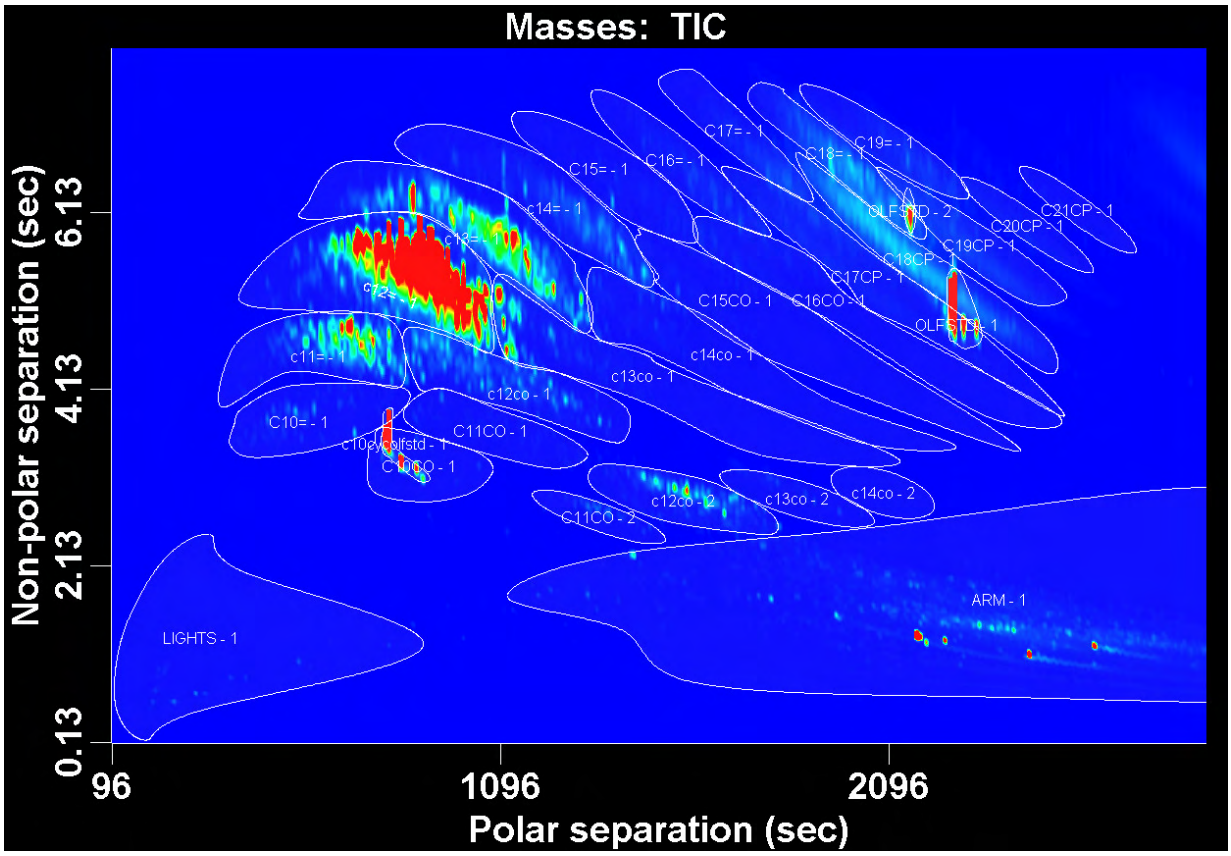

a) 100 °C

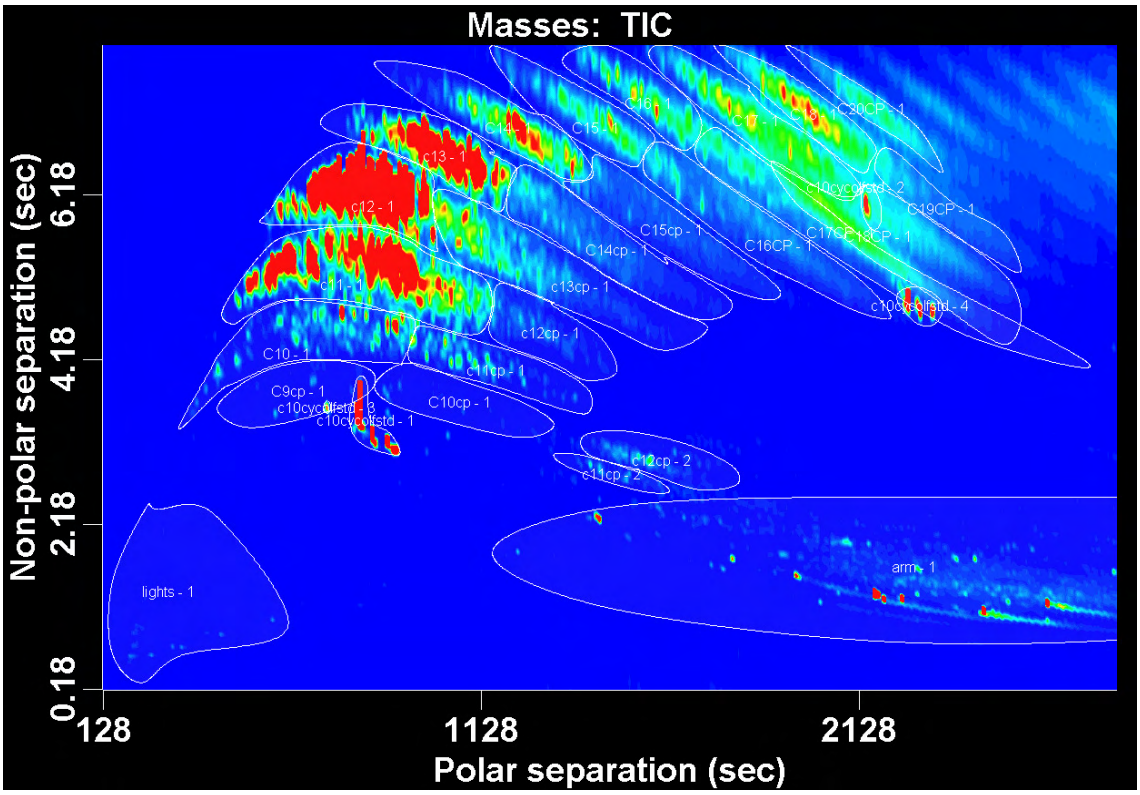

b) 150 °C

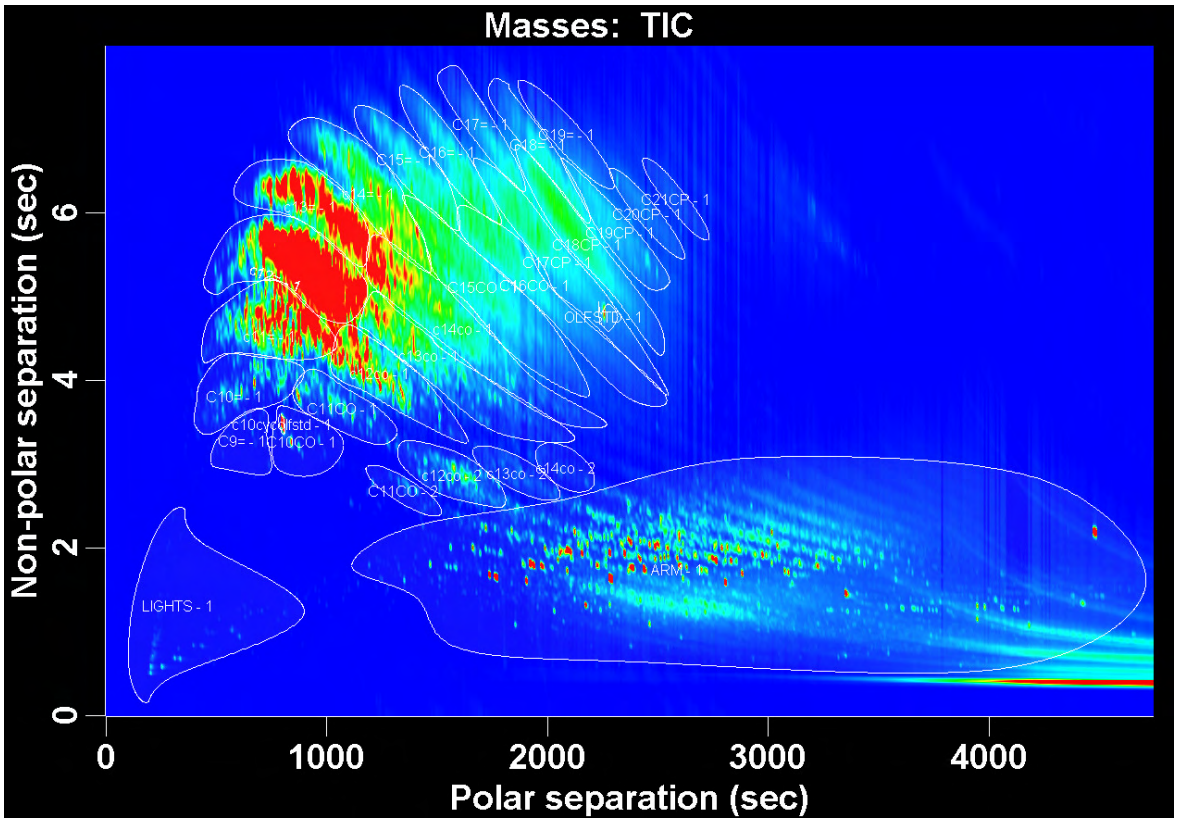

c) 250 °C

Figure 8-3: GCxGC results for 1-hexene product at a) 100 °C, b) 150 °C and c) 250 °C.